Article QR

Title:	**Bivariate and Multivariate Data Cloning through Non Linear Regression Models**
Author (s):	Sajid Hussain[1], Zafar Iqbal[1], Muhammad Mansoor[2], Rashid Ahmed[1]
Affiliation (s):	[1]The Islamia University of Bahawalpur, Pakistan [2]Government S. E. College, Bahawalpur, Pakistan
DOI:	https://doi.org/10.32350/sir.73.01
History:	Received: December 4, 2022, Revised: March 28, 2023, Accepted: March 30, 2022, Published: August 28, 2023
Citation:	Hussain S, Iqbal Z, Mansoor M, Ahmed R. Bivariate and multivariate data cloning through nonlinear regression models. *Sci Inq Rev.* 2023;7(3):1–21. https://doi.org/10.32350/sir.73.01
Copyright:	© The Authors
Licensing:	This article is open access and is distributed under the terms of Creative Commons Attribution 4.0 International License
Conflict of Interest:	Author(s) declared no conflict of interest

Bivariate and Multivariate Data Cloning through Non Linear Regression Models

Sajid Hussain[1*], Zafar Iqbal[1], Muhammad Mansoor[2], and Rashid Ahmed[1]

[1]Department of Statistics, The Islamia University of Bahawalpur, Pakistan
[2]Department of Statistics, Government S. E. College, Bahawalpur, Pakistan

ABSTRACT

Nonlinear regression analysis holds significant popularity in mathematical, engineering, and social science domains. Disciplines like financial matters, biology, and natural chemistry have broadly utilized nonlinear regression models (NLRMs). Cloned datasets have their own importance in such areas which provide the same fit of bivariate and multivariate nonlinear regression models for the actual datasets. This article presents a sequence of cloned datasets that give exactly the same fit of bivariate and multivariate nonlinear regression models.

Keywords: cloned data, nonlinear regression model, fictitious datasets, data visualization.

1. INTRODUCTION

If genuine information is private and cannot be shown, a matching or alternative set of data is required which provide same summary statistics as of the actual data. Cloned data refers to the alternative or matching set of data through mathematical techniques that allow rapid provisioning in testing and developments. Data cloning has its own significance as an alternative method for protecting confidential information and database. Table 1 shows four fictitious distinct cloned datasets (CDSs) created by Anscombe [1] to demonstrate the significance of graphs in statistical analysis. The summary statistics (mean, standard deviation, and correlation) as well as the parameter estimates of the fitted regression equation R^2 and estimated standard deviation of residuals are identical across these four distinct CDSs, however, they were vastly different scatter plots as shown in Figure 1. Dataset I was strongly linear with a single outlier and II appears to follow a parabolic distribution, whereas dataset III appears to adhere to a noisy linear regression model (LRM), and dataset IV appears to follow a vertical line with the regression thrown off by a single outlier. Datesets in Table 1 are significant and frequently used to show how important visible

---

[*] Corresponding Author: sajidhussain060917@gmail.com

methods are. These datasets were also known for their significant use in education. However, the method used to create the datasets was not explained in [1]. A genetic algorithm-based approach was proposed by Chatterjee and Firat [2], who generated 1,000 random datasets with comparable summary statistics and graphics for the basic datasets. Govindaraju and Haslett [3] devised a method for producing datasets by regressing the response on the covariate in the direction of their unconditional sample means, while maintaining identical LRM estimates. As a result, the variability in the response and the covariate decreased in each subsequent cloned dataset. Haslett and Govindaraju's [4] method for creating matched datasets was extended to include a multiple linear regression model, ensuring that the matched datasets have an identical fit to the original data. The idea of data-cloning emerged from both biostatistics [5, 6] and financial time series [7].

Cloning for maximum likelihood estimation using Bayesian software was achieved by the simple device of replicating the original data many times [6]. Fung et al. [8] expressed that the creation of CDSs to anonymize sensitive data was another application for datasets with the same statistical properties, as discussed in [3]. In this instance, it is critical that individual data points were altered, while the data's overall structure remained unchanged.

Haslett and Govindaraju [9] described a straightforward approach for modifying LRM data, while still obtaining the same fitted regression parameters. Ponciano et al. [10] showed how structural parameter non-identifiability can be diagnosed with Data Cloning (DC) and distinguished from other parameter estimability issues, such as when parameters are structurally identifiable but not estimable in a given data set or when they are identifiable and weakly estimable. Bayesian phylogenetics software can be used to diagnose non-identifiability with the DC approach. Additionally, it was demonstrated that DC can be used to examine and eliminate the influence of priors, particularly when prior elicitation was difficult. Finally, DC can be used to investigate at least two significant statistical issues when applied to phylogenetic inference, developing effective sampling strategies for computationally expensive posterior densities, and evaluating the identifiability of discrete parameters, such as the tree's topology.

Data confidentiality is one of the designed goals of tunable encrypted deduplication, see Amvrosiadis and Bhadkamkar [11]. Additionally, it

reduced the risk of data leakage brought by frequency analysis. Furthermore, it was identified that better ways of seeing and exploring data lead to better insights. The "Datasaurus" Cairo dataset was created by Alberto Cairo [12]. This, like Anscombe's Quartet, emphasized the significance of data visualization, despite the dataset's normal summary statistics, the plot it produced depicted a dinosaur. They started with the datasaurus and created additional datasets with the same summary statistics. Additionally, Cairo's Datasaurus data visualization prohibited to solely rely on the summary statistics of the used data.

Resultantly, according to [2], datasets should be as graphically distinct as possible. With different standard deviations but identical means and LRM estimates, [3, 4, 9] data are intended to be graphically comparable. Matejka and Fitzmaurice [13] developed a novel method for creating datasets, which are identical across a variety of statistical properties but visually distinct during the data exploration. To address the primary empirical facts of financial time series, numerous complex parametric stochastic volatility models were proposed in the subsequent literature. The models that Mao et al. [14, 15] proposed incorporated a broader asymmetric volatility function.

Hussain et al. [16] used a simple procedure to clone data for nonlinear regression models having linearizable or nonlinearize regression functions, such as aX^b, ab^X, ae^{bX}, $k\,a^{b^X}$, $ks^X b^{c^X}$, $k+ab^X$, $\dfrac{k}{1+bc^X}$, $A\,[aX_2^{-b} + (1-a)X_1^{-b}]^{-\frac{1}{b}}$. They found that cloned data generated by linearizable or non-linearizable estimable functions of parameters have unchanged estimates. The procedure increased the sample size of cloned data without changing the parameters estimates, which was for n original sample points (x, y). This generated n^2 observations by adding [a_i: $i = 1, 2, …, n$] to the data points y over $\sum_i a_i = 0$. Due to increased sample size, cloned estimates showed smaller standard errors as compared to the original standard errors. This procedure used by [16] was sufficient for the first iteration because in the next iterations, it became tedious work. This procedure was useful for modeling but not for confidentialising or encrypting data, as in the design matrix variables remained unchanged. In this case, the term "confidentializing" referred to making the values of particular variables certain for particular people that cannot be deduced from the data. Our goal in this article is to create datasets with the same fit for nonlinear linear

regression models (NLRMs). [3, 4] methods were used to generate these cloned data sets. To get around the problem in [16], nonlinear regression models with linearizeable regression functions were the prime focus of this article.

Table 1. Anscombe's CDSs with Pairs (x, y_1), (x, y_2), (x, y_3) and (x_4, y_4)

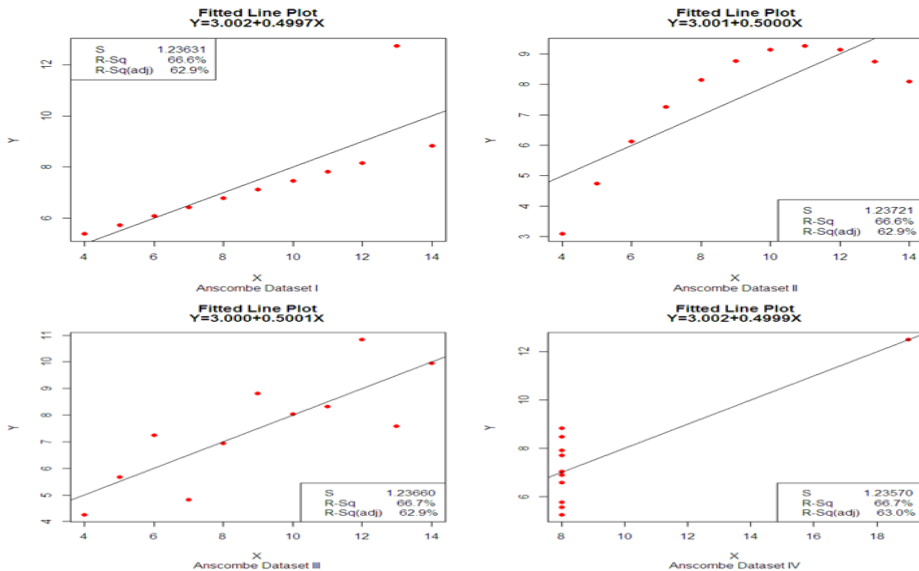| x	y_1	y_2	y_3	x_4	y_4
7	6.42	7.26	4.82	8	7.91
4	5.39	3.10	4.26	19	12.5
11	7.81	9.26	8.33	8	8.47
13	12.74	8.74	7.58	8	7.71
8	6.77	8.14	6.95	8	5.76
5	5.73	4.74	5.68	8	6.89
12	8.15	9.13	10.84	8	5.56
6	6.08	6.13	7.24	8	5.25
10	7.46	9.14	8.04	8	6.58
9	7.11	8.77	8.81	8	8.84
14	8.84	8.10	9.96	8	7.04

Figure 1. Scatter Plots of Anscombe's Datasets with Matched Simple Regression Models

2. THE NONLINEAR REGRESSION MODEL

2.1. The Regression Model (RM)

The Regression Model (RM) talks about the relationship between a response variable Y and one or more covariates $X^{(j)}$. The general model is:

$$Y_i = H\left(X_i^{(1)}, X_i^{(2)}, \dots, X_i^{(m)}; A_1, A_2, \dots, A_p\right) + E_i$$

Here, H is a suitable function that relies on the covariates $X_i^{(1)}, X_i^{(2)}, \dots, X_i^{(m)}$ and parameters $A_1, A_2, \dots, A_p$. The unstructured deviations from H are defined by means of random errors (REs) $E_i \sim N(0, \sigma^2)$.

2.2. The Linear Regression Model

In multiple LRM (MLRM), function H are characterized as linear in the parameters.

$$H\left(X_i^{(1)}, X_i^{(2)}, \dots, X_i^{(m)}; A_1, A_2, \dots, A_p\right) = A_1 \tilde{X}_i^{(1)} + A_2 \tilde{X}_i^{(2)} + \cdots + A_p \tilde{X}_i^{(m)}$$

where $\tilde{X}_i^{(j)}$ can be arbitrary functions of the original covariates $X_i^{(j)}$.

2.3. The Nonlinear Regression Model

In NLRM, function H is regarded in such a way that it can't be written as linear in parameters. In case, there are infinite ways to explain the deterministic part of the model.

2.4. Linearizable Regression Functions (LRFs)

In NLRMs, functions H can be linearized by the transformation of the variable of interest and the explanatory variables. Therefore, the regression is named as function H which is linearizable if it can be converted into a function linear in the parameters.

2.5. A Few Examples of Nonlinear Regression Functions

1- $H(X_i; A_1, A_2) = A_1 X_i^{A_2}$

2- $H(X_i; A_1, A_2) = A_1 A_2^{X_i}$

3- $H(X_i; A_1, A_2) = A_1 e^{A_2 X_i}$

4- $H\left(X_i^{(1)}, X_i^{(2)}; A_1, A_2, A_3\right) = A_1 (X_i^{(1)})^{A_2} (X_i^{(2)})^{A_3}$

2.6. Linearizable Regression Function Model

A LRM with the LRF in the referred example is based on the model given below:

$$\ln(Y_i) = B_1 + B_2 \tilde{X}_i^{(1)} + B_3 \tilde{X}_i^{(2)} + E_i; \ \tilde{X}_i^{(1)} = \ln\left(X_i^{(1)}\right), \tilde{X}_i^{(2)} = \ln\left(X_i^{(2)}\right)$$

Where, E_i follows the normal distribution. This model was back-converted and for this reason, the following equation was obtained:

$$Y_i = A_1 (X_i^{(1)})^{A_2} (X_i^{(2)})^{A_3} \tilde{E}_i \ ; \ \tilde{E}_i = \exp(E_i), i = 1, 2, \ldots, n$$

The errors $\tilde{E}_i$ follows lognormal distributed and contributed multiplicatively. The assumptions about the random deviations were accordingly now appreciably distinct for a model, which was primarily based on:

$$Y_i = A_1 (X_i^{(1)})^{A_2} (X_i^{(2)})^{A_3} + E_i^*$$

with random deviations E_i^* that follows normal distribution and contributed additively.

3. DATA CLONING BY USING REGRESSING Y ON X AND X ON Y

Assuming n paired observations of X and Y say (x_i, y_i) $i = 1, 2, \cdots, n$. The following procedure from [3] would generate a sequence of CDSs by obtaining the same fitted NLRM equations.

3.1. Procedure for Bivariate Nonlinear Regression Model $Y = AX^B$

The simple NLRM (a geometric or power curve) $Y = AX^B$ was linearizable due to logarithmic transformation as $\tilde{Y} = a + B\tilde{X}$ where $\tilde{Y} = \ln(Y), \tilde{X} = ln(X), a = \ln(A)$,and $A = \exp(a)$. The inverse nonlinear regression model (INLRM) of $Y = AX^B$ is $= (\frac{Y}{C})^{\frac{1}{D}}$, which was also linearizable as $\tilde{X} = c + d\tilde{Y}$ where $d = \frac{1}{D}, D = \frac{1}{d}, c = -\frac{\ln(C)}{D}, C = \exp(-\frac{c}{d})$.

1. First fit regression $\tilde{Y}$ on $\tilde{X}$, namely $\tilde{Y}_1 = a + B\tilde{X}$. Also fit inverse regression (IR) $\tilde{X}$ on $\tilde{Y}$, namely $\tilde{X}_1 = c + d\tilde{Y}$.
2. The regression of $\tilde{Y}_1$ on $\tilde{X}_1$ would be $\tilde{Y}_2 = a + B\tilde{X}_1$, preserving same parameter estimates. Likewise, $\tilde{X}_2 = c + d\tilde{Y}_1$. Note that $S_{\tilde{Y}_1}^2 < S_{\tilde{Y}}^2$ and $S_{\tilde{X}_1}^2 < S_{\tilde{X}}^2$.

3. The above method can be iterated with $\tilde{Y}_2$ and $\tilde{X}_2$ as done in step 1 to gain cloning sets of data having the identical linearizable regression equation (LRE). Again $S^2_{\tilde{Y}_2} < S^2_{\tilde{Y}_1} < S^2_{\tilde{Y}}$ and $S^2_{\tilde{X}_2} < S^2_{\tilde{X}_1} < S^2_{\tilde{X}}$ and so on.

4. If preferred, transform back for CDSs, having same coefficients of NLRM. It was noted that variability in Y and X of the cloned datasets fluctuated after every iteration (see Table 2).

Example 1. Consider the variables X= (0.5, 1.5, 2.5, 5.0, 10.0)$^\mathrm{T}$ and Y= (3.4, 7.0, 12.8, 29.8, 68.2)$^\mathrm{T}$, resulting in the nonlinear regression fit

$$\hat{Y} = 5.709057 X^{1.01876} \tag{3.1}$$

Steps 1-4 given above would yield the CDSs proven in Table 2. with exactly the same equation of fitted NLRM as in (**Eq. 3.1**).

Table 2. Cloned Data Sets Having the same Non Linear Regression Fit $Y = AX^B$

	Raw data		First iteration		Second iteration	
	X	Y	X_1	Y_1	X_2	Y_2
	0.5	3.4	0.61884	2.81765	0.51656	3.50135
	1.5	7.0	1.23925	8.62897	1.51542	7.10350
	2.5	12.8	2.21417	14.52011	2.49958	12.83071
	5.0	29.8	4.99031	29.42030	4.92915	29.36222
	10.0	68.2	11.06349	59.61073	9.72023	66.07545
Mean	3.9	24.24	4.02521	22.99955	3.83619	23.77465
Variances	14.425	706.448	18.2784	516.8321	13.50223	657.32050
Correlation	-	0.99684	-	0.99803	-	0.99679
	Third iteration		Fourth iteration		Fifth iteration	
	X_3	Y_3	X_4	Y_4	X_5	Y_5
	0.63657	2.91275	0.53332	3.60356	0.65443	3.00903
	1.25687	8.71936	1.53068	7.20638	1.27437	8.80883
	2.21927	14.51765	2.49918	12.86087	2.22429	14.51524
	4.91979	28.99566	4.86072	28.93958	4.85168	28.58561
	10.73187	57.91217	9.45374	64.05832	10.41665	56.29510
Mean	3.952877	22.61152	3.77553	23.33374	3.88428	22.24276
Variances	17.04036	483.35930	12.65003	612.24240	15.9017	452.4788
Correlation	-	0.99797	-	0.99672	-	0.99791

3.2. Procedure for Bivariate Nonlinear Regression Model $Y = AB^X$

A simple nonlinear regression model (an exponential curve) $Y = AB^X$ was linearizable due to logarithmic transformation as $\tilde{Y} = a + bX$ where

$\tilde{Y} = \ln(Y), a = \ln(A), A = \exp(a), b = \ln(B),$ and $B = \exp(b)$. The inverse nonlinear regression model of $Y = AB^X$ was $X = \ln(\frac{Y}{C})^{\frac{1}{\ln(D)}}$, which was also linearizable, as $X = c + d\tilde{Y}$ where $d = \frac{1}{\ln(D)}, D = \exp(\frac{1}{d}), c = -\frac{\ln(C)}{\ln(D)}, C = \exp(-\frac{c}{d})$.

1. First fit the regression of $\tilde{Y}$ on X specifically $\tilde{Y}_1 = a + bX$. Also, fit the IR of X on $\tilde{Y}$ particularly $X_1 = c + d\tilde{Y}$.
2. The regression of $\tilde{Y}_1$ on X_1 would be $\tilde{Y}_2 = a + bX_1$, maintaing the identical parameter estimates. Similarly, $X_2 = c + d\tilde{Y}_1$. Note that $S^2_{\tilde{Y}_1} < S^2_{\tilde{Y}}$ and $S^2_{X_1} < S^2_X$.
3. The above prcedure can be iterated with $\tilde{Y}_2$ and X_2 as in step 1 to obtain CDSs having the same LRE. Again $S^2_{\tilde{Y}_2} < S^2_{\tilde{Y}_1} < S^2_{\tilde{Y}}$ and $S^2_{X_2} < S^2_{X_1} < S^2_X$ and so on.
4. If preferred, convert back to produce a sequence of CDSs, all with the same NLRM coefficients. Therefore, it was observed that variability in Y of the cloned datasets fluctuated after each and every generation (see Table 3).

Example 2. Consider the variables X= $(0, 1, 2, 3, 4, 5, 6, 7, 8)^T$ and Y= $(0.75, 1.20, 1.75, 2.50, 3.45, 4.70, 6.20, 8.25, 11.50)^T$ and resulting in the nonlinear regression fit

$$\hat{Y} = (0.8573324)(1.392474)^X \qquad (3.2)$$

Steps 1-4 described above would generate the CDSs presented by Table 3 having exactly same NLRM fitted equation as in (**Eq. 3.2**).

Table 3. Cloned Data Sets Having the same Nonlinear Regression Fit $Y = AB^X$

	Raw data		First iteration		Second iteration	
X	Y	X_1	Y_1	X_2	Y_2
0	0.75	-0.3781	0.8573	0.0235	0.7565
1	1.20	1.0332	1.1938	1.0176	1.2070
2	1.75	2.1660	1.6624	2.0118	1.7563
3	2.50	3.2370	2.3148	3.0059	2.5037
4	3.45	4.2041	3.2233	4.0000	3.4486
5	4.70	5.1325	4.4883	4.9941	4.6896
6	6.20	5.9642	6.2499	5.9882	6.1762

	Raw data		First iteration		Second iteration	
	7	8.25	6.8219	8.7028	6.9824	8.2045
	8	11.50	7.8192	12.1184	7.9765	11.4143
Mean	4	4.47778	4	4.53456	4	4.46187
Variances	7.5	12.95069	7.45591	14.67662	7.41209	12.73009
Correlation	-	0.95442	-	0.91709	-	0.95498
	Third iteration		Fourth iteration		Fifth iteration	
	X_3	Y_3	X_4	Y_4	X_5	Y_5
	-0.3524	0.8640	0.0469	0.7629	-0.3268	0.8707
	1.0506	1.2008	1.0352	1.2140	1.0679	1.2078
	2.1768	1.6688	2.0234	1.7626	2.1875	1.6753
	3.2415	2.3193	3.0117	2.5075	3.2459	2.3238
	4.2029	3.2233	4.0000	3.4473	4.2017	3.2233
	5.1258	4.4796	4.9883	4.6793	5.1192	4.4709
	5.9526	6.2256	5.9766	6.1526	5.9412	6.2016
	6.8053	8.6521	6.9648	8.1596	6.7888	8.6021
	7.7968	12.0245	7.9531	11.3298	7.7744	11.9318
Mean	4	4.51756	4	4.44617	4	4.50081
Variances	7.36852	14.41740	7.32521	12.51401	7.28215	14.16366
Correlation	-	0.91777	-	0.95553	-	0.91844

3.3. Procedure for Bivariate Nonlinear Regression Model $Y = Ae^{BX}$

The simple nonlinear regression model (an exponential curve) $Y = Ae^{BX}$ was linearizable due to logarithmic transformation as $\tilde{Y} = a + BX$, where $\tilde{Y} = \ln(Y)$, $a = \ln(A)$, and $A = \exp(a)$. The inverse nonlinear regression model of $Y = Ae^{BX}$ was $X = ln(\frac{Y}{C})^{\frac{1}{D}}$, which was also linearizable as $X = c + d\tilde{Y}$ where $d = \frac{1}{D}, D = \frac{1}{d}, c = -\frac{\ln(C)}{D}, C = \exp(-\frac{c}{d})$.

1. First fit simple LRM of $\tilde{Y}$ on X representing $\tilde{Y}_1 = a + BX$. Also, fit the simple inverse LRM of X on $\tilde{Y}$ describing as $X_1 = c + d\tilde{Y}$.
2. The regression of $\tilde{Y}_1$ on X_1 would be $\tilde{Y}_2 = a + BX_1$, saving the alike parameter estimates. In the same way, $X_2 = c + d\tilde{Y}_1$. Note that $S_{\tilde{Y}_1}^2 < S_{\tilde{Y}}^2$ and $S_{X_1}^2 < S_X^2$.
3. The approach used above can be iterated with $\tilde{Y}_2$ and X_2 as in step 1 to get CDSs with the same LRE. Again $S_{\tilde{Y}_2}^2 < S_{\tilde{Y}_1}^2 < S_{\tilde{Y}}^2$ and $S_{X_2}^2 < S_{X_1}^2 < S_X^2$ and so on.

4. If preferred, transform back to get a sequence of CDSs, all with the same NLRM coefficients. It was observed that variability in Y of the cloned datasets fluctuate after every iteration (see Table 4).

Example 3. Consider the variables X= $(0.5, 0.8, 1.4, 2.0, 2.5)^T$ and Y= $(9.1, 8.5, 7.5, 6.7, 6.1)^T$ and resulting in the nonlinear regression fit

$$\hat{Y} = 9.989049e^{-0.1991399X} \tag{3.3}$$

Here, the CDSs would be yielded as shown in Table 4, using steps 1-4 discussed earlier, to produce same equation of fitted NLRM as given in (**Eq. 3.3**).

Table 4. Cloned Data Sets Having the Same Nonlinear Regression Fit $Y = Ae^{BX}$

	Raw data		First iteration		Second iteration	
	X	Y	X_1	Y_1	X_2	Y_2
	0.5	9.1	0.46924	9.04235	0.50111	9.09792
	0.8	8.5	0.81135	8.51797	0.80076	8.49874
	1.4	7.5	1.43912	7.55866	1.40005	7.50000
	2.0	6.7	2.00487	6.70739	1.99934	6.70089
	2.5	6.1	2.47543	6.07171	2.49875	6.10149
Mean	1.44	7.58	1.44	7.57961	1.44	7.57980
Variances	0.6830	1.532	0.68219	1.51378	0.68138	1.52834
Correlation	-	-0.99617	-	-0.99976	-	-0.99618
	Third iteration		Fourth iteration		Fifth iteration	
	X_3	Y_3	X_4	Y_4	X_5	Y_5
	0.47039	9.04035	0.50222	9.09583	0.47153	9.03835
	0.81209	8.51668	0.80151	8.49748	0.81283	8.51540
	1.43912	7.55859	1.40009	7.50000	1.43912	7.55851
	2.00420	6.70827	1.99868	6.70179	2.00353	6.70916
	2.47420	6.07322	2.49749	6.10298	2.47298	6.07474
Mean	1.44	7.57942	1.44	7.57962	1.44	7.57923
Variances	0.68058	1.51018	0.67977	1.52469	0.67897	1.50657
Correlation	-	-0.99976	-	-0.99618	-	-0.99976

We have generated the cloned data sets for following nonlinear regression models $Y = \frac{1}{A+BX}$, $Y = A + \frac{B}{1+X}$, $Y = A + B\sqrt{X}$, $Y = AX^2 + BX$ and $Y = A + BX + CX^2$ by using the procedure given by [3] and presented, respectively in Table 5-9.

Table 5. Cloned Data Sets Having the Same Non Linear Regression Fit $Y = \frac{1}{A+BX}$; $A = 82.97359, B = -36.58871$

Raw data		First iteration		Second iteration	
X	Y	X_1	Y_1	X_2	Y_2
2.000	0.0615	1.225281	0.102081	1.313470	0.026218
2.000	0.0527	1.188237	0.102081	1.313470	0.025318
0.667	0.0334	1.038642	0.017074	0.648053	0.022237
0.667	0.0258	0.918315	0.017074	0.648053	0.020254
0.400	0.0138	0.458482	0.014633	0.514769	0.015106
0.400	0.0258	0.918315	0.014633	0.514769	0.020254
0.286	0.0129	0.389507	0.013791	0.457862	0.014551
0.286	0.0183	0.701590	0.013791	0.457862	0.017451
0.222	0.0083	-0.196641	0.013360	0.425914	0.011090
0.222	0.0169	0.639830	0.013360	0.425914	0.016789
0.200	0.0129	0.389507	0.013218	0.414932	0.014551
0.200	0.0087	-0.121065	0.013218	0.414932	0.011441

Third iteration		Fourth iteration		Fifth iteration	
X_3	Y_3	X_4	Y_4	X_5	Y_5
0.926740	0.028641	0.970763	0.020381	0.777712	0.021073
0.908248	0.028641	0.970763	0.020104	0.768481	0.021073
0.833572	0.016874	0.638594	0.019057	0.731203	0.016776
0.773506	0.016874	0.638594	0.018291	0.701219	0.016776
0.543963	0.015591	0.572061	0.015855	0.586634	0.016118
0.773506	0.015591	0.572061	0.018291	0.701219	0.016118
0.509531	0.015101	0.543653	0.015545	0.569446	0.015852
0.665320	0.015101	0.543653	0.017056	0.647214	0.015852
0.216933	0.014839	0.527705	0.013327	0.423385	0.015707
0.634490	0.014839	0.527705	0.016734	0.631824	0.015707
0.509531	0.014751	0.522223	0.015545	0.569446	0.015658
0.254660	0.014751	0.522223	0.013577	0.442217	0.015658

Table 6. Cloned Data Sets Having the Same Non Linear Regression Fit $Y = A + \frac{B}{1+X}$; $A = 0.086506, B = -0.091625$

Raw data		First iteration		Second iteration	
X	Y	X_1	Y_1	X_2	Y_2
2.000	0.0615	2.332049	0.055964	1.805105	0.059008

Raw data		First iteration		Second iteration	
X	Y	X_1	Y_1	X_2	Y_2
2.000	0.0527	1.565860	0.055964	1.805105	0.050796
0.667	0.0334	0.705670	0.031542	0.652333	0.032788
0.667	0.0258	0.506758	0.031542	0.652333	0.025696
0.400	0.0138	0.272456	0.021059	0.404582	0.014499
0.400	0.0258	0.506758	0.021059	0.404582	0.025696
0.286	0.0129	0.257787	0.015258	0.296953	0.013659
0.286	0.0183	0.351251	0.015258	0.296953	0.018698
0.222	0.0083	0.187800	0.011526	0.236035	0.009367
0.222	0.0169	0.325711	0.011526	0.236035	0.017392
0.200	0.0129	0.257787	0.010151	0.215011	0.013659
0.200	0.0087	0.193575	0.010151	0.215011	0.009740
Third iteration		Fourth iteration		Fifth iteration	
X_3	Y_3	X_4	Y_4	X_5	Y_5
2.072216	0.053842	1.644782	0.056682	1.863838	0.051862
1.444278	0.053842	1.644782	0.049020	1.340783	0.051862
0.687722	0.031054	0.638878	0.032217	0.671312	0.030599
0.504364	0.031054	0.638878	0.025600	0.502137	0.030599
0.284091	0.021273	0.408885	0.015152	0.295141	0.021472
0.504364	0.021273	0.408885	0.025600	0.502137	0.021472
0.270142	0.015859	0.307342	0.014368	0.281892	0.016421
0.358695	0.015859	0.307342	0.019070	0.365715	0.016421
0.203334	0.012377	0.249424	0.010363	0.218200	0.013172
0.334572	0.012377	0.249424	0.017851	0.342948	0.013172
0.270142	0.011095	0.229361	0.014368	0.281892	0.011975
0.208864	0.011095	0.229361	0.010711	0.223486	0.011975

Table 7. Cloned Data Sets Having the Same Non Linear Regression Fit $Y = A + B\sqrt{X}$; $A = -2.341445, B = 3.011197$

Raw data		First iteration		Second iteration	
X	Y	X_1	Y_1	X_2	Y_2
1.0	1.1	1.389823	0.669752	1.099958	1.208477
1.5	1.3	1.536094	1.346503	1.571153	1.390611
2.0	1.6	1.769221	1.917031	2.033473	1.663810
2.5	2.0	2.105666	2.419675	2.490122	2.028076
3.0	2.7	2.764870	2.874101	2.942743	2.665542

Raw data		First iteration		Second iteration	
X	Y	X_1	Y_1	X_2	Y_2
3.5	3.4	3.513706	3.291989	3.392311	3.303008
4.0	4.1	4.352175	3.680949	3.839463	3.940474
Third iteration		Fourth iteration		Fifth iteration	
X_3	Y_3	X_4	Y_4	X_5	Y_5
1.468250	0.816665	1.195129	1.307264	1.541545	0.950454
1.604771	1.432959	1.637384	1.473126	1.668620	1.511692
1.820930	1.952519	2.064198	1.721920	1.868668	1.984837
2.130380	2.410261	2.481144	2.053645	2.153013	2.401687
2.730323	2.824090	2.891081	2.634163	2.699051	2.778547
3.404599	3.204646	3.295707	3.214682	3.306735	3.125107
4.153208	3.558859	3.696127	3.795200	3.976065	3.447676

Table 8. Cloned Data Sets Having the Same Non Linear Regression Fit $Y = AX^2 + BX; A = 0.4, B = 5.0$

Raw data		First iteration		Second iteration	
X	Y	X_1	Y_1	X_2	Y_2
0	1	0.1933	0.0000	0.0000	1.0107
1	5	0.9156	5.4708	0.9989	5.0388
2	12	2.0321	11.7428	1.9970	12.0451
3	20	3.1495	18.8161	2.9944	20.0064
4	25	3.7859	26.6907	3.9914	24.9641
5	36	5.0621	35.3665	4.9881	35.8353
Third iteration		Fourth iteration		Fifth iteration	
X_3	Y_3	X_4	Y_4	X_5	Y_5
0.1932	0.0000	0.0000	1.0211	0.1931	0.0000
0.9148	5.5123	0.9980	5.0763	0.9140	5.5523
2.0291	11.7893	1.9941	12.0884	2.0263	11.8338
3.1436	18.8311	2.9889	20.0114	3.1377	18.8445
3.7780	26.6377	3.9829	24.9279	3.7701	26.5848
5.0499	35.2093	4.9762	35.6734	5.0376	35.0546

Table 9. Cloned Data Sets Having the Same Non Linear Regression Fit $Y = A + BX + CX^2; A = 1.0, B = -0.20, C = 0.20$

Raw data		First iteration		Second iteration	
X	Y	X_1	Y_1	X_2	Y_2
1.0	1.1	0.99760	1.08571	0.99972	1.09900

1.5	1.3	1.52005	1.29286	1.50226	1.30180
2.0	1.6	1.98929	1.62143	2.00206	1.60299
2.5	2.0	2.44462	2.07143	2.50109	2.00294
3.0	2.7	3.05159	2.64286	2.99979	2.70103
3.5	3.4	3.53894	3.33571	3.49833	3.39798
4.0	4.1	3.95791	4.15000	3.99676	4.09427
Third iteration		Fourth iteration		Fifth iteration	
X_3	Y_3	X_4	Y_4	X_5	Y_5
0.99730	1.08491	0.99945	1.09800	0.99700	1.08412
1.52239	1.29459	1.50450	1.30362	1.52472	1.29631
1.99134	1.62433	2.00410	1.60599	1.99338	1.62719
2.44578	2.07414	2.50217	2.00589	2.44694	2.07680
3.05120	2.64404	2.99959	2.70207	3.05081	2.64518
3.53715	3.33401	3.49667	3.39597	3.53537	3.33230
3.95486	4.14408	3.99355	4.08856	3.95181	4.13819

4. CLONING FOR MULTIPLE NONLINEAR REGRESSION MODEL $Y = A_0(X_i^{(1)})^{A_1}(X_i^{(2)})^{A_2}$ VIA PIVOTS

In accordance with [4], the current approach was extended to a structure of an arbitrary error covariance after discussing data that were independent and identically distributed (iid). Let us give the multiple NLRM in (**Eq. 4.1**).

$$Y_i = A_0(X_i^{(1)})^{A_1}(X_i^{(2)})^{A_2} E_i \tag{4.1}$$

Where Y is response vector, $X = (X^{(1)} : X^{(2)})$ is the covariate data matrix (CDM), $\alpha = (A_0, A_1, A_2)^T$ is parameters vector, and E random error vector.

Eq. 4.1 is linearizable due to logarithmic transfomation, then **Eq. 4.1** becomes $\ln(Y_i) = \ln(A_0) + A_1 \ln(X_i^{(1)}) + A_2 \ln(X_i^{(2)}) + \tilde{E}$. Setting $\tilde{Y} = \ln(Y_i)$, $\tilde{X}^{(1)} = \ln(X_i^{(1)})$, $\tilde{X}^{(2)} = \ln(X_i^{(2)})$, $\tilde{E} = \ln(E_i)$, $B_0 = \ln(A_0)$, $B_1 = A_1$ and $B_2 = A_2$ we get

$$\tilde{Y} = B_0 + B_1 \tilde{X}^{(1)} + B_2 \tilde{X}^{(2)} + \tilde{E} \tag{4.2}$$

where $\tilde{Y}$ is response vector, $\tilde{X} = (\tilde{X}^{(1)} : \tilde{X}^{(2)})$ is CDM, $\beta = (B_0, B_1, B_2)^T$ is unknown parameters vector and $\tilde{E}$ errors vector. When matrix $\tilde{X}$ of rank full as column, estimates of β by ordinary least square (OLS) is $b = (\tilde{X}^t \tilde{X})^{-1} \tilde{X}^t \tilde{Y}$, and fitted multiple LRE is

$$\tilde{Y}_1 = b_0 + b_1 \tilde{X}^{(1)} + b_2 \tilde{X}^{(2)} \qquad (4.3)$$

These consequences follow whether or not $\tilde{Y}$, $\tilde{X}^{(1)}$, and $\tilde{X}^{(2)}$ are mean corrected (MCtD), as here. Due to the MCtD, (**Eq. 4.3**), which can be written as:

$$\hat{y} = b_1 x_1 + b_2 x_2 \qquad (4.4)$$

where $\hat{y} = \tilde{Y} - \bar{\tilde{Y}}$, $x_1 = \tilde{X}^{(1)} - \bar{\tilde{X}}^{(1)}$ and $x_2 = \tilde{X}^{(2)} - \bar{\tilde{X}}^{(2)}$ (In order to avoid any loss of generality, the column of 1 in design matrix X is eliminated following the imply MCtD because it transforms into a column of zeros).

The identified problem here was to create a new response variable vector, Y_{clone}, and a new covariate data matrix, X_{clone}. This can be easily accomplished by transposing back to $\tilde{Y}_{clone}$ and $\tilde{X}_{clone}$, such that

$$b = (\tilde{X}_{clone}^t \tilde{X}_{clone})^{-1} \tilde{X}_{clone}^t \tilde{Y}_{clone}$$

Alternatively, multivariate CDSs to be required $(Y_{clone}, X_{clone}^{(1)}, X_{clone}^{(2)})$ which produced the same multiple NLRM equation as the original dataset $(Y, X^{(1)}, X^{(2)})$.

Returning to the case of iid, how generation of CDSs can be accomplished via manipulating any one covariate, was exhibited, say x_j, where $j = 1,2.$, using the steps below.

1) Iniatially, fit multiple linearizable RM (**Eq. 4.4**), using MCtD data.

2) Select a covariate x_2.

3) Let $\hat{y} = k + b_2 x_2$, where $k = b_1 x_1 = \hat{y} - b_2 x_2$. To obtain the estimated values of $\hat{y}_k$ and $\hat{x}_2$, perform simple RM of $y_k = y - k$ on x_2 and inverse simple regression of x_2 on y_k.

4) Regress x_1 on x_2 and obtain $\hat{x}_1$. Also, obtain $x_{1,2} = x_1 - x_2(x_2^t x_2)^{-1} x_2^t x_1 = (I - x_2(x_2^t x_2)^{-1} x_2^t) x_1$, where I is the identity matrix.

5) Form $y_{k,clone} = \hat{y}_k + \sum b_1 x_{1,2}$.

6) On all newly acquired $x_{1,2}$ and $\hat{x}_2$, perform multiple LREs of $y_{k,clone}$ at the same time, where $\hat{x}_2 = y(y^t y)^{-1} y^t x_2$ in which $y = (1:\hat{y})$ is $n \times 2$.

7) If you prefer, you can add back $\bar{\bar{Y}}$, $\bar{\bar{X}}^{(1)}$, and $\bar{\bar{X}}^{(2)}$ to the cloned data or multiply all of the cloned data by the same scale factor.

8) Transform back to the cloned data in step 7.

9) Repeat from one to eight steps to create a series of datasets with identical NLRM coefficients. At each iteration, a different possible value of j can be chosen.

Example 4. With uncorrelated data and design matrix of full-rank, consider variables X_1, X_2 and Y in Table 9 and resulting in the multiple NLRM fit

$$\hat{Y} = 1.663079 X_1^{0.6163121} X_2^{0.2931787} \tag{4.5}$$

For CDSs in Table 10, 1-9 steps specified above were used (first X_2 was used for manipulation) for which the fitted multiple NLRM equation was exactly the same as in (**Eq. 4.5**).

Table 10. Cloned Data Sets Having the Same Multiple Nonlinear Regression Fit $Y = A_0 X_1^{A_1} X_2^{A_2}$

X_1	X_2	Y	$X_{1,clone}$	$X_{2,clone}$	Y_{clone}
23.81	11.33	22.76	25.583	10.257	24.988
75.83	25.92	76.73	37.324	35.179	40.197
9.46	7.03	8.62	15.945	3.818	16.234
5.71	29.68	10.98	2.473	14.871	7.852
85.78	21.81	86.77	49.689	39.486	45.583
0.37	0.57	0.97	6.672	2.411	4.543
8.82	11.25	11.82	9.540	9.225	13.577
8.99	19.01	16.63	5.928	20.744	11.810
37.65	75.25	67.40	6.780	73.887	19.203
8.43	8.40	8.81	12.012	4.796	14.364
16.10	30.30	21.54	6.839	16.206	14.786
0.64	1.20	1.34	5.718	2.327	5.138
5.28	6.93	12.38	9.021	22.489	11.379
30.40	70.18	58.37	5.847	71.736	17.173
33.66	21.06	29.90	20.152	11.872	25.870
15.72	11.86	14.54	16.178	6.394	19.093
8.44	14.53	17.54	7.172	26.020	12.274
30.20	34.20	29.43	11.444	13.458	21.041
8.89	8.68	11.41	12.282	8.357	14.702

X_1	X_2	Y	$X_{1,clone}$	$X_{2,clone}$	Y_{clone}
5.14	2.84	5.45	20.372	3.117	14.474

Figure 2, represent a matrix plot of raw and cloning data in Table 10, which show the effect on X_2 done by orthogonal manipulation as described in steps 1-9 of the algorithm. Bivariate relationship strength between $X_{2,clone}$ and Y_{clone} is much weaker than X_2 and Y. However, this is not the case with $X_{1,clone}$ and Y_{clone} , because the manipulation was not done with X_1.

Matrix plot of raw data (X_1, X_2, Y) and cloned data (X_{1clone}, X_{2clone}, Y_{clone})
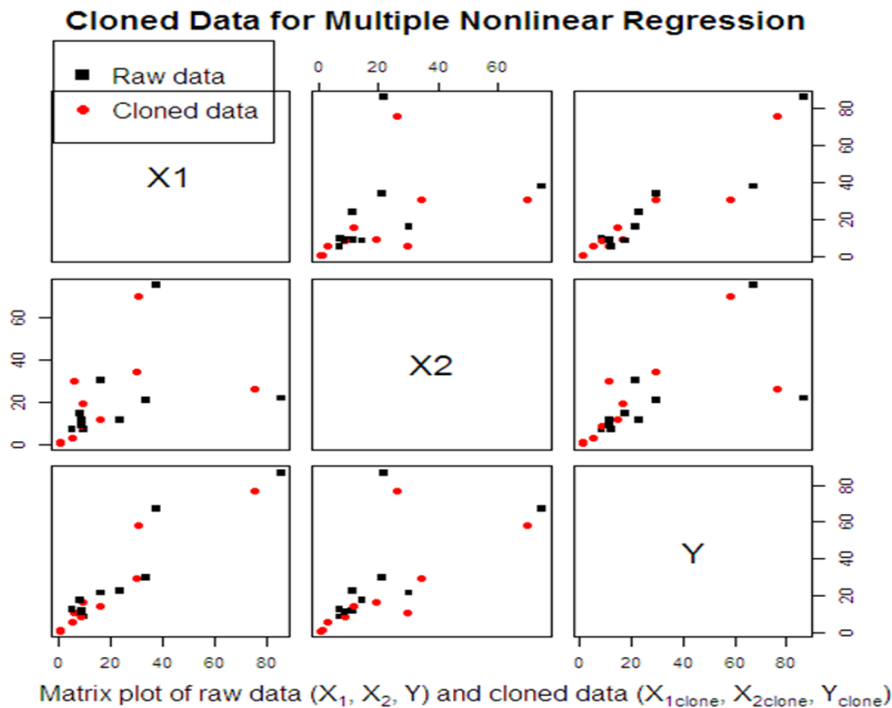
Figure 2. Matrix Plot of raw and cloned data

5. DISCUSSION

This study showed that the parameter estimates of the original datasets discussed in this artical and their generated cloned datasets were identical. As a result, it was identified that data cloning had the potential to be used in a wide range of applications, including data encryption, visualization, and smoothing. The application of encryption was   particularly intriguing because it can be used to generalize the databases even when regression modeling was not desired. In prior literature, cloned datasets were

generated for linear regression models. However, it had equal importance to be generated for the nonlinear regression models. In this context, new methods can be developed for nonlinear regression models to conduct cloning for the datasets or databases.

5.1. Conclusion

CDSs have been presented for bivariate and multivariate NLRMs that have linearizable regression functions including $AX^B, AB^X, Ae^{BX}, \frac{1}{A+BX}, A + \frac{B}{1+X}, A + B\sqrt{X}, AX^2 + BX, A + BX + CX^2$ and $A_0(X_i^{(1)})^{A_1}(X_i^{(2)})^{A_2}$ with exactly the same nonlinear regression coefficients. In terms of bivariate LRFs, the response and a covariate of the CDSs collapsed to their means, which had smaller variability when compared to the original dataset.

REFERENCES

1. Anscombe FJ. Graphs in statistical analysis. *Am Statistic*. 1973;27(1):17–21.

2. Chatterjee S, Firat A. Generating data with identical statistics but dissimilar graphics: A follow up to the Anscombe dataset. *Am Stat*. 2007;61(3):248–254. https://doi.org/10.1198/000313007X220057

3. Govindaraju K, Haslett SJ. Illustration of regression towards the mean. *Int J Matim Edu Sci Technol*. 2008;39(4):544–550. https://doi.org/10.1080/00207390701753788

4. Haslett SJ, Govindaraju K. Cloning data: Generating datasets with exactly the same multiple linear regression fit. *Aust New Zealand J Stat*. 2009;51(4):499–503. https://doi.org/10.1111/j.1467-842X.2009.00560.x

5. Lele SR, Dennis B, Lutscher F. Data Cloning: Easy maximum likelihood estimation for complex ecological models using bayesian markov chian monte carlo methods. *Ecol Lett*. 2007;10:551–563. https://doi.org/10.1111/j.1461-0248.2007.01047.x

6. Lele SR, Nadeem K, Schmuland B. Estimability and likelihood inference for generalized linear mixed models using data cloning. *J Am Stat Assoc*. 2010;105:1617–1625. https://doi.org/10.1198/jasa.2010.tm09757

7. Jacquier E, Johannes M, Polson N. MCMC Maximum likelihood for latent state models. *J Econom*. 2007;137:615–640. https://doi.org/10.1016/j.jeconom.2005.11.017

8. Fung BCM, Wang K, Chen R, Yu PS. Privacy-preserving data publishing: A survey of recent developments. *ACM Comput Surv*. 2010;42(4):e14. https://doi.org/10.1145/1749603.1749605

9. Haslett SJ, Govindaraju K. Data cloning: Data visualization, smoothing, confidentiality, and encryption. *J Stat Plan Infer*. 2012;142:410–422. https://doi.org/10.1016/j.jspi.2011.07.020

10. Ponciano JM, Burleigh JG, Braun EL, Taper ML. Assessing parameter identifiability in phylogenetic models using data cloning. *Syst Biol*. 2012;61(6):955–972. https://doi.org/10.1093/sysbio/sys055

11. Amvrosiadis G, Bhadkamkar M. Identifying trends in enterprisedata protection systems. Paper presented at: USENIX Annual Technical Conference; July 8–10, 2015; Santa Clara, USA.

12. Download the Datasaurus: Never trust summary statistics alone; always visualize your data. Cairo website. http://www.thefunctionalart.com/2016/08/downloaddatasaurus-never-trust-summary.html

13. Matejka J, Fitzmaurice G. Same stats, different graphs: Generating datasets with varied appearance and identical statistics through simulated annealing. Paper presented at: Proceedings of the 2017 CHI Conference on Human Factors in Computing Systems; May 6–11, 2017; Denver Colorado, USA. https://doi.org/10.1145/3025453.3025912

14. Mao X, Ruiz E, Veiga H. Threshold stochastic volatility: Properties and forecasting. *Int J Forec*, 2017;33(4):1105–1123. https://doi.org/10.1016/j.ijforecast.2017.07.001

15. Mao X, Ruiz E, Veiga H, Czellar V. Asymmetric stochastic volatility models: Properties and particle filter-based simulated maximum likelihood estimation. *Econom Stat*. 2020;13:84–105. https://doi.org/10.1016/j.ecosta.2019.08.002

16. Hussain S, Daniyal M, Ogundokun RO, Muhammad YS, Iqbal Z, Ahmed, R. Cloning data with unchanged estimates of estimable non-

linear functions of parameters. *F1000Research*. 2022;10:e106. https://doi.org/10.12688/f1000research.28297.2

Article QR

Title:	**Rising Arsenic Level in Drinking Water: A Study of Schools and Local Areas of Multan, Pakistan**
Author (s):	Muhammad Zohaib Zulfiqar[1], Faiza Rao[1,2], Anam Rao[3], Syeda Fizza Raza Zaidi[1]
Affiliation (s):	[1]University of Central Punjab Lahore, Pakistan. [2]Xiamen University, Xiamen, Fujian 361102, China. [3]Center to Advance Level Research and Development (SMC-Pvt) Ltd Multan, Pakistan.
DOI:	https://doi.org/10.32350/sir.73.02
History:	Received: June 20, 2022, Revised: March 22, 2023, Accepted: March 25, 2023, Published: August 28, 2023.
Citation:	Zulfiqar MZ, Rao F, Rao A, Zaidi SFR. Rising arsenic level in drinking water: A study of schools and local areas of Multan, Pakistan. *Sci Inq Rev.* 2023;7(3):22–31. https://doi.org/10.32350/sir.73.02
Copyright:	© The Authors
Licensing:	This article is open access and is distributed under the terms of Creative Commons Attribution 4.0 International License
Conflict of Interest:	Author(s) declared no conflict of interest

Rising Arsenic Level in Drinking Water: A Study of Schools and Local Areas of Multan, Pakistan

Muhammad Zohaib Zulfiqar[1], Faiza Rao[1,2*], Anam Rao[3], and Syeda Fizza Raza Zaidi[1]

[1]Department of Zoology, University of Central Punjab, Lahore, Pakistan
[2]Fujian Provincial Key Laboratory of Reproductive Health Research, School of Medicine, Xiamen University, China
[3]Center to Advance Level Research and Development (SMC-Pvt) Ltd Multan, Pakistan

ABSTRACT

Water is the basic need for the survival of all living organisms; however, its contamination has caused disastrous effects on human health. Almost 80% of the total population in Pakistan is forced to use unsafe drinking water due to the scarcity of clean water sources. To assess, the risk involved and to monitor the amount of Arsenic and bacterial growth in drinking water, water samples were collected from different government schools and underdeveloped areas of Multan, Pakistan. Moreover, water samples were collected by randomly visiting areas and were sent for laboratory analysis to determine and detect the arsenic amount along with other parameters including aesthetic, physical, chemical, and bacteriological growth. The results indicated that all the data collected from Govt. schools and developed locality were having a large amount of arsenic in drinking water. A huge amount of Coliform growth was found in the Peer colony water, which indicated a highly unhealthy intensity of pollutant water for the population residing in this area. Therefore, urgent and regular monitoring of drinking water in Multan was required to prevent such contamination.

Keywords: arsenic, coliform, health risk, water pollution, water scarcity

1. INTRODUCTION

Water holds the second most significant position after oxygen, which is essentially important for human survival. Therefore, water is an essential component of life not only for human beings but for all living organisms. In some living organisms, approximately 90% of the body weight consists of water. The majority of the world's population is suffering from water

---

*Corresponding Author: rao.faiza@yahoo.com

scarcity, due to unsafe and unsuitable water consumption, which has been regarded as a fundamental right for nations. As indicated in a study, the heart and brain mainly comprise almost 73% of water, whereas 83% of water is found in the lungs. Water plays a vital role in our body by maintaining the body temperature, functions as a shock absorber for sensitive parts of the body like the brain and spinal cord, which aids in the growth of body cells, forms saliva that helps in digestion, and maintains the moisture in the mucosal membrane. Various human activities have caused impurity and toxicity in water, which has resulted in water contamination, which is a leading health problem nowadays. Harmful metals, such as arsenic, iron, and cobalt are easily and excessively found in water. These metals have affected different organs of the body, such as kidney dysfunction, cancer, nervous system disorder, skin lesions, and immune and gastrointestinal disorders. According to a case study, almost five million children have lost their life because they were subjected to bad water consumption and toxic water intake [1].

In many areas, fecal matter is mixed with water due to poor sanitation systems and leakage of pipes in poorly developed areas. This contamination may worsen health problems, which may lead to serious health problems [2]. Different pathogenic bacteria are found in drinking water such as *Shigella sonnei*, *Salmonella enterica*, and other bacteria. These bacteria were chiefly disseminated by fecal excretion [3]. Coliform bacterium was found in the feces of warm-blooded animals, which cause severe disease when exposed to water [4].

However, Pakistan has faced water toxicity issues due to its poor sanitation systems. In some areas, these detrimental chemicals and pathogens have caused major health problems by putting massive people's life at stake. According to WHO and UNICEF, approximately 1.1 billion people worldwide are suffering due to the nonexistence of pure drinking water [5]. Many other water-borne diseases like hepatitis, diarrhea, and cryptosporidium are increasing rapidly due to the flawed sanitary system. As per Child Rights International Network, nearly 250,000 children have faced a high death rate, due to the high impurity and toxicity of drinking water [6]. In industrial areas of Pakistan, water gets contaminated when exposed to injurious chemicals. Furthermore, it was also identified that in underdeveloped areas of Pakistan, when drinking water is mixed with sewage water it caused many health issues even leading to death [7]. The

quantity of arsenic found in drinking water was quite high in secondary schools of Vehari (mostly ranging between 12.9µg/L-19.5µg/L), which predominantly affected the health of students [8]. Highly populated cities like Karachi, Lahore, Rawalpindi, and others face severe drinking water pollution due to human activities, rendering it unsuitable for consumption [9].

Many developing countries like Pakistan are facing the common issue of water scarcity. Pakistan has ranked as the 7th country, which faces water pollution and water scarcity problem. Exterior as well as interior water is contaminated with arsenic. Arsenic is a carcinogen that causes cancer [10]. Chlorination is an effective method to extract toxic chemicals and microbes from the water, making it suitable for drinking [11].

2. MATERIALS AND METHODS

The current study was conducted in different government schools and some local underdeveloped areas of Multan like Mumtazabad, Peer Colony, Chungi no. 8, Northern Bypass, and Ghanta Ghar Multan, to find out the amount of arsenic in the drinking water. The Environmental Protection Agency (EPA) has set the standard for arsenic in drinking water to be 10 micrograms per liter. This study considered all the physical, bacteriological, synthetic, and aesthetic analysis reports issued by the water quality laboratory in Multan to conduct further analysis.

2.1. Sample Collection

For this purpose, the researcher randomly visited government schools and collected water samples from the cooler, electric cooler, drinking water bottles, water fountains, and taps. Sterile 250mL plastic bottles were used for the sampling purpose. During collection of samples gloves were used by the collector. The bottles were filled up to 240mL leaving the headspace of the bottle, capped the bottles immediately, and delivered to the lab on the same day of their collection.

2.2. Bacterial Detection

For the detection of total coliform, fecal coliform, and E. coli petri, petrifilm calculation plates were used. Place Petrifilm EL plate on a leveled surface and lift the top to place 1ml of sample onto the center of the bottom film. Now release the top film and allow it to drop. Place the spreader on top of the film and gently apply pressure to distribute it evenly. Lift the

spreader and wait for one minute for the gel to solidify. Now incubate the petri film count plates on the clear side up at a temperature of 30°C for almost 48 hours. In, the end the bacterial colonies growing on petrifilm were identified with a magnifier.

2.3. Arsenic Test

Arsenic was analyzed in the drinking water samples by using a hydride generation atomic absorption spectrometer (HG-AAS). All samples were tested thrice for better results.

3. RESULTS AND DISCUSSION

Drinking water samples from different schools identified a high level of arsenic (15µg/l-75µg/l). None of the selected schools' arsenic level in drinking water was normal. The graph given below presented a level of arsenic in school water available for school children.
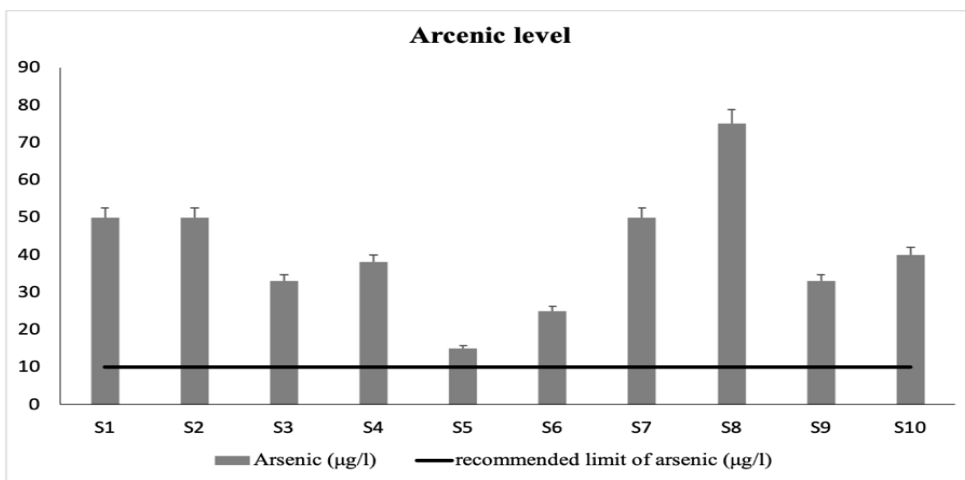
Figure 1. Arsenic Level in Drinking Water of Different Schools

The first step was to collect samples from different schools located in different areas of Multan. The above graph presents the level of arsenic in different schools. The schools are presented with symbols and numbers from S1-S10. According to the results sample collected from S5 indicated arsenic 15µg/l, which is the lowest value as compared to other samples collected, however, they were still unsafe to drink. The highest value of arsenic was evaluated in S8 School with 70µg/l. These values of arsenic

were also informed in schools and later schools set up filter water for children.

A direct link between drinking water and health was noticed in the samples. The consumption of arsenic in drinking water can lead to various problems like skin diseases, stomach diseases, and cancers. Also, in order to check the concentration of arsenic in water, its distribution was also analyzed across different locations in Multan City.
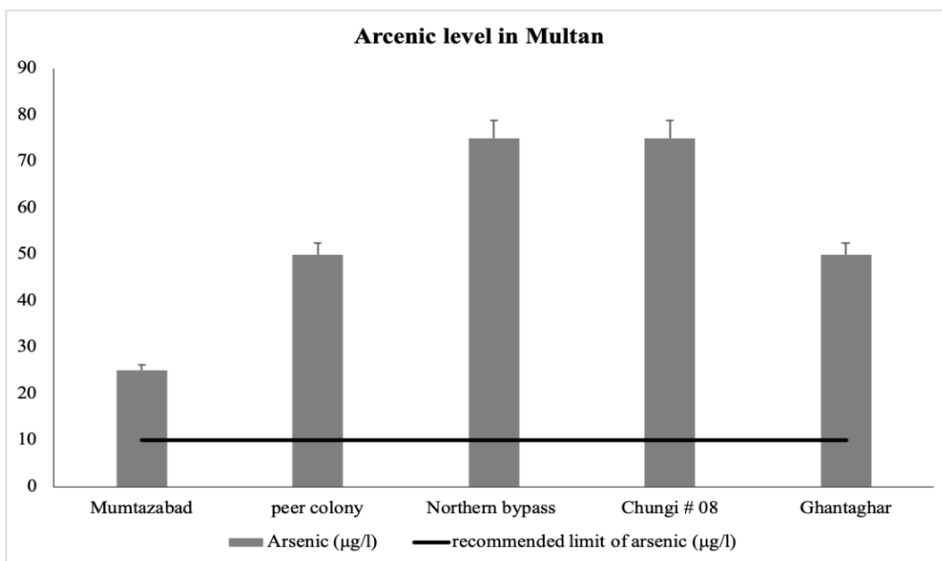
Figure 2. Arsenic Data in Drinking Water of Different Locations in Multan

The above graph presents arsenic values tested from the water samples collected from different areas of the Multan, Pakistan. These areas were selected randomly. The lowest level of arsenic found in selected areas was Mumtazabad with 25µg/l and highest value in areas Northern Bypass and Chungi no.8 with 75µg/l. However, even the lowest value found in Mumtazabad water was still high to consume. The other two areas Ghanta Ghar and Peer colony both were found with 50µg/l arsenic in drinking water. The presence of arsenic in these areas can be due to high amount present in the ground water plus the rusting of pipes and the contamination of water due to high industrialization in these areas. A small survey was also conducted related to different skin, eyes, kidney, stomach, and other diseases in order to recognize conditions of people using this water. This

area according to our small survey indicated people with skin, stomach diseases, and eyes issues each house. Although detail planning and data collection is required to find the complete detail of types of skin, stomach, and eyes diseases related to arsenic in water. All the data collected was depicted in the graphs to determine the purity of water. In drinking water supplies, arsenic is a significant problem because of its toxicity. In this research, the aesthetic, physical, chemical, and bacteriological analysis reports were incorporated, which were issued by the water laboratory, Multan, Pakistan.

According to previous research, arsenic was calculated (0->50µg/l) in 2005 Multan City, while [12] the updated data of 2022 presented the maximum value calculated of arsenic in the Multan, which is 75µg/l. There are limitations applied here but still it gave us an idea about the increase of arsenic level in the city water from 2005-2022, which is an alarming situation.

There is another issue of bacterial colonies in the drinking water. Various samples from different areas of Multan for *E. coli* and Coliform bacterial colonies were tested. None of the water was found with disease causing bacteria except Peer colony water. The petri film was observed very carefully and was found with colonies of total coliform. Five colonies were found countable, while others were not in range of counting due to the presence on gridline and out of the circle. The coliform bacteria present in the water sample of Peer colony was further evaluated for the presence of fecal coliform. Peer colony was found with 2 colonies of fecal coliform. These results were evaluated thrice and calculated as per ml of sample and the presented colony numbers are the mean of all results. The results presented in Table 1 indicates absence of *E. coli* and presence of coliform bacteria with specifically indication of some colonies of fecal coliform bacteria. Such type of bacteria was hazardous for human health. This presence opens a new research study to be setup in Peer colony. The presence of total coliform and fecal coliform bacteria in water indicated risk of contracting a water borne illness increase in this area. There are other publications which have presented a high percentage of arsenic in Multan but no specific areas were mentioned that can be compared with future studies [13]. In parallel, another ongoing study sheds light on arsenic levels, underscoring groundwater contamination and echoing our findings of elevated concentrations. Together, these revelations emphasize an

immediate call for proactive mitigation strategies to address arsenic contamination in Sindh's water sources. Elevated levels, influenced by natural processes and human activities, exceed WHO limits, necessitating urgent action to mitigate health risks and ensure the safety of the water supply [14, 15].

Table 1. Identification of Bacterial Colonies in the Water of Peer Colony Houses (Per Sample)

Sr No.	Water Quality Parameters	Heights Desirable Level	Result
1	Total Coliform	0/100 ml (PSQCA)	5
2	Fecal Coliform	0/100 ml (PSQCA)	2
3	E. coli	Negative	Negative

A prior study conducted on the localized areas of Multan presented no signs of coliform bacteria, however, this study found the presence of total coliform and fecal coliform in Multan city from every one out of five areas of the collected samples. This difference can be due to the area selection or it can be due to clean water present in 2005. After the positive result of peer colony bacterial contamination, there should be a selection of many more areas to confirm other species and chemicals present in the water.

3.1. Conclusion

The current study identified that in many cases, groundwater was found to be polluted with high amounts of arsenic, which has caused major health issues, especially in young children and adults. Notably, if groundwater is recharged directly from the land surface, which has a historical association with industrial usage or the disposal waste, there exists a significant risk of high arsenic concentrations in the groundwater. For this purpose, new technologies for purification should be developed to achieve high quality drinking water to avoid any future health disasters and exposure due to the toxic elements present in the drinking water. Hence, it was identified that Multan water still requires an extensive study with large study samples to cover major external and internal factors in order to find specific areas where arsenic level is high, which should be considered serious for health issues.

REFERENCES

1. Haydar S, Arshad M, Aziz JA. Evaluation of drinking water quality in urban areas of Pakistan: A case study of southern Lahore. *Pak J Eng Appl Sci*. 2009;5:16–23.

2. Daud MK, Nafees M, Ali S, et al. Drinking water quality status and contamination in Pakistan. *BioMed. Res Int.* 2017;2017:e7908183. https://doi.org/10.1155/2017/7908183

3. Nazeer S, Hashmi MZ, Malik RN. Heavy metals distribution, risk assessment and water quality characterization by water quality index of the River Soan, Pakistan. *Ecol Indicat*. 2014;43:262–270. https://doi.org/10.1016/J.ECOLIND.2014.03.010

4. Nabeela F, Azizullah A, Bibi R, et al. Microbial contamination of drinking water in Pakistan--a review. *Environ Sci Pollut Res Int*. 2014;21(24):13929–13942. https://doi.org/10.1007/s11356-014-3348-z

5. Meeting the MDG drinking water and sanitation target: A mid-term assessment of progress. World Health Organization; 2004. https://apps.who.int/iris/bitstream/handle/10665/43021/9241562781.pdf?sequence=1&isAllowed=y

6. Pakistan: Unsafe water kills 250,000 children annually. Child Rights International Network Web site. https://archive.crin.org/en/library/news-archive/pakistan-unsafe-water-kills-250000-children-annually.html. Updated April 19, 2011. Accessed December 31, 2022.

7. Arain MB, Ullah I, Niaz A, et al. Evaluation of water quality parameters in drinking water of district Bannu, Pakistan: Multivariate study. *Sustain Water Qual Ecol*. 2014;3-4:114–123. https://doi.org/10.1016/j.swaqe.2014.12.005

8. Murtaza B, Nazeer H, Natasha, et al. Hydrogeochemical investigation of arsenic in drinking water of schools and age dependent risk assessment in Vehari District, Punjab Pakistan: A multivariate analysis. *Environ Sci Pollut Res*. 2020;27(24):30530–30541. https://doi.org/10.1007/s11356-020-09334-7

9. Bhutta MN, Chaudhry MR, Chaudhry AH, Yasmin N. Groundwater quality and availability in Pakistan. Seminar on Strategies to Address

the Present and Future Water Quality Issues; 6–7, 2002; Islamabad, Pakistan. https://inis.iaea.org/search/searchsinglerecord.aspx?recordsFor=SingleRecord&RN=36058280

10. Nawaz S, Ali Y. Factors affecting the performance of water treatment plants in Pakistan. *Water Conserv Sci Eng*. 2018;3(3):191–203. https://doi.org/10.1007/s41101-018-0051-9

11. Khanoranga, Khalid S. An assessment of groundwater quality for irrigation and drinking purposes around brick kilns in three districts of Balochistan province, Pakistan, through water quality index and multivariate statistical approaches. *J Geochem Explor*. 2019;197:14–26. https://doi.org/10.1016/j.gexplo.2018.11.007

12. Aziz JA. Management of source and drinking-water quality in Pakistan. *East Mediterr Health J*. 2005;11(5-6):1087–1098.

13. Gul M, Mashhadi AF, Iqbal Z, Qureshi TI. Monitoring of arsenic in drinking water of high schools and assessment of carcinogenic health risk in Multan, Pakistan. *Human Ecol Risk Assess*. 2020;26(8):2129–2141. https://doi.org/10.1080/10807039.2019.1653167

14. Ali W, Aslam MW, Feng C, et al. Unraveling prevalence and public health risks of arsenic, uranium and co-occurring trace metals in groundwater along riverine ecosystem in Sindh and Punjab, Pakistan. *Environ Geochem Health*. 2019;14:2223–2238. https://doi.org/10.1007/s10653-019-00278-7

15. Asfandyar S, Shihua Q, Zaheer M. Arsenic contamination, subsequent water toxicity, and associated public health risks in the lower Indus plain, Sindh province, Pakistan. *Environ Sci Pollut Res Int*. 2019;26(30):30642–30662. https://doi.org/10.1007/s11356-018-2320-8

Article QR

Title:	**Exploring Breast Cancer Texture Analysis through Multilayer Neural Networks**
Author (s):	Aalia Nazir[1], Hafeez Ullah[1], Ghulam Gilanie[1], Shabbir Ahmad[1], Zahida Batool[1], Asghar Gadhi[2]
Affiliation (s):	[1]The Islamia University of Bahawalpur, Pakistan [2]Bahawalpur Institute of Nuclear Medicine, Bahawalpur
DOI:	https://doi.org/10.32350/sir.73.03
History:	Received: February 23, 2023, Revised: June 2, 2023, Accepted: June 7, 2023, Published: August 28, 2023.
Citation:	Nazir A, Ullah H, Gilanie G, Ahmad S, Batool Z, Gadhi A. Exploring breast cancer texture analysis through multilayer neural networks. *Sci Inq Rev.* 2023;7(3):32–47. https://doi.org/10.32350/sir.73.03
Copyright:	© The Authors
Licensing:	This article is open access and is distributed under the terms of Creative Commons Attribution 4.0 International License
Conflict of Interest:	Author(s) declared no conflict of interest

Exploring Breast Cancer Texture Analysis through Multilayer Neural Networks

Aalia Nazir[1*], Hafeez Ullah[1], Ghulam Gilanie[1], Shabbir Ahmad[1], Zahida Batool[1], and Asghar Gadhi[2]

[1] Institute of Physics, The Islamia University of Bahawalpur, Pakistan
[2] Bahawalpur Institute of Nuclear Medicine, Bahawalpur, Pakistan

ABSTRACT

Breast cancer is a significant health problem for women globally; however, timely detection can reduce female morbidity and mortality. Early breast screening has become imperative for all women, though, adequate screening facilities are necessarily required in developing countries like Pakistan, where breast cancer is a leading cause of death. To encounter this chronic disease, various image processing techniques have been introduced to automatically diagnose breast cancer from digital mammograms. The current study deployed data from a population of 35 participants. The mammograms used for screening were 5 normal, 15 benign, and 15 malignant patients. The breast images were marked by the radiologist and the system was trained with normal, benign, and malignant classes. Moreover, Multilayer Neural Networks (MNN) based texture analysis methodology was adopted to distinguish normal, benign, and malignant breast images. Reportedly, an automated approach was used to detect breast conditions after conducting the analysis of digital mammograms. Statistical parameters, namely sum, mean, variance, standard deviation, kurtosis, skewness, energy, and entropy were calculated, analyzed, and compared for the normal, malignant, and benign breast images. The results indicated a 100% accuracy after the analysis. The results of the extracted statistical parameters were promising and reliable in distinguishing between normal, malignant, and benign breast mammograms, again indicating the need for early detection of the disease to minimize the risk of breast cancer among women.

---

[*] Corresponding Author: alia.nazir@iub.edu.pk

1. INTRODUCTION

Breast cancer is one of the most common cancers among women, which affects women's physical and mental health and is even life-threatening globally. The overall frequency is increasing, and the risk factors are well-documented [1].

There are several features, which are responsible for this disease like obesity, radiation exposure, family history, fat-enriched food, and pre-malignant injuries. Breast cancer once detected can become worse with a change in lifestyle [2, 3]. Breast cancer is the second major cause of mortality worldwide and in Pakistan every 1 woman out of 9 is suffering from this chronic disease. This can be due to the lack of medical facilities and unawareness, which are major causes of delayed diagnosis [4, 5]. It has been a challenging task to detect breast cancer at an earlier stage to lower the mortality rate. The risk of breast cancer among women aged less than 40 years is smaller, whereas an increased rate has been noticed in women between 45-55 years, resultantly causing an increase in mortality rate [6]. Mammography is an affordable, low-radiation test recommended for early detection of breast cancer [7, 8]. This test can be performed on both pre-symptomatic and symptomatic women; however, it is less efficient for women who are lower than 40 due to dense breasts [9]. Though, women at later stages can feel a lump, a hard loop within the breast or under the arm, swelling, changes in the mass of the breast, redness, and dimpling or creasing of skin. Countries with low-income and underdevelopment, such as Pakistan, face a scarcity of resources for essential diagnosis or detection. Delays in medical care may contribute to the spread of breast cancer's morbidity and mortality [10]. Michell *et al*. Identified that the addition of digital breast tomosynthesis (DBT) in conventional mammography increases the accuracy rate in cancer assessment [11].

The human nervous system is a compound neural system and our body collects external signals through dendrites. These signals are collected till a threshold level to make an action. A large number of neurons are interrelated to study input and optimize its output by means of computing and processing. Artificial Neural Network (ANN) is used in training a learned system by processing these signals in medical imaging so, that decisions can be automated. Computer-aided Detection Systems (CAD) trained using machine learning models, help radiologists, medical

practitioners, radiation oncologists or physicians in the accurate and more definite detection of breast cancer in the early stage [12]. CAD systems have been used in many medical institutes for clinical diagnosis as referred by doctors [13]. For the feature extraction process, curvelet moments are also very beneficial in giving reduced features and enhancing accuracy in the diagnosis of breast cancer [14]. An automated feature extraction process is utilized in diagnosing architecture distortion in the breast, which causes malignancy by applying texture models and vector machine classifiers on the region of interest [15]. A multivariate feature can also be used for extraction by applying a genetic algorithm and obtaining feature descriptive in two categories, which classify malignant and benign breasts and reduces the workload of radiologists [16]. Furthermore, the grey level co-occurrence matrix is used for feature extraction in different orientations to differentiate masses and non-masses, by combing the grey level with the wavelet approach through which the results are enhanced [17]. ANN-PSO (artificial neural network with particle swarm optimization) method has been used by Zhang *et al* to extract the intensity and shape features, which tested and then distinguished normal and abnormal breast mammograms [18]. The particle swarm optimized wavelet neural network (PSOWNN) technique was applied to breast mammograms by Sathyaa *et al* and the Receiver Operating Characteristic (ROC) curve indicated the sensitivity and specificity as indicated by Dheeba et al. [19, 20].

From the analysis of texture, an automated method was proposed to classify different breast tissues as normal, malignant, or benign. This method provided the radiographic details of breast lesions.

Breast tumors can be benign or malignant. Benign is not dangerous, it can grow but doesn't spread in surroundings. However, malignant is cancerous and can spread in the entire body and cause destruction [21, 22]. Therefore, in this study, an automated approach has been proposed to classify breast cancer as normal, benign, or malignant. This work explored ways to prevent this disease and provide a new taxonomy for breast cancer risk assessment.

2. MATERIALS AND METHODS

A dataset of mammograms, correspondingly collected from 35 subjects was obtained from the Bhawal Victoria Hospital. The women

who were considered for scanning ranged from age 45-55 years having either normal, benign, or malignant breast cancer stage. All patients were duly informed and the ethics review board signed for further process. Medial-lateral oblique and craniocaudal images were acquired and statistical mammographic data were analyzed. The following steps were taken to successfully classify breast conditions including normal, benign or malignant.

i. The mammograms having high intensity and contrasts were input to the developed system. The developed system consisted of an architecture based upon 12-layered multi-layered neural networks (MNN).

ii. Segmentation of Region of Interest (ROI), which had a suspicious area with distinguished surroundings was marked by the domain experts.

iii. Texture features, namely, sum, mean, variance, standard deviation, kurtosis, skewness, energy, and entropy extracted from each of the segmented ROIs belonging to normal, benign, and malignant stages.

iv. Training of the system using these extracted texture features through MNN using Matlab2020a was conducted on 70% of the total data.

v. Evaluation of the proposed developed system was based on the standard evaluation measurement, such as accuracy.

3. RESULTS

In this research, statistical methods were used to extract texture features. Using image classification and segmentation methods was a more reliable approach, which ensured higher reliability in the obtained results. The feature extraction method underlying the statistical procedure consisted of the sum of the following parameters, namely mean (pixel value), variance (square root of deviation), energy (uniformity), standard deviation (pixel deviation from the mean), skewness (pixel asymmetry), kurtosis (flatness or peak), and entropy (random measurements). Normal, malignant, and benign breast mammograms and their bilateral statistical data were analyzed. There are usually two models for image projection, namely Craniocaudal (CC), a view from the apex, which allows for enhanced imaging of the central and internal breast regions, and Mediolateral Oblique (MLO) that provides an improved view of the gland from a specific side view.
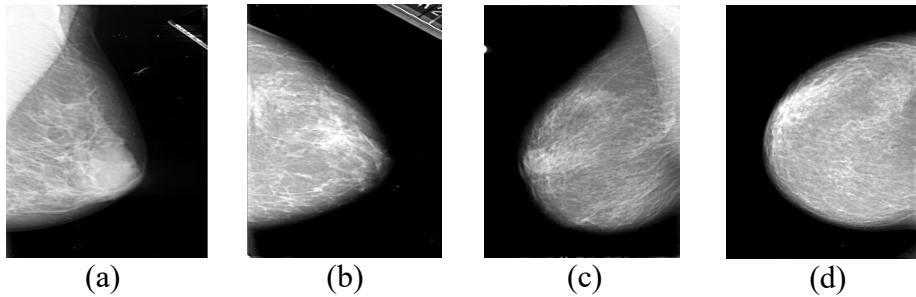
Figure 1. (a) Case 1 (L-MLO), (b) Case 2 (R-CC), (c) Case 35 (R-MLO), and (d) Case 35 (R-CC`)
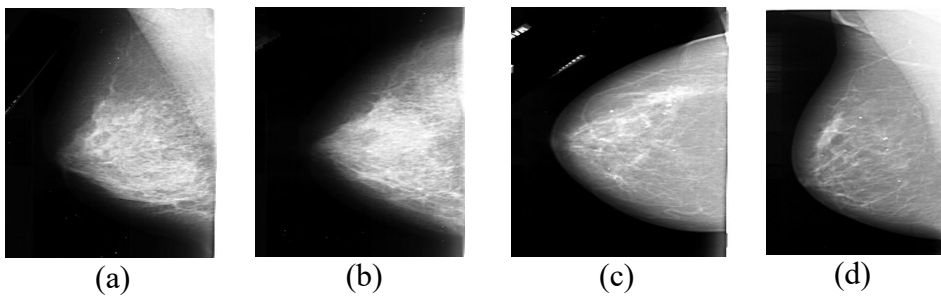
Figure 2. (a) Case 7 (R-MLO), (b) Case 7 (L-CC), (c) Case 19 (L-MLO), and (d) Case 19 (R-CC)

Figures 1 and 2 show a normal case in which no tumor was detected on mammography screening of the two selected subjects.
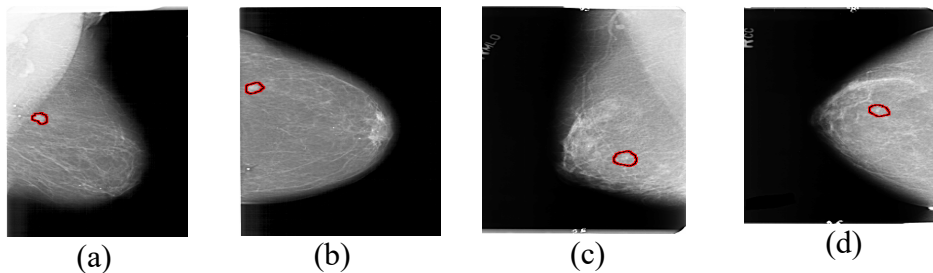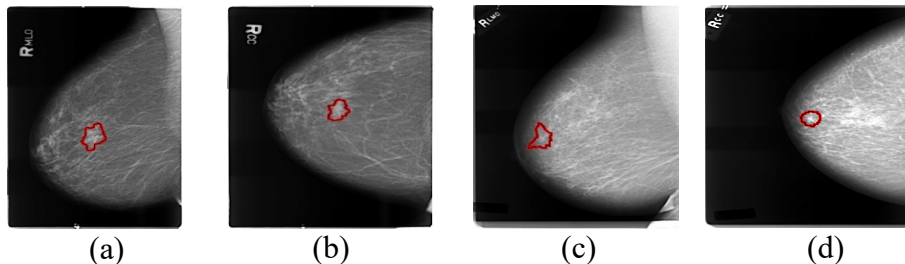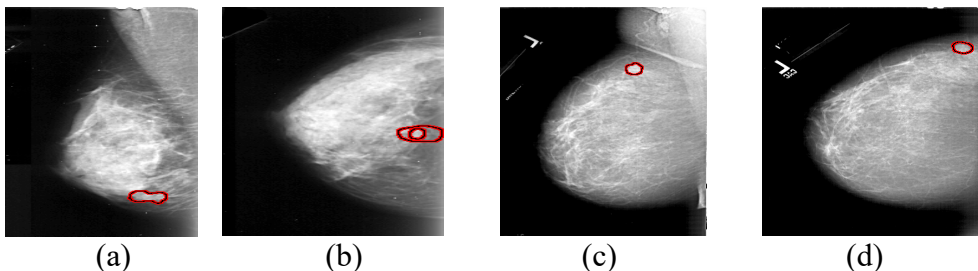

Figure 3. (a) Case 1 (L-MLO), (b) Case 1 (L-CC), (c) Case 2 (L-MLO), and (d) Case 2 (L-CC)

Figure 3 contains randomly selected left mammograms from two different subjects. The regions highlighted in these MLO and CC images are malignant breast lesions. Benign areas are brighter due to their higher intensity. Figure 4, shows right mammograms of two cases containing malignant areas in MLO and CC image projections. In Figure 4, Case 3 R

(MLO and CC) shows abnormalities, lesion-like masses, foci, asymmetric dense margins, and unclear partially malignant pathology (a, b). Case 4 R (MLO and CC) showed abnormalities, with lesion-like mass morphology and suspiciously malignant irregular margins in parts (c, d). The selected area is the tumor-containing lesion.

(a)   (b)   (c)   (d)

Figure 4 (a) Case 3 (R-MLO), (b) Case 3 (R-CC), (c) Case 4 (R-MLO), and (d) Case 4 (R-CC)

(a)   (b)   (c)   (d)

Figure 5. (a) Case 1 (L-MLO), (b) Case 1 (L-CC), (c) Case 2 (L-MLO), and (d) Case 2 (L-CC)

(a)   (b)   (c)   (d)
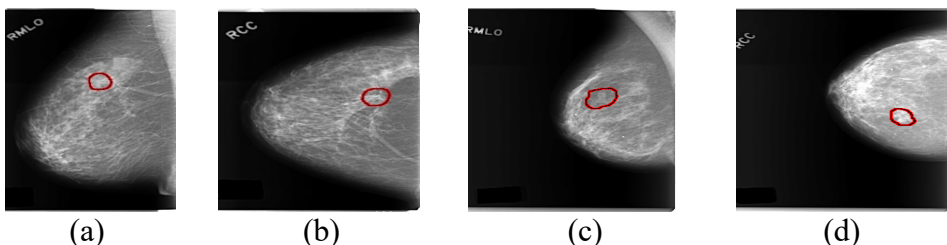
Figure 6. (a) Case 3 (R-MLO), (b) Case 3 (R-CC), (c) Case 4 (R-MLO), and (d) Case 4 (R-CC).

Mammograms of the left breast for case 1 and case 2 are shown in Figure 5, with the mediolateral and craniocaudally view with affected highlighted areas. This study has dealt with images of benign breasts having calcification, pleomorphic distribution, and architectural distortions

as shown in Figure 6. Case 3 R (MLO) is abnormal. Lesion-type classification, pleomorphic distribution, and clustered benign mammogram are shown in Figure 6 (a). Case 3 R (CC) is abnormal lesion-type calcification, pleomorphic distribution clustered, and architectural distortion margins speculated benign as shown in Figure 6 (b). Case 4 R (MLO and CC) shows abnormality lesion-type mass and shape round margins obscured benign as shown in Figure 6 (c, d). Red enclosed areas in the normal and benign breasts are the regions of interest, which are segmented and processed for statistical feature extraction of mammograms.

Texture parameters extracted from normal ROIs of the selected 35 patients age ranging from 45-55 are shown in Table I. Texture analysis was performed on 35 women with bilaterally normal breasts. Data from all the patients were collected and summarized below, showing medial-lateral oblique and craniocaudal views.

Table 1. Statistical Parameters in Mediolateral Oblique and Craniocaudal view of Normal Right and Left Breast

Statistical Parameters	Normal (MLO) (Average values)		Normal (CC) (Average values)	
	Right Breast	Left Breast	Right Breast	Left Breast
Sum	53.0	50.00	43.0	42.00
Mean	81.3	81.67647	66.4	65.470588
Variance	68.0	6768.161	63.0	6470.7764
Standard deviation	82.0	82.04567	79.0	80.050905
Skewness	0.49	0.455200	0.86	0.8279944
Kurtosis	-1.20	-1.272985	-0.60	-0.7750828
Entropy	26.0	2651414	21.0	21112641.1
Flatness	0.46	0.475726	0.52	0.53155200
Energy	3.2 E-05	3.268E-05	4.0 E-05	4.16294E-05

Table 1 provides textural parameters, such as, sum, mean, variance, standard deviation, skewness, kurtosis, entropy, flatness, and energy, along with maximum, minimum, and mean ranges for all normal mammograms.

The statistical characteristics of all the patients with malignancies were determined and presented in Table 2.

Table 2. Numerical Analysis of Right and Left Malignant Breast in MLO and CC view

Statistical Parameters	Malignant (MLO) (Average values)		Malignant (CC) (Average values)	
	Right Breast	Left Breast	Right Breast	Left Breast
Sum	5754958.9	5665979.1	4779375.86	4332792.4
Mean	78.371429	77.400000	62.6571429	59.828571
Variance	6171.9399	6381.0684	5749.74924	5489.5443
Standard deviation	78.195735	79.510718	75.2393183	73.539115
Skewness	0.5173302	0.5314520	0.89566069	0.9520324
Kurtosis	-1.0368810	-1.0458932	-0.48604212	-0.2584942
Entropy	30025540	28286342	23421773.6	21287130
Flatness	0.4867556	0.4924317	0.55017747	0.5496571
Energy	2.727E-05	2.9818E-05	3.49926E-05	3.8034E-05

Table 3 summarizes the texture parameters of the image window pixels, including the maximum, minimum, and mean values of the left and right benign breasts, with promising results. Reportedly, maximum and minimum values are now equal to absolute values.

Table 3. Pixel Parameters of Right and Left Benign Breast Images

Statistical Parameters	Benign (MLO) (Average values)		Benign (CC) (Average values)	
	Right Breast	Left Breast	Right Breast	Left Breast
Sum	5798909.86	5172456	4832506.3	5066756.51
Mean	73.2285714	66.485714	62.200000	65.2857143
Variance	5685.44068	5397.0492	5488.9733	5285.80702
Standard deviation	74.9817381	73.053862	73.571646	72.37847995

Statistical Parameters	Benign (MLO) (Average values)		Benign (CC) (Average values)	
	Right Breast	Left Breast	Right Breast	Left Breast
Skewness	0.68503344	0.7359084	0.9761847	0.80500920
Kurtosis	-0.7213016	-0.604295	-0.1948880	-0.41404877
Entropy	28338321.9	25325634	214942223	24647141.59
Flatness	0.51946173	0.5318824	0.5694440	0.536184773
Energy	2.727E-05	2.9818E-05	3.49926E-05	3.8034E-05

The results for the left and right benign breasts are shown in Table 3. To obtain reliable results and conclusions about the texture parameters of all normal, malignant, and benign breast images, comparisons were made numerically, to classify the results of normal and benign breast data by using MNN. The proposed approach was analyzed and found to be a reliable approach for the assessment. Digital data from previous mammograms of benign and healthy breasts were used for differentiation. Texture parameters are compared in Table 4 for maximum and minimum values for both of the selected cases.

Table 4. Comparison of Right MLO view Texture Parameters of Normal and Benign Breast Mammograms

Statistical Parameters	Right normal (MLO) (Average Values)	Right benign (MLO) (Average values)	% Differences
Sum	5383731.714	5798909.86	-7.1595896
Mean	81.34285714	73.2285714	11.0807648
Variance	6807.459804	5685.44068	19.7349544
Standard deviation	82.28868257	74.9817381	9.74496545
Skewness	0.491937579	0.68503344	-28.187801
Kurtosis	-1.20984084	-0.7213016	67.730231
Entropy	26957357.8	28338321.9	-4.8731329
Flatness	0.468915193	0.51946173	-9.730559
Energy	3.23365E-05	2.75458E-05	17.3917621

4. DISCUSSION

Normal, benign, and malignant mammograms were analyzed and the extracted textural features were presented in medial-lateral and

craniocaudal (CC) views. Subtle and obscure areas are enhanced using algorithms to make areas of interest easier to see and texture extraction methods are more useful in these areas. In this research, mammograms were used to train and test the proposed model to automatically classify normal, benign, and malignant breast images based on their texture. Each mammogram contains 20 slices of both views (MLO and CC) along the left and right breast. Therefore, $35 \times 2 \times 20 \times 2$ slices were used for training and testing the reported system. Of these total 2800 slices, 1848 slices were used for training the reported system and the remaining 952 slices were used for testing the reported system. Reportedly, two clues to malignant tumors are identified, namely microcalcifications and masses. These texture features were used to train the proposed method using MNNs and then compared to the literature [23, 24], both types yielded up to 90% of accuracy in discriminating benign or malignant abnormalities.

The statistical analysis examined each category's sum, mean, variance, entropy, skewness, and other pixel features of left and right breasts. Variations in these parameters, such as maximum, minimum, and mean values, were used to classify normal and benign tumor, including breast and the areas of microcalcification. In this work, MLO-mapped parameters of mammograms of healthy and malignant breasts were used in which clear differences in all values were noticed.

Differences between all parameters and maximum, minimum, and mean values demonstrated the intelligent classification of normal and benign breasts. This study's results were promising for various statistical approaches to describe and analyze image textures. By analyzing the variance of all outcomes, it was concluded that a distinction is required between the normal and benign cases with 100% accuracy. Different values are also agreed upon for normal and abnormal benign images. The observed variance for normal cases ranges from 8831.9-3896.8 and all findings for abnormal benign cases are above the maximum for normal images. Therefore, the variance parameter gave 100% results from benign to normal images. Furthermore, it was observed that normal and abnormal benign cases could achieve different ranges of kurtosis 88% of the time, with 89% of perfect results. For the rest of the parameters, a clear result was also noticed. This demonstrated good results obtained in a large number of breast cancer cases and benign cases. These were further compared on various parameters of normal, benign, and malignant breasts

by plotting kurtosis, energy, flatness and distortion on the x-axis and their intensity on the y-axis. Data were obtained from random patients and parameters were plotted with intensity. The variation in values of normal, malignant, and benign breast mammograms can be clearly observed graphically.
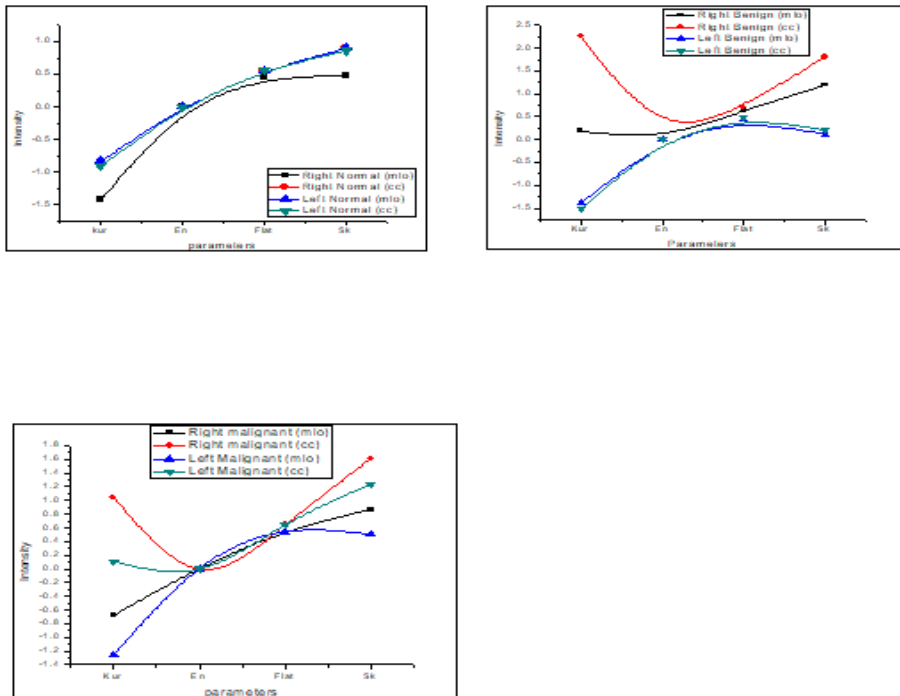

Figure 7. (a) The normal breast parameters of right and left mammogram in MLO and CC view, (b) Parameters of benign breast images along with intensities, and (c) Malignant breast mammogram parameters along with intensities.

Figure 7(a) shows the changes in kurtosis, energy, flatness, and skewness of left and right mammograms of a normal breast in craniocaudal and medial-lateral views. The parameters compared with the benign mammography parameters are shown in Fig. 7(b). In Fig. 7(b), the hyperintensities of the right benign image in CC view and MLO show the variation of values in normal parameters. The kurtosis parameter has a high intensity, which decreased at the energy point and increased again with flatness and strain but increase in the value at cc and then decreases

gradually. Comparing these two charts with the malignant breast image, the deviations from normal values are larger than the benign image parameters, as shown in Fig. 7(c). Intensity fluctuations in right malignant CC views are rather instantaneous and different from benign and normal breast parameters. The left malignant tumor (MLO, CC) and right malignant MLO also showed strange curves, which were different from the normal breast curve. This artificial texture analysis approach would play an important role in the future. Furthermore, the research aims to test these methods with other classifiers or segmentation schemes and in more realistic texture interpretation situations. These results showed that there is considerable performance variability between different texturing methods. These results are supported by previous comparative studies in this field. Hence, the feature extraction results may assist radiologists in the early screening of breast mammograms and discrimination between healthy and unhealthy breasts by analyzing the numerical data.

4.1. Conclusion

The current study, aimed to propose a multi-layered neural network (MNN) approach to demonstrate the potential to distinguish between healthy, benign, and malignant breast mammograms in breast region analysis and segmentation. Texture analysis and comparison parameters of statistical data such as mammogram sum, variance, mean, kurtosis, standard deviation, skewness, energy, entropy, and flatness were used to obtain the results. It was obvious from the results that this feature extraction modality was reliable for diagnosing cancerous or malignant breasts. Therefore, it was recommended that early detection could increase the survival rates among women possessing breast cancer. Moreover, screening tests are mandatory for all women, especially in developing countries like Pakistan, where cancer mortality is relatively higher than in other developed countries.

REFERENCES

1. Li H, Zhuang S, Li D, Zhao J, Ma Y. Benign and malignant classification of mammogram images based on deep learning. *Biomed Signal Proc Control*. 2019;51:347–354. https://doi.org/10.1016/j.bspc.2019.02.017

2. Morman NA, Byrne L, Collins C, Reynolds K, Bell JG. Breast cancer risk assessment at the time of screening mammography: Perceptions

and clinical management outcomes for women at high risk. *J Gen Counsel*. 2017;26(4):776–784. https://doi.org/10.1007/s10897-016-0050-y

3. Puliti D, Bucchi L, Mancini S, et al. Advanced breast cancer rates in the epoch of service screening: The 400,000 women cohort study from Italy. *Eur J Cancer*. 2017;75:109–116. https://doi.org/10.1016/j.ejca.2016.12.030

4. Khan NH, Duan SF, Wu DD, Ji XY. Better reporting and awareness campaigns needed for breast cancer in Pakistani women. *Cancer Manag Res*. 2021;13:212–2129. https://doi.org/10.2147/cmar.s270671

5. Menhas R, Umer S. Breast cancer among Pakistani women. *Iran J Public Health*. 2015;44(4):586–587.

6. Pisano ED, Gatsonis C, Hendrick E, et al. Diagnostic performance of digital versus film mammography for breast-cancer screening. *New Eng J Med*. 2005;353(17):1773–1783. https://doi.org/10.1056/nejmoa052911

7. Sung H, Ferlay J, Siegel RL, et al. Global cancer statistics 2020: GLOBOCAN estimates of incidence and mortality worldwide for 36 cancers in 185 countries. *Cancer J Clinic*. 2021;71(3):209–249.

8. Zahoor S, Lali IU, Khan MA, Javed K, Mehmood W. Breast cancer detection and classification using traditional computer vision techniques: A comprehensive review. *Curr Med Imag Form Curr Med Imag Rev*. 2021;16(10):1187–1200. https://doi.org/10.2174/1573405616666200406110547

9. Elizalde A, Pina L, Etxano J, Slon P, Zalazar R, Caballeros M. Additional US or DBT after digital mammography: Which one is the best combination? *Acta Radiol*. 2016;57(1):13–18.

10. Selove R, Kilbourne B, Fadden MK, et al. Time from screening mammography to biopsy and from biopsy to breast cancer treatment among Black and White, non-HMO Medicare women beneficiaries not participating in a health maintenance organization. *Women Health Issue*. 2016;26(6):642–647. https://doi.org/10.1016/j.whi.2016.09.003

11. Galván-Tejada C, Zanella-Calzada L, Galván-Tejada J, et al. Multivariate feature selection of image descriptors data for breast

cancer with computer-assisted diagnosis. *Diagnostics*. 2017;7(1):e9. https://doi.org/10.3390/diagnostics7010009

12. Jiang J, Trundle P, Ren J. Medical image analysis with artificial neural networks. *Comput Med Imag Graph*. 2010;34(8):617–631. https://doi.org/10.1016/j.compmedimag.2010.07.003

13. Fujita H. AI-based computer-aided diagnosis (AI-CAD): The latest review to read first. *Radiol Phy Technol*. 2020;13(1):6–19. https://doi.org/10.1007/s12194-019-00552-4

14. Michell MJ, Iqbal A, Wasan RK, et al. A comparison of the accuracy of film-screen mammography, full-field digital mammography, and digital breast tomosynthesis. *Clin Radiol*. 2012;67(10):976–981. https://doi.org/10.1016/j.crad.2012.03.009

15. Dhahbi S, Barhoumi W, Zagrouba E. Breast cancer diagnosis in digitized mammograms using curvelet moments. *Compute Biol Med*. 2015;64:79–90. https://doi.org/10.1016/j.compbiomed.2015.06.012

16. Kamra A, Jain V, Singh S, Mittal S. Characterization of architectural distortion in mammograms based on texture analysis using support vector machine classifier with clinical evaluation. *J Digit Imaging*. 2016;29(1):104–114. https://doi.org/10.1007/s10278-015-9807-3

17. Kulkarni DA, Bhagyashree. SM, Udupi GR. Texture analysis of mammographic images. *Int J Comput Appl*. 2010;5(6):12–17. https://doi.org/10.5120/919-1297

18. Zhang C, Shao H, Li Y. Particle swarm optimisation for evolving artificial neural network. Paper presented at: SMC 2000 conference proceedings. 2000 IEEE International Conference on Systems, man and Cybernetics; October 8–11, 2000; Nashville, TN, USA. https://doi.org/10.1109/ICSMC.2000.884366

19. Sathya DJ, Geetha K. Mass classification in breast DCE-MR images using an artificial neural network trained via a bee colony optimization algorithm. *ScienceAsia*. 2013;39(3):294–305. https://doi.org/10.2306/scienceasia1513-1874.2013.39.294

20. Dheeba J, Singh NA, Selvi ST. Computer-aided detection of breast cancer on mammograms: A swarm intelligence optimized wavelet

neural network approach. *J Biomed Info*. 2014;49:45–52. https://doi.org/10.1016/j.jbi.2014.01.010

21. Sharma M, Dubey RB, Gupta S. Feature extraction of mammograms. *Int J Adv Comput Res*. 2012;2(3):201–209.

22. Ranjbarzadeh R, Sarshar NT, Ghoushchi SJ, et al. MRFE-CNN: Multi-route feature extraction model for breast tumor segmentation in Mammograms using a convolutional neural network. *Ann Oper Res*. https://doi.org/10.1007/s10479-022-04755-8

23. Kayode AA, Afolabi BS, Ibitoye BO. Preparing mammograms for classification task: Processing and analysis of mammograms. *Int J Info Eng Elect Bus*. 2016;8(3):57–66. https://doi.org/10.5815/ijieeb.2016.03.07

24. Chan HP, Sahiner B, Petrick N, et al. Computerized classification of malignant and benign microcalcifications on mammograms: Texture analysis using an artificial neural network. *Phy Med Biol*. 1997;42(3):549–567. https://doi.org/10.1088/0031-9155/42/3/008

Article QR

Title:	**Fluidic Simulation and Optimization of Microchannels for Retinal Vein Occlusion (RVO) by Using Fuzzy Technique**
Author (s):	Muhammad Javaid Afzal[1], Farah Javaid[2], Muhammad Ilyas Yasin[3], Shahzadi Tayyaba[4], Muhammad Waseem Ashraf[5]
Affiliation (s):	[1]Department of Physics, Govt. Islamia Graduate College Civil Lines Lahore, Pakistan [2]Department of Physics, Govt. APWA College (W) Lahore, Pakistan [3]Department of Firearms Acadiana Criminalistics Laboratory, New Iberia Louisiana – USA [4]Department of Information Sciences, University of Education, Township Campus, Lahore, Pakistan [5]Department of Electronics, Govt. College University, Lahore, Pakistan
DOI:	https://doi.org/10.32350/sir.73.04
History:	Received: May 3, 2023, Revised: June 14, 2023, Accepted: June 15, 2023, Published: August 28, 2023
Citation:	Afzal MJ, Javaid F, Yasin MI, Tayyaba S, Ashraf MW. Fluidic simulation and optimization of microchannels for Retinal Vein Occlusion (RVO) by using fuzzy technique. *Sci Inq Rev.* 2023;7(3):48–67. https://doi.org/10.32350/sir.73.04
Copyright:	© The Authors
Licensing:	This article is open access and is distributed under the terms of Creative Commons Attribution 4.0 International License
Conflict of Interest:	Author(s) declared no conflict of interest

UMT

A publication of
The School of Science
University of Management and Technology, Lahore, Pakistan

Fluidic Simulation and Optimization of Microchannels for Retinal Vein Occlusion (RVO) by Using Fuzzy Technique

Muhammad Javaid Afzal[1*], Farah Javaid[2], Muhammad Ilyas Yasin[3], Shahzadi Tayyaba[4], and Muhammad Waseem Ashraf[5]

[1]Department of Physics, Govt. Islamia Graduate College Civil Lines Lahore, Pakistan
[2]Department of Physics, Govt. APWA Graduate College (W), Lahore, Pakistan
[3]Department of Firearms Acadiana Criminalistics Laboratory, New Iberia Louisiana – USA
[4]Department of Information Sciences Division Science and Technology, University of Education, Lahore, Pakistan
[5]Department of Electronics, Govt. College University, Lahore, Pakistan

ABSTRACT

A microelectromechanical system (MEMS) is a diminutive machine having electronic and mechanical components with a size ranging from 20 µm-1 mm. In this present-day world, MEMS fabrication techniques have remodeled the conventional approaches towards system fabrication. Microfluidics is an eminent domain of MEMS in which small volumes of fluids are disciplined in micro-channels having dimensions in the submillimeter to achieve the desired outputs. Microfluidics have revolutionized the realm of compact system fabrication through preeminent inventions like lab-on-a-chip technology. Microchannels of various architectures are fabricated to employ microfluidic systems depending upon the required function of the device. In ophthalmology, Retinal Vein Occlusion (RVO) is an ailment in which small veins that take away blood from the human eye's retina are blocked or fissured, causing vision loss. Therefore, in this study, four micro-channels with different architectures, namely, sinusoidal, U-shaped, spiral, and curvilinear, were simulated by using the fuzzy technique to investigate the optimization of fluids for the implantation process to fix the RVO elixir. The two most critical parameters in retinal vein flow rate and velocity were taken at the output for optimization. Hence, fuzzy fluidic simulation revealed that curvilinear micro-channels were the best fit for biomedical implantation to treat RVO malady.

---

[*] Corresponding Author: javaidphy@gmail.com

Keywords: biomedical implants, curvilinear microchannel, fuzzy logic, microchannels, retinal vein occlusion

1. INTRODUCTION

A device with electrical and mechanical components as its integral parts and a size less than 1mm but greater than one micron falls in the category of MEMS [1]. Applications of MEMS have greatly revolutionized almost every field of scientific research. Additionally, MEMS based devices are widely employed in routine life; including automobile airbag accelerometers, keyless entry mechanisms, heat exchanging systems for cooling microsystems, lab-on-a-chip technology, micro drug delivery mechanisms, and many more. In the 1990s, an essential sector of MEMS, microfluidics study, came into the limelight with its astonishing applications in the fabrication of MEMS-based devices. In microfluidics systems, small volumes of fluids, usually the norm in the range of microliters (µl) to picoliters (pl) are controlled and manipulated in micro-ducts having dimensions from tens to hundreds of micrometers to obtain desired outputs [2]. Inkjet printers proved to be a prominent commercial success for microfluidics-based MEMS [3]. Microfluidics-based devices greatly benefited medical science by providing biochips, especially diagnosis applications [4].

Micro-channels are an imperative part of any microfluidic device [5]. The small volume of fluids is contained and manipulated in micro-channels of hydraulic diameter customarily below than1mm. Originally the concept of micro-channels was suggested by Tuckerman and Pease of Stanford Electronics Laboratories [6]. Micro-heat exchangers have widely employed micro-channels containing small qualities of fluids for heat exchange. These micro-heat exchangers play a significant role in the gas turbine engines, air conditioning, and heat pumps. It is because of the modest velocities at which fluids moving via microchannels, low Reynolds numbers are obtained [7]. Primarily, this paper is based on Retinal Vein Occlusion (RVO) for all three micro-channels. The human eye's lens focuses on all the incoming light onto the retina, located in the rear of the eyeball. The optical nerve transmits information from the retina to the brain, where it is processed to recognize images. Retinal vein occlusion (RVO) occurs when a clot blocks blood flow in the retinal vein. Hence, this research describes the maximal and typical blood flow rates in the human retinal veins.

1.1. Microchannel Shapes

Depending upon the intended purpose, micro-channels of different morphology were concocted. For example, to reinforce the flow pattern like parallel, serpentine, crossed, oblique, and ratchet morphology of microchannels could have adopted the architecture application. The shape of the microchannel is always an important factor to obtain the required results. Computational fluid dynamics (CFD) is often employed to optimize the desired microchannel shape [8]. The design of different alphabets like J, Y, T, U, and S can be a choice for purpose-based on its applications [9]. The other viable architectures include triangular, spiral, double spiral, trapezoidal, rectangular, circular, square, coil, double coil, curved, curvilinear, concentric, and sinusoidal with ascending and descending orders. The preferred choice of shape may vary greatly depending upon the desired results. Fluids exhibit differently in different shapes of microchannel. The flow rate and speed of the fluid in the microchannel are considered most meaningful for its suitability in any application. The chemistry of blood remained the same in all micro-channels [10].

Four micro-channels were subjected for the fluid optimization in the current study, which are briefly discussed below.

1.1.1. Sinusoidal Microchannel. A sinusoidal shape microchannel comprised of periodic repetitions of oscillations [11]. Sinusoidal microchannels of defined wavelength and amplitude have been employed in previous research for heat dissipation and mass transformation [12]. Studies have showed that sinusoidal micro-channels exhibit excellent flow conditions for the blood-like fluid. Blood flow at curves tends to lose its streamlined flow; however, regained its normal tendon after the curves. Such micro-channels have been employed for biomedical implantations for varicose veins. Such micro-channels possessed excellent qualities for dissipation of heat because of the morphology [13]. Curvatures helped to resist and streamlining the flow by making it easier to homogenize in the fluids.

Figure 1. Sinusoidal Microchannel

1.1.2. Spiral Microchannel. A coil-like microchannel called a spiral would have more complexity with increasing numbers of twists. Therefore, the current study's application demanded minimum twist in channels. Continuous centrifugal force made the blood lose its streamline flow [14]. Morphology of retinal veins can easily afford the implantation of spiral micro-channels. Blood rheology easily allowed the use of a spiral channel for implantation purposes [15]. Such micro-channels have been widely employed in mass transit systems [16].
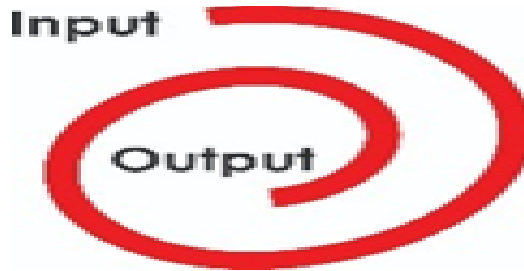
Figure 2. Spiral Microchannel

1.1.3. U-Shaped Microchannels. Researchers have been employing U-Shaped microchannels in fluid dynamics effectively [17]. A big advantage of a U-shape is its ability to adjust its length as per need [18]. The single curve in such a channel tends to offer minimum parametric changes as compared to other shapes [19]. However, Its biomedical application is well investigated in previously done research [20].
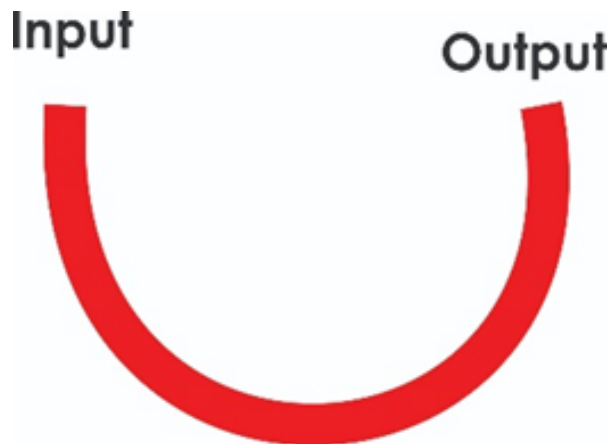
Figure 3. U-Shaped Microchannel

1.1.4. Curvilinear Microchannel. A microchannel comprising of curving boundaries or edges is called a curvilinear microchannel. Blood particles in its plasma offer the same behaviour to curvilinear morphology fabricated microchannel as that of natural response to veins [21]. More prone to extendable flexibility, its suitability for biomedical implants is favourable [22]. With the increased number of curves, the cell separation task can be obtained from such micro-channels [23].

Figure 4. Curvilinear Microchannel

1.2. Microchannels in Humans

Biological systems in human organs, namely, brain, liver, lungs, kidney, heart, and eyes contain many micro-channels majorly performing the critical functions of mass and heat transfer [24]. Cells can also migrate via micro-channels in a body structure [25]. It is believed that a comprehensive microchannel mass transfer mechanism work in human biological systems. Human tissues contain a complex network of micro-channels, which can be used to regulate routine tissue operations [26]. Primarily, blood composed of two major components; plasma and red blood cells. Plasma is a Newtonian fluid and red blood cells are intransigent spherical particles [27]. Blood bank viscosity is based on the percentage of blood that is made up of red blood cells. Characteristics of flowing blood like blood pressure, velocity, flow rate, the flow pattern is affected by the structure of the microchannel. Naturally occurring micro-channels in human biological system vary in morphology, which depends upon the function they are performing [28]. However, most micro-channels of human biological systems are elastic and can assume different morphology with the varying position of the human body [29]. Similarly, the diameter of this microchannel also responded to

the varying volume and pressure of blood and adjusted accordingly to tolerate the instant conditions.

1.3. Retinal Vein Occlusion

The lens of the human eye focuses on all coming rays to form an image on the inner side of the eye sphere to a place called the retina [30]. Nerve cells surrounding the retina convert the coming light into signals, which are transmitted to the brain via optical nerve for image recognition. Blockage of blood flow in the retinal vein because of a clot is called retinal vein occlusion (RVO). RVO is one of the most commonly occurring retinal vascular disease with an estimated 16 million effete globally [31]. A person affected by RVO may suddenly lose partial or full vision permanently without pain. So far iRVO is incurable; therefore, damage once done is irreversible but ophthalmologists can treat patients to stop further deterioration. Individuals suffering from diabetes and high blood pressure are more prone to RVO [32]. Other commonly found reasons for RVO include hypertension, high cholesterol, smoking, glaucoma, and excessive weight [33].

Furthermore, RVO is additionally categorized into two types; Central Retinal Vein Occlusion (CRVO) and Branch Retinal Vein Occlusion (BRVO). In CRVO the main retinal vein carrying blood is blocked/raptured, whereas BRVO affects a small branch of the main retinal vein. Both central and branch retinal veins have diameters in the range of µm with the central vein having a larger diameter as compared to the other branches. In certain cases, blocked vessels caused the leakage of jelly-like fluid into the retina resulting in small spots. These spots hampered the transmission of optical signals, which can be further used for the formation of an image. In other cases, some new unusual blood vessels may be caused by the retina; a process called neovascularization. These newly developed vessels leak the blood or fluid giving rise to RVO [34].

Different imaging tests are used to see the footsteps of RVO in the human eye, which include fluorescein Angiography, Optical Coherence Tomography, and Fundus Autofluorescence [35]. In retinal veins of human's maximum blood velocity and average flow rate as 54 mm/s and 2.04 nanoliters/ sec, respectively. Retinal veins carry blood away from the retina are quite similar to the microchannels.

1.3.1. Current Treatments. Current ophthalmology techniques to treat RVO include anti-vascular endothelial growth factor drug injections, retina opening massage, clot-busting medication, steroid treatment, Panretinal photocoagulation, focal laser treatment, and hyperbaric oxygen therapy [36]. These treatments deal with the issues arising from RVO to prevent further damage.

1.3.2. Challenges. There is no treatment or medication, which can completely unblock retinal veins [35]. Until now, RVO is incurable; ophthalmologists only manage the damage and prevent further deterioration. Vision problems, such as blurring or complete loss of sight in one eye, may appear unexpectedly. Complications from RVO include ocular edoema and haemorrhage. These conditions can cause blindness if not treated at the right time.

1.4. Biomedical Implants

Biomedical implants referred to placing natural or fabricated devices or tissues inside or on the surface of the human body to accomplish specific tasks. There may be different reasons for biomedical implants, which may include a missing body organ for supplemental support and monitoring body functions [37]. Hence, the implanted devices or tissues may be removed when they are no longer needed for the process. Primarily, operational surgery was required for the implantation. Most commonly implanted devices included implantable cardioverter defibrillators (ICDs), artificial hips, heart pacemakers, breast implants, spine screws, bone supporting rods, artificial spinal discs, intrauterine devices, metal supports for traumatic fracture repair, artificial knees, coronary stents, ear tubes, and artificial eye lenses.

The interdisciplinary nature of biomedical implantation covering various fields like physics, chemistry, electronics, bioengineering, biotechnology, biophysics, pharmaceutics, and others in conjunction with micro and nanotechnology made this a frequent choice to fix chronic syndromes by many researchers [38].

1.4.1. Bioengineered Microchannels. In bypass surgery and dialysis, bioengineered veins provided a definite advantage to replace faulty natural veins with fabricated veins. Micro-channels for implantation to treat varicose veins problem were reported in the research [39]. Different materials

can opt for microchannel fabrication depending upon their application. Initially, metal and ceramic-based micro-channels got the attention of previous researchers [40]. Furthermore, Polymer-based micro-channels got the attention of researchers because of their biomedical compatibility. Especially the polymers with non-toxic and elastic properties gained an obvious advantage over metal-based micro-channels [41]. Polyvinylchloride, polypropylene, polyurethane, polyamide, polyethylenterephthalate, polyetherimide, and other synthetic polymers are among tried options for the fabrication of bio-engineered veins. Polydimethylsiloxane (PDMS) with its non-toxic properties has gained the attention of researchers in last decade. Therefore, the current study investigated fluidic simulation and optimization of microchannels for Retinal Vein Occlusion (RVO).
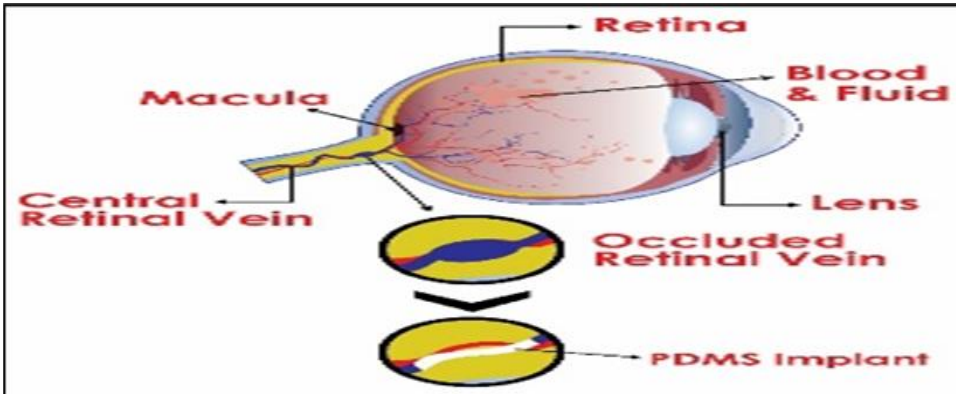
Figure 5. Proposed Microchannel Implantation to Treat RVO

2. FUZZY TECHNIQUE

Artificial intelligence software enabled the researcher to deal with complex problems uncomplicatedly. Contrary to binary logic fuzzy logic provided a more accurate picture of the system by considering all possibilities. Instead of overlooking at the implications of minutia, the fuzzy technique comprehensively enveloped all possible happenings. Fuzzy logic was beneficial in managerial sciences, business research, economics, scientific research, and various other engineering and social sciences fields.

In MEMS technology mainly micro-size components are dealt with, where simulations of possible happening allow to save time, money, and energy for the process. Researchers have applied fuzzy techniques in the field of microfluidics to manage the fabrication and operation of devices

[42]. The fuzzy simulation depicted fluid flow properties and related outcomes well in advance. Morphology and geometry of micro-channels and other research employed in microfluidic devices were being predicted by fuzzy and ANSYS simulation for perfect outcomes [20, 43–49].

2.1. Fuzzy Simulation of Microchannels for RVO

In the current study, four types of micro-channels architecture sinusoidal, U-shaped, spiral, and curvilinear were subjected to fuzzy parametric estimations to analyze the suitability for biomedical implantation to treat RVO. This microchannel architecture was selected to see the morphology of retinal veins. Moreover, the material used for fabrication can augment the evaluation of perfect-fit choices.

For this purpose, four Fuzzy Logic Control (FLC) models one for each microchannel was prepared. Membership functions for each model was defined and rules were prepared by using "if and then" statements.

3. RESULTS AND DISCUSSION

The outcomes are discussed below for all three sinusoidal, curvilinear, and U-shaped microchannel.

3.1. Sinusoidal Microchannel

For sinusoidal microchannel, Fuzzy Inference System (FIS) variables and their ranges are shown in Table 1.

Table 1. FIS Variables and their Ranges for Sinusoidal Microchannel

Input FIS Variables and Their Ranges			Output FIS Variables with Their Ranges	
Pressure	Diameter	Reynold Number	Flow Rate	Velocity
10-100 KPa	100-1000 µm	100-200	1-3 nL/s	40-60 mm/s

The output critical for a retinal vein is flow rate and velocity. The range of Reynolds numbers was taken to take all possibilities into account.
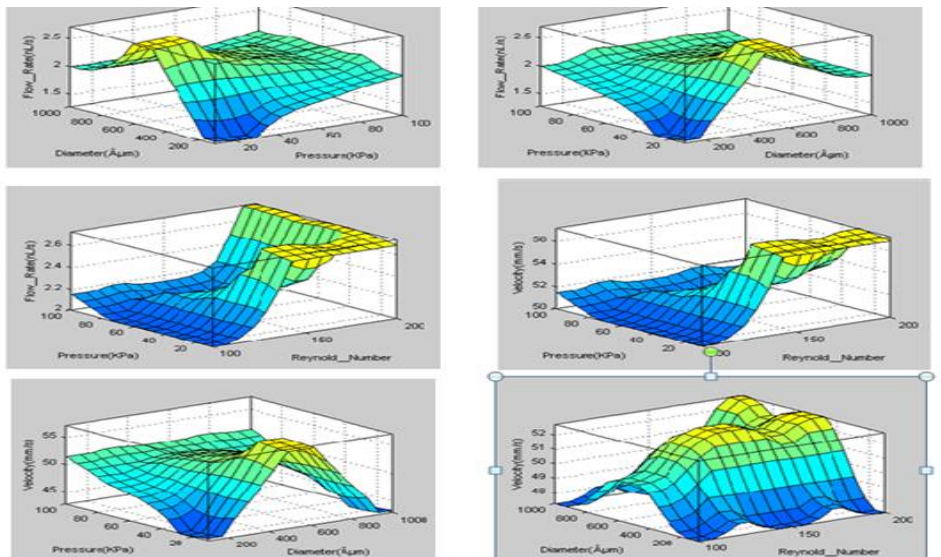
Figure 6. 3D Representation of Variations of Velocity and Flow rate in Sinusoidal microchannel

Flow rate showed a great variance in response to varying pressure. Only for pressure near 85 KPa flow rate remained in the acceptable value near 2nL/s. Response of flow rate to variations in Reynold's number and diameter of the microchannel was spread over a wide range, showing variation in inputs for each unit change. This variation in the flow rate was a response to minor changes in all three input parameters, which made this the least compatible for the intended purpose. Velocity variations follow the same pattern of changes, which were followed in response for the input changes in the microchannel simulation.

3.2. Spiral Microchannel

Fore spiral microchannel Fuzzy Inference System (FIS) variables and their ranges are shown in Table 2.

Table 2. FIS Variables and their Ranges for Spiral Micro-channels

Input FIS Variables and Their Ranges			Output FIS Variables with Their Ranges	
Pressure	Diameter	Friction	Flow Rate	Velocity
20-100 KPa	100-800 µm	0-1 N	1-3 nL/s	40-60 mm/s
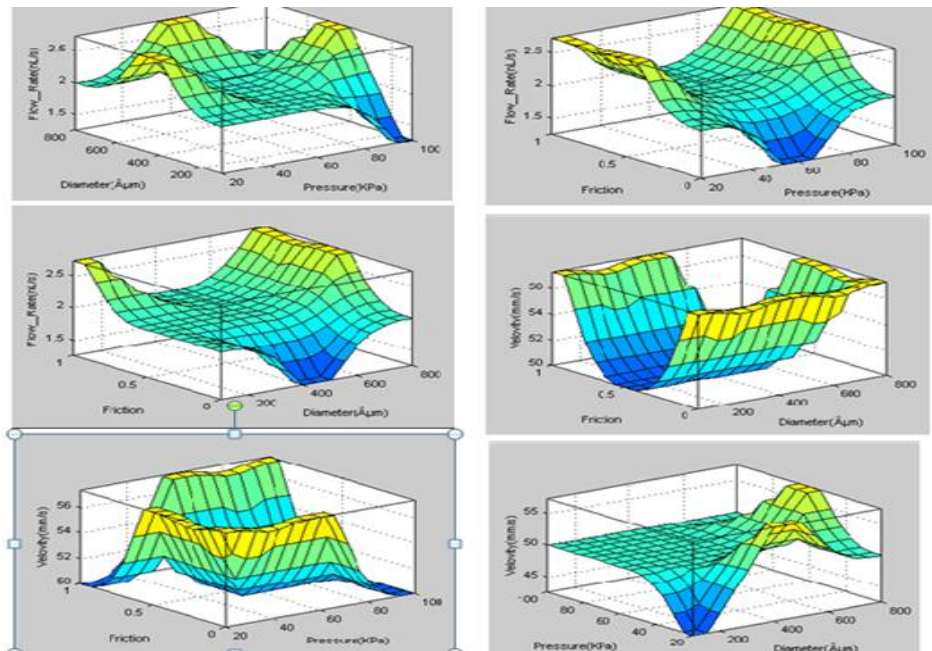
Figure 7. 3D Representation of Variations of Velocity and Flow rate in Spiral Microchannel

For variations in pressure, the flow rate varies to 2-2.75 nL/S. Only for 40-80 KPa pressure ranges, the flow rate remained in acceptable ranges near 2.1 nL/s. whereas in larger diameters the flow rate tends to increase constantly. Moreover, flow rate and velocity showed the same response of variations in the diameter of the microchannel. However, velocity remained constant near 5 mm/s for the pressure range of 55-10 KPa.

3.3. U-Shaped Microchannel

Fore U-Shaped microchannel Fuzzy Inference System (FIS) variables and their ranges are shown in Table 3.

Table 3. FIS Variables and their Ranges for U-Shaped Micro-Channel

Input FIS Variables and Their Ranges		Output FIS Variables with Their Ranges	
Pressure	Diameter	Velocity	Flow Rate
10-100 KPa	100-1000 µm	1-3 nL/s	40-60 mm/s

For low diameters up to 600 µm, the flow rate maintains a constant value of 2nL/s, however, an increased flow rate was noticed in the range of 600-950 µm that goes up to 2.7 nL/s. Contrarily, all pressures flow rate remained constant near 2nL/s. Minor changes in pressure and diameter made velocity vary to a great extent.
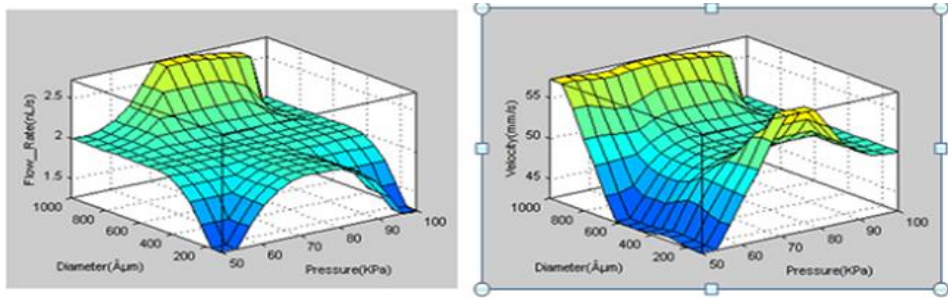
Figure 8. 3D Representation of Variations of Velocity and Flow rate in U-Shaped Microchannel

3.4. Curvilinear Microchannel

Fore U-Shaped microchannel Fuzzy Inference System (FIS) variables and their ranges are shown in Table 4.

Table 4. FIS Variables and their Ranges

Input FIS Variables and Their Ranges			Output FIS Variables and Their Ranges	
Pressure	Diameter	Friction	Flow Rate	Velocity
20-100 KPa	100-800 µm	0-1 N	1-3 nL/s	40-60 mm/s

Curvilinear micro-channels possess the quality of U-Shape and sinusoidal micro-channels. Moreover, its morphological appearance resembles the natural retinal veins, which gives it a clear advantage over the other types.

From the graphical representation it is quite obvious that for a diameter in the range of 400-600µm its flow rate and velocity exhibit the ideal optimization. The most suitable situation in the curvilinear microchannel is that in the pressure range 50-100 KPa flow rate remains constant near 2 nL/s. Moreover, the flow rate also maintains a constant value near 2nL/s when the diameter of the channel ranges between 400-100 µm. Velocity for any certain diameter maintains a constant value, which is ideal for the proposed application.
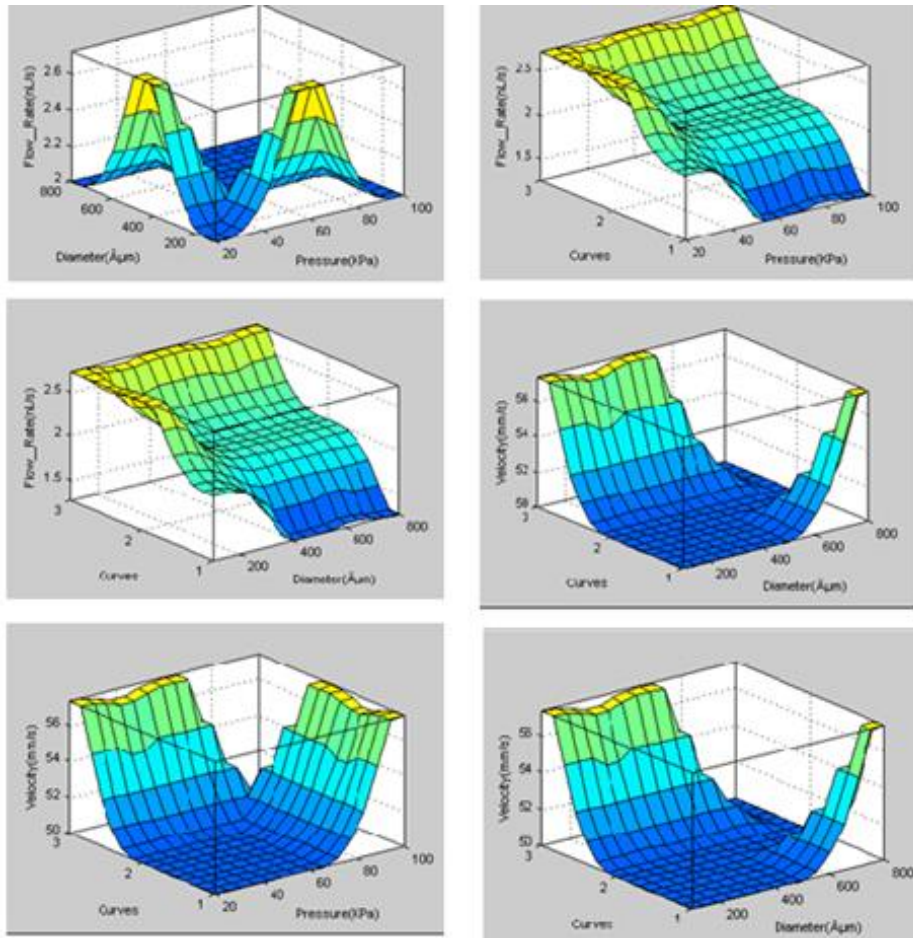
Figure 9. 3D Representation of Variations of Velocity and Flow rate in Curvilinear Microchanne

3.5. Comparative Discussion

A comparison of most optimum values was figured out through fuzzy parametric estimations, which is given below in Table 5. Both the flow rate and the velocity were compared with the Mamdani values to find the percentage errors. Fuzzy rule views provided us with the ease to see all possible parameters for the optimal outputs.

Although the percentage error in all four cases was quite negligible, the actual blood velocity and average flow rate values 54 mm/s and 2.04 nano-liters/ sec, respectively fall close in all simulated microchannels.

Table 5. Flow Rate and Velocity Results

Microchannel Type	Quantity	FUZZY Value	Mamdani Value	%age Error
Sinusoidal	Flow Rate	2.18 nL/s	2.15 nL/s	1.4%
	Velocity	50.7 mm/s	50.5 mm/s	0.4%
Spiral	Flow Rate	2.19 nL/s	2.16 nL/s	1.4%
	Velocity	51.6mm/s	51.9mm/s	0.6%
U-Shape	Flow Rate	2.0 nL/s	2.3 nL/s	1.5%
	Velocity	50 mm/s	50.2 mm/s	0.4%
Curvilinear	Flow Rate	2.06 nL/s	2.04 nL/s	0.1%
	Velocity	51.8 mm/s	51.5 mm/s	0.6%

3.6. Conclusion

The current study aimed to provide a fluidic stimulation by using Fuzzy parametric estimations technique, which provided optimal behaviours for all four micro-channels. The output optimization of four simulated micro-channels revealed that the curvilinear micro-channel best suited the implantation to treat RVO. Blood flow rate and velocity are the least divergent in a curvilinear microchannel. Although the simulated values of curvilinear micro-channels are a little lower than the practical value, this small deficiency is negligible in the context of associated flow rate. For the three simulations, the combination of two output parameters remained divergent from the actual case requirements.

REFERENCES

1. Gad-el-Hak M. *MEMS: Introduction and Fundamentals*. CRC press; 2005.

2. van Heeren H. Standards for connecting microfluidic devices? *Lab Chip.* 2012;12(6):1022–1025.

3. Singh M, Haverinen HM, Dhagat P, Jabbour GE. Inkjet printing—process and its applications. *Adv Mater.* 2010;22(6):673–685. https://doi.org/10.1002/adma.200901141

4. Gubala V, Harris LF, Ricco AJ, Tan MX, Williams DE. Point of care diagnostics: Status and future. *Anal Chem*. 2011;84(2):487–515. https://doi.org/10.1021/ac2030199

5. Abdelgawad M, Wheeler AR. Low-cost, rapid-prototyping of digital microfluidics devices. *Microfluid Nanofluid*. 2008;4(4):349–355. https://doi.org/10.1007/s10404-007-0190-3

6. Won Y, Cho J, Agonafer D, Asheghi M, Goodson KE. Fundamental cooling limits for high power density gallium nitride electronics. *IEEE Transac Comp Pack Manufac Technol*. 2015;5(6):737–744. https://doi.org/10.1109/TCPMT.2015.2433132

7. Liu C, Hu G, Jiang X, Sun J. Inertial focusing of spherical particles in rectangular microchannels over a wide range of Reynolds numbers. *Lab Chip*. 2015;15(4):1168–1177. https://doi.org/10.1039/C4LC01216J

8. Tonomura O, Kano M, Hasebe S. Shape optimization of microchannels using CFD and adjoint method. In: Pierucci S, Ferraris GB, ed. *Computer Aided Chemical Engineering*. Vol 28. Elsevier; 2010:37–42. https://doi.org/10.1016/S1570-7946(10)28007-0

9. Liang L, Xuan X. Continuous sheath-free magnetic separation of particles in a U-shaped microchannel. *Biomicrofluid*, 2012;6(4):e044106. https://doi.org/10.1063/1.4765335

10. Fujiwara H, Ishikawa T, Lima R, et al. Red blood cell motions in high-hematocrit blood flowing through a stenosed microchannel. *J Biomech*. 2009;42(7):838–843. https://doi.org/10.1016/j.jbiomech.2009.01.026

11. Bruckmann A, Klefenz F, Wunsche A. A neural net for 2D-slope and sinusoidal shape detection. *Int J Comput*. 2014;3(1):21–26.

12. Toghraie D, Abdollah MM, Pourfattah F, Akbari OA, Ruhani B. Numerical investigation of flow and heat transfer characteristics in smooth, sinusoidal and zigzag-shaped microchannel with and without nanofluid. *J Therm Anal Calorim* 2018;131(2):1757–1766. https://doi.org/10.1007/s10973-017-6624-6

13. Ghani IA, Kamaruzaman N, Sidik NA. Heat transfer augmentation in a microchannel heat sink with sinusoidal cavities and rectangular ribs. *Int J Heat Mass Trans*. 2017;108:1969–1981. https://doi.org/10.1016/j.ijheatmasstransfer.2017.01.046

14. Kuntaegowdanahalli SS, Bhagat AA, Kumar G, Papautsky I. Inertial microfluidics for continuous particle separation in spiral microchannels. *Lab Chip*. 2009;9(20):2973–2980. https://doi.org/10.1039/B908271A

15. MacInnes JM, Ortiz-Osorio J, Jordan PJ, Priestman GH, Allen RW. Experimental demonstration of rotating spiral microchannel distillation. *Chem Eng J.* 2010;159(1-3):159–169. https://doi.org/10.1016/j.cej.2010.02.030

16. Peng XY, Li PC, Yu HZ, Ash MP, Chou WL. Spiral microchannels on a CD for DNA hybridizations. *Sens Actuator B Chem*. 2007;128(1):64–69. https://doi.org/10.1016/j.snb.2007.05.038

17. Zhang TT, Jia L, Zhang J, Jaluria Y. Numerical simulation of fluid flow and heat transfer in U-shaped microchannels. *Numer Heat Trans*. 2014;66(3):217–228. https://doi.org/10.1080/10407782.2013.873288

18. Vishnubhatla KC, Bellini N, Ramponi R, Cerullo G, Osellame R. Shape control of microchannels fabricated in fused silica by femtosecond laser irradiation and chemical etching. *Optic Exp*. 2009;17(10):8685–8695. https://doi.org/10.1364/OE.17.008685

19. Kockmann N, Engler M, Haller D, Woias P. Fluid dynamics and transfer processes in bended microchannels. *Heat Trans Eng*. 2005;26(3):71–78. https://doi.org/10.1080/01457630590907310

20. Afzal MJ, Tayyaba S, Ashraf MW, Hossain MK, Afzulpurkar N. Fluidic simulation and analysis of spiral, U-shape and curvilinear nano channels for biomedical application. 2017 IEEE International Conference on Manipulation, Manufacturing and Measurement on the Nanoscale (3M-NANO); August 7–11, 2011, Shanghai, China. https://doi.org/10.1109/3M-NANO.2017.8286277

21. Özbey A, Karimzadehkhouei M, Akgönül S, Gozuacik D, Koşar A. Inertial focusing of microparticles in curvilinear microchannels. *Sci Rep*. 2016;6:e38809. https://doi.org/10.1038/srep38809

22. Lee MG, Choi S, Park JK. Inertial separation in a contraction–expansion array microchannel. *J Chromat A*. 2011;1218(27):4138–4143. https://doi.org/10.1016/j.chroma.2010.11.081

23. Wewala WA, Kasi JK, Kasi AK, Afzulpurkar N. Design, simulation and comparison of ascending and descending curvilinear microchannels for

cancer cell separation from blood. *Biomed Eng*. 2013;25(3):e1350037. https://doi.org/10.4015/S1016237213500373

24. Korin N, Bransky A, Dinnar U, Levenberg S. A parametric study of human fibroblasts culture in a microchannel bioreactor. *Lab Chip*. 2007;7(5):611–617. https://doi.org/10.1039/B702392H

25. Ko YG, Co CC, Ho CC. Directing cell migration in continuous microchannels by topographical amplification of natural directional persistence. *Biomaterials*. 2013;34(2):353–360. https://doi.org/10.1016/j.biomaterials.2012.09.071

26. Huang GY, Zhou LH, Zhang QC, et al. Microfluidic hydrogels for tissue engineering. 2011;3(1):e012001. https://doi.org/10.1088/1758-5082/3/1/012001

27. Kim J, Antaki JF, Massoudi M. Computational study of blood flow in microchannels. *J Comput Appl Math*. 2016;292:174–187. https://doi.org/10.1016/j.cam.2015.06.017

28. Yaginuma T, Oliveira MS, Lima R, Ishikawa T, Yamaguchi T. Human red blood cell behavior under homogeneous extensional flow in a hyperbolic-shaped microchannel. *Biomicrofluidics*. 2013;7(5):e054110. https://doi.org/10.1063/1.4820414

29. Parker KJ. A microchannel flow model for soft tissue elasticity. *Phys Med Biol*. 2014;59(15):e4443. https://doi.org/10.1088/0031-9155/59/15/4443

30. Atchison DA, Smith G. Optics of the human eye. *Encyclo Mod Opt*. 2000;5:43–63.

31. Rogers S, McIntosh RL, Cheung N, et al. The prevalence of retinal vein occlusion: pooled data from population studies from the United States, Europe, Asia, and Australia. *Ophthalmology*. 2010;117(2):313–319. https://doi.org/10.1016/j.ophtha.2009.07.017

32. Wong TY, Klein R. *The Epidemiology of Eye Diseases in Diabetes*. John Wiley & Sons, Ltd; 2008.

33. Lee JY, Yoon YH, Kim HK, et al. Baseline characteristics and risk factors of retinal vein occlusion: A study by the Korean RVO Study Group. *J Korean Med Sci*. 2013;28(1):136–144. https://doi.org/10.3346/jkms.2013.28.1.136

34. Chhablani J, Stewart M, Paulose R, Gallego-Pinazo R, Dolz-Marco R. Clinical characteristics and treatment outcomes of recurrent central retinal vein occlusions. In: *Seminars in Ophthalmology*. 2nd ed., Taylor & Francis; 2018:191–197.

35. MacDonald D. The ABC s of RVO: A review of retinal venous occlusion. *Clinic Experiment Optoom*. 2014;97(4):311–323. https://doi.org/10.1111/cxo.12120

36. Schachat AP, Zarbin MA. Anti-vascular endothelial growth factor drugs to reduce diabetic retinopathy progression. *Ophthalmol Retina*. 2018;2(10):985–987. https://doi.org/10.1016/j.oret.2018.08.004

37. Pinho T, Neves M, Alves C. Multidisciplinary management including periodontics, orthodontics, implants, and prosthetics for an adult. *Am J Orthod Dento Ortho*. 2012;142(2):235–245. https://doi.org/10.1016/j.ajodo.2010.10.026

38. Arsiwala A, Desai P, Patravale V. Recent advances in micro/nanoscale biomedical implants. *J Controll Rel*. 2014;189:25–45. https://doi.org/10.1016/j.jconrel.2014.06.021

39. Afzal MJ, Tayyaba S, Ashraf MW, Hossain MK, Uddin MJ, Afzulpurkar N. Simulation, fabrication and analysis of silver based ascending sinusoidal microchannel (ASMC) for implant of varicose veins. *Micromachines*. 2017;8(9):e278. https://doi.org/10.3390/mi8090278

40. Kalluri H, Kolli CS, Banga AK. Characterization of microchannels created by metal microneedles: formation and closure. *The AAPS J*. 2011;13(3):473–481. https://doi.org/10.1208/s12248-011-9288-3

41. Husny J, Cooper-White JJ. The effect of elasticity on drop creation in T-shaped microchannels. *J Non-NewFluid Mech*. 2006;137(1-3):121–136. https://doi.org/10.1016/j.jnnfm.2006.03.007

42. Abdel-Hamid W, Abdelazim T, El-Sheimy N, Lachapelle G. Improvement of MEMS-IMU/GPS performance using fuzzy modeling. *GPS Solu*. 2006;10(1):1–11. https://doi.org/10.1007/s10291-005-0146-6

43. Tayyaba S, Afzal MJ, Sarwar G, Ashraf MW, Afzulpurkar N. Simulation of flow control in straight microchannels using fuzzy logic.

International Conference on Computing, Electronic and Electrical Engineering (ICE Cube); April 11–12, 2016, Quetta, Pakistan. https://doi.org/10.1109/ICECUBE.2016.7495226

44. Afzal MJ, Javaid F, Tayyaba S, Ashraf MW, Punyasai C, Afzulpurkar N. Study of charging the smart phone by human movements by using MATLAB fuzzy technique. 15th International Conference on Electrical Engineering/Electronics, Computer, Telecommunications and Information Technology (ECTI-CON); July 18–21, 2018, Chiang Rai, Thailand. https://doi.org/10.1109/ECTICon.2018.8619882

45. Afzal MJ, Javaid F, Tayyaba S, Ashraf MW, Yasin MI. Study of constricted blood vessels through ANSYS fluent. *Biologia*. 2020;66(2):197–201.

46. Afzal MJ, Javaid F, Tayyaba S, Sabah A, Ashraf MW. Fluidic simulation for blood flow in five curved Spiral Microchannel. *Biologia*. 2019;65(2):1–15.

47. Afzal MJ, Tayyaba S, Ashraf MW, Sarwar G. Simulation of fuzzy based flow controller in ascending sinusoidal microchannels. 2nd International Conference on Robotics and Artificial Intelligence (ICRAI); November 1–2, 2016; Rawalpindi, Pakistan. https://doi.org/10.1109/ICRAI.2016.7791243

48. Tayyaba S, Ashraf MW, Ahmad Z, Wang N, Afzal MJ, Afzulpurkar N. Fabrication and analysis of polydimethylsiloxane (PDMS) microchannels for biomedical application. *Processes*. 2021;9(1):e57. https://doi.org/10.3390/pr9010057

49. Afzal MJ, Tayyaba S, Ashraf MW, et al. A review on microchannel fabrication methods and applications in large-scale and prospective industries. *Evergreen*. 2022;9(3):764–808.

Article QR

Title:	**Epidemiology of Type-II Diabetes and its Risk Factors in Punjab, Pakistan: A Retrospective Study**
Author (s):	Rana Muhammad Mateen[1], Asma Tariq[2], Mureed Hussain[1], Muhammad Irfan Fareed[1], Waseem Sajjad[1], Imran Tipu[1], Rukhsana Parveen[3]
Affiliation (s):	[1]University of Management and Technology, Lahore, Pakistan [2]Institute of Biochemistry and Biotechnology, University of the Punjab, Lahore, Pakistan [3]Centre for Applied Molecular Biology, University of the Punjab, Lahore, Pakistan
DOI:	https://doi.org/10.32350/sir.73.05
History:	Received: February 17, 2023, Revised: July 10, 2023, Accepted: July 10, 2023, Published: August 28, 2023
Citation:	Mateen RM, Tariq A, Hussain M, Fareed MI, Sajjad W, Tipu I, Parveen R. Epidemiology of type-II diabetes and its risk factors in Punjab, Pakistan: A retrospective study. *Sci Inq Rev.* 2023;7(3):68–81. https://doi.org/10.32350/sir.73.05
Copyright:	© The Authors
Licensing:	This article is open access and is distributed under the terms of Creative Commons Attribution 4.0 International License
Conflict of Interest:	Author(s) declared no conflict of interest

Epidemiology of Type-II Diabetes and its Risk Factors in Punjab, Pakistan: A Retrospective Study

Rana Muhammad Mateen[1], Asma Tariq[2], Mureed Hussain[1], Muhammad Irfan Fareed[1], Waseem Sajjad[1], Imran tipu[1*], and Rukhsana Parveen[3]

[1]Department of Life Sciences, School of Science, University of Management and Technology, Lahore, Pakistan
[2]Institute of Biochemistry and Biotechnology, University of the Punjab, Lahore, Pakistan
[3]Centre for Applied Molecular Biology, University of the Punjab, Lahore, Pakistan

ABSTRACT

Type-II diabetes is the most common type of diabetes, which has affected more than 465 million people globally and has become the ninth leading cause of mortality. The current study aims to determine risk factors associated with type-II diabetes such as BMI, cholesterol levels, physical activity, and smoking along with co-morbidities associated with this disease. The data was collected from the province of Punjab, Pakistan. For this purpose, a survey was performed for investigating the prevalence of type II diabetes and associated risk factors combined with it. A sample size of 265 patients was collected and interviewed through a questionnaire who were observed having type-II diabetes. A questionnaire was designed to record these patients' responses. The questionnaire contained sub-categorizes, such as participants characteristics, lifestyle, and comorbidities associated with the disease. The findings indicated that the mean BMI was 25.62 in the studied cohort. However, 78% of the patients had a family history of diabetes. Moreover, 76% of the participants were reported to be non-smokers and 75.67% of the participants reported atypical features associated with this disease. It was also observed that 13 % of the patients with low BMI (less than 18.5) had gastrointestinal diseases and 14.72% of the patients with a BMI greater than 18.5 but less than 25 had hypertension, and 8.30 % of the patients with more than 30 BMI also had hypertension. High BMI was found to be a major risk factor associated with type-II diabetes in this study population. The patients observed with high BMI were also more prone towards comorbidities associated with this disease. However, data suggested that most of the patients had familial type-II diabetes.

---

* Corresponding Author: Imran.tipu@umt.edu.pk

Keywords: BMI, diet, diabetes, lifestyle, risk factor

1. INTRODUCTION

Non-communicable diseases (NCDs) are non-infectious and non-transmissible among people. These are chronic diseases arising due to genetic, environmental, and physiological factors. Globally, in 2010 34.5 million deaths were caused by these NCDs [1]. It has been found that more than 60% of the global deaths occurred due to NCD in Korea, Japan, and China by following the static lifestyle, increased fat and protein intake in the diet are the major cause of increased mortality rate [2]. The mortality rate in Korea due to NCDs increased from 39.4% in 1983-56.0% in 2011 [3]. In 2009, heart diseases, cerebrovascular disease, and neoplasm were identified with the prevailing causes of death resulting in more than 50% of the total amount of death [4]. For minimizing NCDs there must be a comprehensive understanding of the complete disease spectrum starting from health promotion and risk factor promotion to the rehabilitation. Among all, risk factor monitoring has been proven to be an efficient strategy in reducing NCDs [5]. The major cause of NCD includes the consumption of tobacco and alcohol, unhealthy dietary intake, and a sedentary lifestyle. In China, Japan, and Korea the transition in the diet pattern is the major cause of the rapid growth of NCD. They transformed their diet from the traditional vegetable pattern to an unhealthy diet, such as fast food and oily food. The protection and treatment of risk factors is proven to be more efficient in reducing mortality due to NCDs. Several public health centers target risk factor for preventing NCDs. Among China, Japan, and Korea some valuable achievements in risk factors have been noticed in the past few years. They have improved their dietary lifestyle [6].

In the Western countries the major cause of cardiovascular disease is high BMI (body mass index) according to previous epidemiological research [7], while in Asian countries low BMI is a major cause of cardiovascular death [8]. Prior studies have also indicated that people can prevent themselves from diabetes type II by having a healthy lifestyle routine. Different lifestyle factors have contributed to type II diabetes [9]. The risk factors for diabetes include obesity, weight gain, and physical inactivity, which can independently act as a risk factor [10].

According to the International Diabetes Federation (IDF), it was estimated that approximately 463 million of the adults worldwide (20-79

years of age) were suffering from type-II diabetes mellitus and by 2045 this number is expected to rise by 700 million. Furthermore, it was identified that 79% of the diabetic adults were living in low income countries. Moreover, 1 in every 2 individuals are undiagnosed diabetes patients. Globally, diabetes mellitus has caused over 4.2 million deaths and 374 million individuals have been found to have an increased risk of developing mellitus type-II diabetes.

Pakistan falls under the top 10 countries for absolute increasing rate due to diabetes prevalence, which reached 17.1% in 2019. A comparison with previously reported figures was drawn in this study, which suggested a 148% increased percentage of this disease. Additionally, over 19 million adults in Pakistan were estimated with having diabetes, while 8.5 million out of these were undiagnosed [11]. This study focused on the prevalence of diabetes with associated risk factors and some atypical features (the features which are unusual and not the part of diagnostic procedures), which may or may not be linked to diabetes mellitus in Punjab, Pakistan.

2. METHODOLOGY

The current study deployed a cross-sectional survey to investigate the prevalence of NCDs and associated risk factors combined with the lifestyle and dietary controls of diabetic patients. The survey was conducted in Punjab province of Pakistan having a population of 220,892,340 as of 2020 [12]. The sample size was calculated using the formula as described earlier [13].

A questionnaire consisting of 27 questions was designed for the survey, which was divided into three parts, namely comprising sub-sections as participants characteristics, lifestyle-related questions, and questions-related to comorbidities. Participants' characteristics consisted of several questions related to the general information about the participants, such as their gender, age, weight, height, and family history. Participant's weight was converted into pounds similarly participant's height was recorded in feet was converted into inches to calculate the BMI of every participant [14].

A population of 265 participants were chosen having all type-II diabetes. The participants were made aware regarding the questions included in the survey, with each question being verbally explained to them by the conducting team. Furthermore, a written consent form was first filled

out by all the participants. Most of the lifestyle-related questions had 'yes' or 'no' answers. The analysis was compiled on Microsoft Excel with the descriptive analysis function and co-relations were analysed by using the AND function in MS Excel.

3. RESULTS
3.1. Participants Characteristics

Among the selected participants 39.8% of the participants were males. Most of the participants belonged to the age group 50-59(25%), while the age group 20-29 contained the least of the participants (1.14%). Table 1 summarizes the characteristics of the participants. The mean height in inches of the participants was $62.37 \pm$ S.D (standard deviation) of 9.7 inches. Similarly, the mean weight in pounds was $145.12 \pm$ S.D of 2.54 lbs and mean BMI was found to be $25.62 \pm$ S.D of 8. It was also observed that 78% of the participants had a family history of diabetes disease.

Table 1. Participants' Characteristics of the Study ($n= 265$)

Indices	Number	Percentage
Gender		
Males	105	39.8%
Females	159	60.2%
Age		
<=19	51	19.32%
20-29	3	1.14%
30-39	16	6.06%
40-49	50	18.94%
50-59	66	25.00%
60-69	45	17.05%
70=>	33	12.50%
BMI		
<18.5	64	24.81%
18.5-24.9	65	25.19%
25-30	57	22.09%
>30	72	27.91%
Family History		
Yes	207	78%

Indices	Number	Percentage
No	58	22%
(Mean BMI = 25.62 ± 8)		
(Mean Weight in Pounds = 145.12 ± 2.54 = 2.54)		
(Mean height in inches = 62.37 ± 9.7)		

3.2. Lifestyle Behaviour

The questionnaire targeted the participants who spent their holidays, while evaluating their diet and physical activity, which was significantly related to their disease. The exercise was among the foremost asked question in which 43.3% of the participants answered positively that they were actively engaged in exercise, while 28.35% answered "a few days a week", whereas the same percentage answered "No". When asked to choose between the work type, sedentary, mobile, and moderately active", 43.68% of the participants chose sedentary, while only 17.24% chose mobile. (Table 2)

Another question of self-evaluation was considered to ask the participants whether they have checked their daily sugar intake or not. The results indicated that 75.67% of the participants chose Yes, which was a positive response. Participants were also asked about their dinner and sleep timings to calculate the interval between these activities. It was indicated that 18% of the participants went to sleep in 2 hours, while 42% of the participants went to sleep right after 2 hours of having dinner, whereas 32% the participants were those who took 2-5 hours of sleep. Additionally, there were 3% of the participants who took more than 5 hours of sleep. However, 2% of the participants had insomnia.

When asked about smoking habits, 14% of the participants were smokers, while 76% were non-smokers. Additionally, 2% of the participants claimed that they quit and 7% said that they smoked On and off, while 1% of the participants answered Sometimes.

Table 2. Lifestyle Behaviour of the Type-II Diabetic Patients (*n*= 265)

Indices	Number	Percentage
Exercise		
Daily	113	43.30%
A few Days in a week	74	28.35%
No	74	28.35%

Indices	Number	Percentage
Work Type		
Sedentary	114	43.68%
Moderately Active	102	39.08%
Mobile	45	17.24%
Check on Daily sugar intake		
Yes	199	75.67%
No	64	24.33%
Time interval between dinner and sleep		
<2 hours	47	18%
Insomnia	5	2%
2 hours	111	42%
2 to 5 hours	86	32%
More than 5 Hours	7	3%
Smoking		
Yes	37	14%
No	202	76%
Sometimes	2	1%
Quit	5	2%
On and off	18	7%
Check on Daily Sugar Level		
Yes	150	57%
No	113	43%

3.3. Atypical Features

Participants were asked about atypical symptoms, which they might have that may or may not be linked to their diabetic health profile. These are given in Table III. However, these patients were asked about dizziness or weakness, around 199 (75.67%) participants agreed that they had these symptoms. Whereas 143(54.37%) of the participants reported the feeling pain or a burning sensation in their body. Additionally, 189(71.86%) reported numb feet and 53(20.15%) participants reported foot sores, while body ulcers were also reported by 58 (22.05%) of the participants.

Table 3. Atypical Features Associated with Type-II Diabetic Patients (*n*=265)

Indices	*n* (Percentages)	*n* (Percentages)
Atypical Features	Yes	No
dizziness/weakness	199(75.67%)	64(24.33%)
Feel of pain or Burning	143(54.37%)	120(45.63%)
Numb feet	189(71.86%)	74(28.14%)
foot Sores	53(20.15%)	210(79.85%)
Body ulcers	58 (22.05%)	205(77.95%)
Amputation	29 (11.03%)	233(88.59%)

3.4. Co-analysis

Table 4 highlights the relationship between different categories of questions. A percentage of 6.79% of the participants were mentioned having all the symptoms as given in Table 3, while 80% of the participants had at least one of these symptoms (Table 3). When a link between lifestyle and work type of the participants was made, it was found that 16.98% of the participants had a sedentary lifestyle and did not exercise at all. The participants, which had a mobile lifestyle and exercised daily were observed to be 18(6.79%), while 19(7.17%) participants had a moderately active lifestyle and exercised a few days in a week. It was observed that patients with low BMI (less than 18.5) were indulged in stomach, liver, and intestine diseases with a percentage of 13%. Participants with BMI greater than 18.5 but less than 25 had Hypertension (14.72%) and patients with more than 30 BMI had hypertension as well (8.30%).

Table 4. Co-analysis of Different Risk Factors in Type-II Diabetic Patients (n=265)

Serial No.	Indices	Participants (Percentage)
1.	Participants that have at least one of the mentioned symptoms	212(80.00%)
2.	Participants that have a sedentary lifestyle and do not exercise	45(16.98%)
3.	Participants that have a moderately active lifestyle and exercise a few days in a week	19(7.17%)

Serial No.	Indices	Participants (Percentage)
4.	Participants that have a mobile lifestyle and exercise daily	18(6.79%)
5.	Participants that have all the mentioned symptoms	18(6.79%)
6.	Participants with <18.5 BMI and have stomach, liver or intestine diseases	35(13%)
7.	People with <25 BMI and have Hypertension	39(14.72%)
8.	People with >30 BMI and have hypertension	22(8.30%)

Table 5 gives the prevalence of co-morbidities with diabetes. Hypertension was the most common disease with 81.89% of the participants suffering from it. Blood cholesterol was the second highest with 81.51% of the participants. Additionally, 58.49% of the participants reported heart disease. However, other (40.75%) reported diseases related to Stomach, intestine, and liver, while in a separate category of GI diseases, 40.75% of the participants were identified with these diseases. Among all only 2.26% of the participants reported having paralysis issue.

Table 5. Prevalence of Co-morbidities with Type –II Diabetes

HT	217 (81.89%)
Cholesterol	216(81.51%)
Heart Diseases	155(58.49%)
Stomach Liver Intestine	80(30.19%)
GI	108(40.75%)
Paralysis	6(2.26%)

4. DISCUSSION

Non communicable diseases (NCDs) have been linked with effective lifestyle behaviours. It has been reported that a successful change in lifestyle caused a 58% reduction in the diabetic incidence rate [15]. However, in developing countries, more than 80% of the deaths have been reported as a result of cardiovascular diseases and diabetes [16]. Behavioural risk factors and physiological risk factors have been reported to be the primary causes for NCDs [17]. Physical activity has been inversely related to different

diseases, such as diabetes [18]. Nevertheless, even today, there are quite less solutions that deal with physical inactivity. Reportedly, data collected from Brazil reported that 61% of the adults did not reach satisfactory levels of physical activity [19].

Hayes, L., et al studied the prevalence of diabetes in Pakistan before and after the physical activity of Pakistani population and its risk factors, which are associated with diabetes. He indicated that Pakistanis are less physically active than European people [20]. This corroborates with the current study in which 7.17% participants were found to have a moderately active lifestyle and people who were indulged in exercising were more active. A good percentage of participants approximately 43.68% had a sedentary work type and 16.98% out of these did not considered physical exercising as a part of active lifestyle behaviour.

Diabetes is also linked with sleep disturbances [21], which was actively found in this study, 2% of the participants reported insomnia, while 3% of the participants took more than 5 hours to sleep after taking dinner. It is worth mentioning that a considerable amount, approximately 32% took 2-5 hours of sleep, which could either be a lifestyle choice or can also be the cause of sleep disturbances [22]. 5% of the participants had sleep disorders, which can also be linked to diabetes.

Reportedly, this study identified that patients having diabetes were diagnosed with body ulcers and foot sores, which were 22.05% and 20.15%, respectively. According to some previous studies, there are serious complications among patients suffering from diabetes contributing to morbidity and mortality [23]. Noticeably, patients who were often prescribed inappropriate antibiotics worsened the situation leading to adverse effects, unlikely to heal. Diabetics with active ulcers have healing rates up to 75%. The amputation rate in this study's findings is 11.03%, while 15-20% of the amputations are of prior studies [24].

An extensive number of the participants, approximately 71.86% reported numbness of feet, which can be an indication of diabetic neuropathy [25]. Furthermore, it was observed in this study that diabetic patients who are overweight (25-30 BMI) and obese (>30 BMI) suffered from hypertension. This association corresponds with the results of previous findings. Moreover, higher levels of BMI was linked to the increasing blood pressure of patients and the gradient observed strongly suggested that there

could be a direct effect of BMI on blood pressure disregarding other clinical factors [26]. The results of these findings indicated a mean BMI of $25.62 \pm 8.$ with males having a mean BMI of 25.69 and females having a BMI of 29.58 as compared to the body mass index 24.1 and 24.7, respectively of diabetic patients in Japan [27].

Several studies conducted in Asia identified Stroke and coronary heart diseases are also associated with comorbid conditions of diabetes. Moreover, these studies indicated diabetes as a leading cause of death in patients and with reported stroke rate of 42%, respectively [28]. However, no valuable association was found between BMI and stroke in the epidemiologic report of Japan [29]. Smoking has been reported as a significant associated risk factor for developing diabetes with 44% of the increased risk rate [30]. Cigarette smoking induces insulin resistance and inadequate compensatory insulin secretion responses.

4.1. Conclusion

The study was conducted on a population sample of 265 participants, which were suffering from the diabetes. Noticeably, high BMI was found to be a major risk factor associated with type-II diabetes in this study population. Moreover, patients having a high BMI were also more prone towards comorbidities associated with this disease. Markedly, proper diet and exercise can reduce the risk of type-II diabetes among patients.

REFERENCES

1. Lozano R, Naghavi M, Foreman K, et al. Global and regional mortality from 235 causes of death for 20 age groups in 1990 and 2010: a systematic analysis for the global burden of disease study 2010. *Lancet*. 2012;380(9859):2095–2128. https://doi.org/10.1016/S0140-6736(12)61728-0

2. Takasu N, Yogi H, Takara M, et al. Influence of motorization and supermarket-proliferation on the prevalence of type 2 diabetes in the inhabitants of a small town on Okinawa, Japan. *Inter Med*. 2007;46(23):1899–1904. https://doi.org/10.2169/internalmedicine.46.0387

3. Khang Y-H. Burden of noncommunicable diseases and national strategies to control them in Korea. *J Preven Med Public Health*. 2013;46(4):155–164. https://doi.org/10.3961/jpmph.2013.46.4.155

4. Ikeda N, Inoue M, Iso H, et al. Adult mortality attributable to preventable risk factors for non-communicable diseases and injuries in Japan: a comparative risk assessment. *Plos Med*. 2012;9(1):e1001160. https://doi.org/10.1371/journal.pmed.1001160

5. Kim HC, Oh SM. Noncommunicable diseases: current status of major modifiable risk factors in Korea. *J Prev Med Public Health*. 2013;46(4):165–172. https://doi.org/10.3961/jpmph.2013.46.4.165

6. Mitrakas A, Zaitch D. Law, cybercrime and digital forensics: trailing digital suspects. In: Nemati H, ed., *Information Security and Ethics: Concepts, Methodologies, Tools, and Applications*. IGI Global; 2018:1681–1700. https://doi.org/10.4018/978-1-59904-937-3.ch115

7. Prospective Studies Collaboration. Body-mass index and cause-specific mortality in 900 000 adults: collaborative analyses of 57 prospective studies. *Lancet*. 2009:373(9669);1083–1096. https://doi.org/10.1016/S0140-6736(09)60318-4

8. Chen Y, Copeland WK, Vedanthan R. Association between body mass index and cardiovascular disease mortality in east Asians and south Asians: pooled analysis of prospective data from the Asia Cohort Consortium. *BMJ*. 2013;347:ef5446. https://doi.org/10.1136/bmj.f5446

9. Hu FB, Manson JE, Stampfer MJ, et al. Diet, lifestyle, and the risk of type 2 diabetes mellitus in women. *New Eng J Med*. 2001;345(11):790–797. https://doi.org/10.1056/NEJMoa010492

10. Hu FB, Sigal RJ, Rich-Edwards JW, et al. Walking compared with vigorous physical activity and risk of type 2 diabetes in women: a prospective study. *JAMA*. 1999;282(15):1433–1439. https://doi.org/10.1001/jama.282.15.1433

11. International Diabetes Federation. IDF diabetes atlas. IDF Diabetes Atlas Web site. https://www.diabetesatlas.org/upload/resources/material/20200302_133351_IDFATLAS9e-final-web.pdf. Accessed November 26, 2022

12. Punjab population 2020. Worldometer Web site. https://www.worldometers.info/world-population/pakistan-population/#:~:text=Pakistan%202020%20population%20is%20estimated,of%20the%20total%20world%20population. Accessed November 26, 2020.

13. Charan J, Biswas T. How to calculate sample size for different study designs in medical research? *Ind J Phsychol Med.* 2013;35(2):121–126. https://doi.org/10.4103/0253-7176.116232

14. Center for Disease Control and Prevention. https://www.cdc.gov/healthyweight/assessing/bmi/childrens_bmi/childrens_bmi_formula.html. Accessed November 8, 2020.

15. Hu FB. Globalization of diabetes: the role of diet, lifestyle, and genes. *Diabetes Care*. 2011;34(6):1249–1257. https://doi.org/10.2337/dc11-0442

16. Fuster V, Kelly BB, Vedanthan R. Promoting global cardiovascular health: moving forward. *Circulation*. 2011;123(15):1671–1678. https://doi.org/10.1161/CIRCULATIONAHA.110.009522

17. Islam SM, Purnat TD, Phuong NT, Mwingira U, Schacht K, Fröschl G. Non-Communicable Diseases (NCDs) in developing countries: a symposium report. *Global Health*. 2014;10:e81. https://doi.org/10.1186/s12992-014-0081-9

18. Ramires V, Becker L, Sadovsky A, Zago A, Bielemann R, Guerra P. Evolution of epidemiological research on physical activity and sedentary behavior in Brazil: update of a systematic review. *Revis Brasil de Ativid Física Saúde*. 2014;19(5):529–529. https://doi.org/10.12820/rbafs.v.19n5p529

19. Brasil. Ministério da Saúde. 2020 https://www.saude. gov.br/images/pdf/2020/April/16/Boletim-epidemiologico-SVS-16.pdf. Accessed November 8, 2020.

20. Hayes L, White M, Unwin N, et al. Patterns of physical activity and relationship with risk markers for cardiovascular disease and diabetes in Indian, Pakistani, Bangladeshi and European adults in a UK population. *J Public Health*. 2002;24(3):170–178. https://doi.org/10.1093/pubmed/24.3.170

21. Resnick HE, Redline S, Shahar E. Diabetes and sleep disturbances: findings from the Sleep Heart Health Study. *Diabetes Care*. 2003;26(3):702–709. https://doi.org/10.2337/diacare.26.3.702

22. Oosterman JE, Wopereis S, Kalsbeek A. The circadian clock, shift work, and tissue-specific insulin resistance. *Endocrinology*. 2020:161(12):ebqaa180. https://doi.org/10.1210/endocr/bqaa180

23. Nyamu PN, Otieno CF, Amayo EO, McLigeyo SO. Risk factors and prevalence of diabetic foot ulcers at Kenyatta National Hospital, Nairobi. *East Afr Med J*. 2003;80(1):36–43. https://doi.org/10.4314/eamj.v80i1.8664

24. Vadiveloo T, Jeffcoate W, Donnan PT, et al. Amputation-free survival in 17,353 people at high risk for foot ulceration in diabetes: a national observational study. *Diabetologia*. 2018;61(12):2590–2597. https://doi.org/10.1007/s00125-018-4723-y

25. Franse LV, Valk GD, Dekker JH, Heine RJ, Van Eijk JT. Numbness of the feet'is a poor indicator for polyneuropathy in Type 2 diabetic patients. *Diabetic Med*. 2000;17(2):105–110. https://doi.org/10.1046/j.1464-5491.2000.00223.x

26. Landi F, Calvani R, Picca A. Body mass index is strongly associated with hypertension: results from the longevity check-up 7+ study. *Nutrients*. 2018;10(12):e1976. https://doi.org/10.3390/nu10121976

27. Yokomichi H, Nagai A, Hirata M, et al. Serum glucose, cholesterol and blood pressure levels in Japanese type 1 and 2 diabetic patients: BioBank Japan. *J Epidemiol*. 2017;27(Supplement_III):S92–S97. https://doi.org/10.1016/j.je.2016.12.013

28. Asia Pacific Cohort Studies Collaboration. The effects of diabetes on the risks of major cardiovascular diseases and death in the Asia-Pacific region. *Diabetes Care*. 2003;26(2):360–366. https://doi.org/10.2337/diacare.26.2.360

29. Oki I, Nakamura Y, Okamura T, et al. Body mass index and risk of stroke mortality among a random sample of Japanese adults: 19-year follow-up of NIPPON DATA80. *Cerebrovasc Dis*. 2006;22(5-6):409–415. https://doi.org/10.1159/000094860

30. Willi C, Bodenmann P, Ghali WA, Faris PD, Cornuz J. Active smoking and the risk of type 2 diabetes: a systematic review and meta-analysis. *JAMA*. 2007;298(22):2654–2664. https://ddoi.org/10.1001/jama.298.22.2654

Article QR

Title:	**Screening of Actinomycetes Isolated from Soil and their Antimicrobial Activity against Plant Pathogens**
Author (s):	Rahat Zamir[1,2], Sumaira Mazhar[1], Huma Shafique[1], Roheela Yasmeen[1]
Affiliation (s):	[1]Lahore Garrison University, Pakistan [2]Government College University, Lahore Pakistan
DOI:	https://doi.org/10.32350/sir.73.06
History:	Received: August 16, 2022, Revised: March 16, 2023, Accepted: July 10, 2023, Published: August 28, 2023
Citation:	Zamir R, Shafique H, Yasmeen R, Mazhar S. Screening of actinomycetes isolated from soil and their antimicrobial activity against plant pathogens. *Sci Inq Rev.* 2023;7(3):82–94. https://doi.org/10.32350/sir.73.06
Copyright:	© The Authors
Licensing:	This article is open access and is distributed under the terms of Creative Commons Attribution 4.0 International License
Conflict of Interest:	Author(s) declared no conflict of interest

UMT

A publication of
The School of Science
University of Management and Technology, Lahore, Pakistan

Screening of Actinomycetes Isolated from Soil and their Antimicrobial Activity against Plant Pathogens

Rahat Zamir[1,2], Sumaira Mazhar[1*], Huma Shafique[1] and Roheela Yasmeen[1]

[1]Department of Biology, Lahore Garrison University, Pakistan
[2]Government College University, Lahore Pakistan

ABSTRACT

Actinomycetes abundantly present in soil are renowned for various secondary metabolites production with a wide range of use in diverse fields of life. Many reports are available on the use of actinomycetes for the regulation of pathogenic microbes in plants. For this purpose, this study used thirteen Actinomycetes strains, which were isolated from the fields of Piplan (district Mianwali) Punjab, Pakistan. However, out of thirteen, only seven were found active for the production of both primary and secondary screening. The active seven actinomycetes (AW1, AW2, AW3, AW4, AM1, AC1, and AC2) were separated for their microbial potential against pathogenic strains (*Escherichia coli* and *Staphylococcus aureus*) isolated from the same agriculture soil. About 42.85% of isolated actinomycetes (three out of seven) showed antagonistic properties against *S. aureu* and *E. coli* in primary screening. Thus, it was noticed that the three strains (AW3, AM1, and AC1) had great antimicrobial potential, which showed the most promising results. Whereas in Secondary screening only AC1 showed the best result with ethyl acetate extract as compared to ethanol, methanol, and chloroform. Hence, It was concluded that actinomycetes isolates had great potential for antibacterial activity and they can be used in agriculture industry for the regulation of plant pathogens.

Keywords: Actinomycetes, antimicrobial, metabolites, piplan, primary screening, secondary screening

1. INTRODUCTION

Actinomycetes belong to a group of bacteria placed in order in Actinomycetales, having a distinguished taxonomic group in the bacterial domain; however, with fungi, they share certain morphological features [1]. They are aerobic, spore formers, and Gram-positive. In soil, they create thread-like filaments [2]. They display filamentous growth, producing substrate or aerial mycelium, occasionally coccoid to rod in shape [3].

* Corresponding Author: humashafique@lgu.edu.pk

Actinomycetes DNA has high G+C content in the range of 57-75% [4]. Out of eighteen main lineages of the bacterial domain, Actinomycetes are one of the prime taxonomic units [5]. They cultivate as hyphae and are characteristically capable of the production of soil earthy smell [4, 6]. According to [7] around 100 actinomycetes genera are found in soil and several species, which are primarily found as soil inhabitants.

However, reportedly in the previous literature, Actinomycetes existed as an appearing group of microorganisms, which were extensively dispersed in natural ecosystems around the world [8, 9]. Furthermore, the species had been found in a divergent aquatic environment containing deep ocean sediments [10–12].

It is also known that the Actinomycetes are producers of many secondary metabolites [13]. In actinomycetes, about 70–80% of secondary metabolites are produced by *Streptomyces* genera (almost 500 species); while other genera have less contribution, for example, *Micromonospora, Saccharopolyspora, Actinoplanes,* and *Amycolatopsis* [14]. They have a broad range of utilization within the agricultural, medical, and pharmaceutical industries. In medicine, secondary products are used as antibiotics, antitumors, antiviral, and anti-infection agents [15–17]. Furthermore, actinomycetes would manufacture plant growth promoters to boost plant growth and facilitate the institution of plants under stressed conditions [18, 19]. Secondary metabolites produced by actinomycetes facilitate other microbes by forming mutualistic and symbiotic interactions with them to protect their host from pathogenic microbes [20]. There is scarce data from fields of Piplan (district Mianwali) about the isolation of ascomycetes and their antimicrobial activity from the rhizospheric region of the crops. Therefore, the current study aimed to investigate the isolation of actinomycetes from (fields of piplan) and the use of these strains against pathogenic strains, which were isolated from crops such as maize (*Zea mays*), cotton (*Gossypium*), and wheat (*Triticum aestivum*). The current study would significantly highlight the applications of isolated actinomycetes for the control of plant pathogens strains.

2. MATERIALS AND METHODS

2.1. Collection of Soil Samples

Soil samples were collected from the rhizospheric region of the crops such as wheat (*Triticumaestivum*), cotton (*Gossypium*), and maize (*Zea mays*) for the isolation of actinobacteria.

The soil samples were sited in polythene bags (sterile) during the month of November 2017.

The samples were desiccated at ambient temperature for continuous 2 days and sieved. The sieved soils were then used for the actinomycetes isolation.

2.2. Isolation and Characterization of Actinobacteria

For isolation purpose, enrichment of Actinomycetes in the samples was carried out by physical [21] and chemical treatment [22]. Following physical and chemical treatment 1 gm of soil sample was serially diluted and spread on ISP media supplemented with 50 g/ml antifungal agent nystatin [23]. The isolated actinobacteria (13 strains) were sub-cultured and incubated for 7–12 days at 28°C. However, only seven selected colonies of actinobacteria were noticeably characterized both morphologically and biochemically [24].

2.3. Test Organisms

Pathogenic soil bacterial strains, such as *S. aureus* and *E. coli* were isolated from the same soil samples, which were used to assess the antagonistic activity of actinomycetes. Glycerol stock was prepared to store bacterial strains. It can be used by subculturing when required.

2.4. Primary Screening for the Antibacterial Activity of Actinomycetes

In primary screening, a modified cross-streak process was used to assess antimicrobial activity [25]. From each plate, an isolated colony of actinomycetes was picked and streaked on the modified nutrient agar surface.

A single streak of actinomycetes isolates was created for each isolate, which passed down the middle of the plate and incubated at 28°C for 5-7 days [26]. An upright ribbon growth of the actinomycetes was observed on the plates, followed by the inoculation within 24 hours old culture

pathogenic soil bacterial strains i.e. *E. coli* and *S. aureus*. Then, the plates were further incubated for 24 h at 37 °C [27]. The inhibition zone was measured and recorded after the incubation.

2.5. Secondary Screening for the Antibacterial activity of Actinomycetes

The Agar well diffusion process along with crude extracts of ethanol, ethyl acetate, chloroform, and methanol was used in the secondary screening of the isolate. Submerged fermentation bioactive compound production was done by Chaudhary et al. [2]. A conical 250 ml flask was taken with 50 ml of ISP broth, which was inoculated with Actinomycetes isolates. After the incubation was done at 30°C in a shaking incubator at 150-rpm rotation for continuous 7 days. When fermentation was done and centrifuged at medium twice for 10 min at 10,000 rpm to take out cells and debris and harvested them for fermented broth. Collected crude extracts were tested against test microorganisms (*S. aureus* and *E.coli*) via a method of agar well diffusion [28, 29]. Both test microorganism and cell concentrations were adjusted at 0.5 McFarland turbidity standards. A sterilized cotton swabs were used to inoculate the strains on nutrient agar plates. A sterilized micro tip (1000 µl) was used to bore wells in the plates. Then, the wells were poured with 20, 50, and 100 µl of each crude extract. The plates were incubated at 37°C for 24 h [2]. After incubation, the zone of inhibition was measured and noted for the record.

3. RESULTS AND DISCUSSION

In the last few years, actinomycetes seemed extensively studied in various undiscovered locations in distinct parts of the globe (including Pakistan). However, there are no reports of isolation of actinomycetes from, District: Mianwali Punjab (Pakistan). Therefore, attempts have been made to isolate actinomycetes from this undiscovered area to find new species. From Soil samples, 7 actinomycetes strains (out of 13) were isolated and labeled as Actinomycete wheat 1 (AW1), Actinomycete wheat 2 (AW2), Actinomycete wheat 3 (AW3), Actinomycete wheat 4 (AW4), Actinomycete maize 1 (AM1), Actinomycete cotton 1(AC1), and Actinomycete cotton 2 (AC2). In the current study overall, 53.8 % isolates of actinomycetes were found to be gram-positive organisms and the results were similar with Subhan et al. [30] who identified 55 % isolates of actinomycetes as gram-positive. Furthermore, two pathogenic bacterial

strains (*E.coli* and *S. aureus*) were also isolated, which were characterized both morphologically and biochemically (see Table 1).

Table 1. Morphological and Biochemical Characteristics of Bacterial Strains Isolated from Agricultural Soil

Sr. No.	GS	S	M	C	Sp	F	C	O	In	MR	VP	Cit	Nit	U	H$_2$S
S. aureus	+	Cocci	-	-	-	-	+	-	-	+	+	+	+	+	-
E. Coli	-	Rods	+	-	-	+	+	-	+	+	-	-	+	-	-

Note. GS: Gram Staining; S: Shape; M: Motility; C: Capsule; Sp: Spore; F: Flagella; C: Catalase; O: Oxidase; In: Indole Production; MR: Methyl Red; VP: Voges-Proskauer; C: Citrate Utilization; Nit: Nitrate Reduction; U: Urease; H$_2$S: H$_2$S Production

The morphological characterization of all the seven isolates showed dry and rough to the powdery and smooth texture of isolates. Moreover, the colonies were chalky white, dry, nodular, and sticky on isolation agar of actinomycetes. The morphological and biochemical characteristics suggested that the isolates were representative of genus Actinomycetes (see Table 2). The characteristics of the genus were also in line like the previous findings of Gurung et al. [31] and Anwar et al. [32].

Table 2. Biochemical Characteristics of Actinomycetes Bacterial Strains

Biochemical Test	Isolated strains of Actinomycetes						
	AW1	AW2	AW3	AW4	AC1	AC2	AM1
Catalase	+	-	+	+	+	+	+
Citrate Utilization	+	-	+	+	+	+	-
Urease	+	+	-	-	+	-	+
Methyl Red	+	+	+	+	+	+	+
Voges-Proskauer	-	+	+	+	-	-	-
Melanin Production	+	+	+	-	+	-	+
H$_2$S Production	-	-	+	-	-	-	-
Nitrate Reduction	+	+	+	+	+	-	+
Motility	-	-	-	-	-	-	-
Starch Hydrolysis	+	+	+	+	+	+	+

Note. AW1: Actinomycete wheat 1; AW2: Actinomycete wheat 2; AW3: Actinomycete wheat 3; AW4: Actinomycete wheat 4; AM1: Actinomycete maize 1; AC1: Actinomycete cotton 1 and AC2: Actinomycete cotton 2

In the current study, a soil sample was collected from the surface and rhizospheric region of crops at the depth and it has been found that as a result of appropriate pH and water condition in depth, actinomycetes

quantity at depth is quite higher than the surface of the soil and similar findings were also reported Basavaraj et al. [33].

For antimicrobial potential, strains of actinomycetes were assessed. By perpendicular streak method, primary screenings were performed [29]. Firstly, the perpendicular streak method (primary screening) was used to test actinomycetes strains and it was concluded that three (AW3, AM1, and AC1) out of seven strains (AW1, AW2, AW3, AM1, AC1, AW4, and AC2) (see Table3) showed activity against test *S. aureus* and *E. coli* (gram-positive and gram-negative bacteria). This broad-spectrum activity of actinomycetes may be attributable to the production of more than one antimicrobial compound, which compels the strains more effectively against the both tested bacteria [31]. An overall 42.5% activity of actinomycetes (three out of seven strains) was recorded and founding was in close agreement with Seipke et al. [34] who stated 45 % of isolates; whereas Remya and Kumar [35] reported that 47 % of isolates showed broad-spectrum activity in the primary screening. However, a lower antimicrobial activity of actinomycetes of 38 % (51 out of 134 actinomycetes) were compared to this study, which was reported by Sharma et al. [36]. Similarly, findings of low antimicrobial activity of actinomycetes were reported by [37, 38]. Moreover, Belyagoubi et al. [39] reported a very high level of 72.86 % of antimicrobial activity of actinomycetes as compared to this study's findings.

Table 3. Primary Screening against Bacterial Isolates

Bacterial Isolate	Actinomycetes and zone of inhibition (mm)						
	AW1	AW2	AW3	AW4	AM1	AC1	AC2
Staphylococcus aureus	10.5	0	10.5	0	20.5	20.6	0
Escherichia coli	0	10.5	20.5	0	10.5	20.8	0

Table 4. Secondary Screening Results

Bacterial Isolate	Actinomycetes		
	AW3	AM1	AC1
Staphylococcus aureus	-	-	+
Escherichia coli	-	-	+

For secondary screening, three actinomycetes (AW3, AM1, and AC1) isolates were selected based on the primary screening (see Table 4). The Agar well method was used to perform secondary screening of active

isolates [28, 29]. A finding of secondary screening was conclusive. In all three actinomycete isolates only Actinomycetes AC1 showed great potential for antimicrobial activity as compared to those strains, which exhibit activity in primary screening but did not give antimicrobial activity in secondary screening. The reason behind this is maybe when growing on a solid medium the modification in the morphology of actinomycetes (filamentous mycelia) while in liquid broth (fragmenting mycelia) [28] and mostly actinomycetes are poor fermenters. Actinomycetes release active compounds, which became inactive or stick to the liquid medium component or in broth they modified chemically is also the possibility [31, 40].

Table 5. Zone of Inhibition in mm with Ethyl Acetate Extract

Bacterial Isolate	Zone of inhibition (mm)		
	20μL	50 μL	100 μL
Staphylococcus aureus	3.1	5.5	12
Escherichia coli	2.9	5.1	10

Different solvents were used for the isolation of antimicrobial metabolites including ethyl acetate, ethanol, chloroform, and methanol from the broth. This method is called a solvent extraction method. Only ethyl acetate extract of actinomycetes AC1 exhibited antimicrobial potential against *Staphylococcus aureus* and *Escherichia coli*. The recorded activity of AC1 against *Staphylococcus aureus* was measured by inhibition zone as 3.1, 5.5 and 12 mm with 20, 50, and 100 mg/L concentrated extracts of ethyl acetate respectively. However, the recorded activity of AC1 against *E.coli* was measured by inhibition zone as 2.9, 5.1, and 10 mm with 20, 50, and 100 mg/L concentrated extracts of ethyl acetate respectively (Table:5). It was noticed in the present study, that fermented broth with other solvents did not extract any antimicrobial metabolite as no inhibition zone was observed with any concentration. Gurung et al. [31] findings with other solvents suggest the failure of metabolite extraction may be due to the existence of polar functional group in a secondary metabolite that form metabolite soluble in water and insoluble in solvent, the use of inappropriate solvents and inadequate shaking of the mixture.

3.1. Conclusion

The current study showed that isolates of Actinomycetes, found in Piplan soil of Mianwali, had the potential to use it as sources for the novel

antibacterial compounds against pathogenic microorganisms of soil. Isolate AC1 exhibited the highest activity in secondary screening against both gram-positive and gram-negative test bacteria. However, further work in this research is required about AC1 for its practical application in this field.

REFERENCES

1. Hirsch CF, Christensen DL. Novel method for selective isolation of actinomycetes. *Appl Environ Microbiol*. 1983;46(4):925–929. https://doi.org/10.1128/aem.46.4.925-929.1983.

2. Chaudhary HS, Yadav J, Shrivastava AR, Singh S, Singh AK, Gopalan N. Antibacterial activity of actinomycetes isolated from different soil samples of Sheopur (A city of central India). *J Adv Pharma Technol Res*. 2013;4(2):118–123. https://doi.org/10.4103%2F2231-4040.111528

3. Adegboye MF, Babalola OO. Taxonomy and ecology of antibiotic producing actinomycetes. *Afr J Agric Res*. 2012;7(15):2255–22561. https://doi.org/10.5897/AJARX11.071

4. Boroujeni ME, Arijit D, Prashanthi K, Sandeep S, Sourav B. Enzymatic screening and random amplified polymorphic DNA fingerprinting of soil streptomyces isolated from Wayanad district in Kerala, India. *J Biol Sci*. 2012;12(1):43–50. https://doi.org/10.3923/jbs.2012.43.50

5. Jeffrey LS. Isolation, characterization and identification of actinomycetes from agriculture soils at Semongok, Sarawak. *Afr J Biotechnol*. 2008;7(20): 3697–3702

6. Sprusansky O, Stirrett K, Skinner D, Denoya C, Westpheling J. The bkdR gene of Streptomyces coelicolor is required for morphogenesis and antibiotic production and encodes a transcriptional regulator of a branched-chain amino acid dehydrogenase complex. *J Bacteriol*. 2005;187(2):664–671. https://doi.org/10.1128/jb.187.2.664-671.2005

7. Yamamoto Y, Kouchiwa T, Hodoki Y, Hotta K, Uchida H, Harada KI. Distribution and identification of actinomycetes lysing cyanobacteria in a eutrophic lake. *J Appl Phycol*. 1998;10:391–397. https://doi.org/10.1023/A:1008077414808

8. Singh R, Dubey AK. Diversity and applications of endophytic actinobacteria of plants in special and other ecological niches. *Front Microbiol*. 2018;9:e1767. https://doi.org/10.3389/fmicb.2018.01767

9. Tandale A, Khandagale M, Palaskar R, Kulkarni S. Isolation of pigment producing actinomycetes from soil and screening their antibacterial activities against different microbial isolates. *Int J Curr Res Life Sci*. 2018;7(6):2397–2402.

10. Arifuzzaman M, Khatun MR, Rahman H. Isolation and screening of actinomycetes from Sundarbans soil for antibacterial activity. *Afr J Biotechnol*. 2010;9(29):4615–4619.

11. Ayoubi H, Mouslim A, Moujabbir S, et al. Isolation and phenotypic characterization of actinomycetes from Rabat neighborhood soil and their potential to produce bioactive compounds. *Afr J Microbiol Res*. 2018;12(8):186–191. https://doi.org/10.5897/AJMR2017.8761

12. Kirby BM, Roes-Hill ML, Cary SC, Burton SG, Tuffin IM, Cowan DA. Actinobacterial Diversity Associated with Antarctic Dry Valley Mineral Soils. In: de Bruijn FJ, ed. *Handbook of Molecular Microbial Ecology II: Metagenomics in Different Habitats*. Wiley-Blackwell; 2011:125–33. https://doi.org/10.1002/9781118010549.ch13

13. George M, Anjumol A, George G, Hatha AM. Distribution and bioactive potential of soil actinomycetes from different ecological habitats. *Afr J Microbiol Res*. 2012;6(10):2265–2271. https://doi.org/10.5897/AJMR11.856

14. Berdy J. Bioactive microbial metabolites. *J Antibiot*. 2005;58(1):1–26. https://doi.org/10.1038/ja.2005.1

15. Chen Y, Zhou D, Qi D, Gao Z, Xie J, Luo Y. Growth promotion and disease suppression ability of a Streptomyces sp. CB-75 from banana rhizosphere soil. *Front Microbiol*. 2018;8:e2704. https://doi.org/10.3389/fmicb.2017.02704

16. Gallagher KA, Fenical W, Jensen PR. Hybrid isoprenoid secondary metabolite production in terrestrial and marine actinomycetes. *Curr Opinion Biotechnol*. 2010;21(6):794–800. https://doi.org/10.1016/j.copbio.2010.09.010

17. Igarashi Y. Screening of novel bioactive compounds from plant-associated actinomycetes. *Actinomycetologica*. 2004;18(2):63–66. https://doi.org/10.3209/saj.18_63

18. Bonjar GS. Broadspectrim, a Novel Antibacterial from Streptomyces sp. *Biotechnology*. 2004;3:126–130.

19. Srivastava S, Patel JS, Singh HB, Sinha A, Sarma BK. Streptomyces rochei SM 3 induces stress tolerance in chickpea against Sclerotinia sclerotiorum and NaCl. *J Phytopathol*. 2015;163(7-8):583–592. https://doi.org/10.1111/jph.12358

20. Seipke RF, Kaltenpoth M, Hutchings MI. Streptomyces as symbionts: An emerging and widespread theme? *FEMS Microbiol Rev*. 2012;36(4):862–876. https://doi.org/10.1111/j.1574-6976.2011.00313.x

21. Seong CN, Choi JH, Baik KS. An improved selective isolation of rare actinomycetes from forest soil. *J Microbiol*. 2001;39(1):17–23.

22. Oskay M. Comparison of Streptomyces diversity between agricultural and non-agricultural soils by using various culture media. *Sci Res Essays*. 2009;4(10):997–1005.

23. Taechowisan T, Peberdy JF, Lumyong S. Chitinase production by endophytic Streptomyces aureofaciens CMUAc130 and its antagonism against phytopathogenic fungi. *Ann Microbiol*. 2003;53(4):447–462.

24. Ali B, Sabri AN, Ljung K, Hasnain S. Quantification of indole-3-acetic acid from plant associated Bacillus spp. and their phytostimulatory effect on Vigna radiata (L.). *World J Microbiol Biotechnol.* 2009;25:519–526. https://doi.org/10.1007/s11274-008-9918-9

25. Holt JG. *Bergey's manual of systemic bacteriology*. UK: Cambridge University Press; 1989.

26. Hemashenpagam N. Purification of secondary metabolites from soil actinomycetes. *Int J Microbiol Res*. 2011;3(3):148–156.

27. Bizuye A, Moges F, Andualem B. Isolation and screening of antibiotic producing actinomycetes from soils in Gondar town, North West Ethiopia. *Asian Pacific J Trop Dis*. 2013;3(5):375–381. https://doi.org/10.1016/S2222-1808(13)60087-0

28. Budhathoki S, Shrestha A. Screening of actinomycetes from soil for antibacterial activity. *Nepal J Biotechnol*. 2020;8(3):102–110. https://doi.org/10.3126/njb.v8i3.33664

29. Wahab A, Shumaila S, Subhan SA, Ali ST, Mujahid TY. Isolation and identification of actinomycetes isolated from Karachi soil and screening of antimicrobial compounds. *Int J Curr Res*. 2015;7(2):12760–12765.

30. Subhan SA, Wahab A, Mujahid TY, Abbas T, Khan I, Idrees S. Screening of actinomycetes from indigenous soil for production of extracellular metabolites. *Int J Curr Res.* 2015;7:12078–12083. https://doi.org/10.1016/S2222-1808(13)60087-0

31. Gurung TD, Sherpa C, Agrawal VP, Lekhak B. Isolation and characterization of antibacterial actinomycetes from soil samples of Kalapatthar, Mount Everest Region. *Nepal J Sci Technol*. 2009;10:173–182. https://doi.org/10.3126/njst.v10i0.2957

32. Anwar S, Ali B, Sajid I. Screening of rhizospheric actinomycetes for various in-vitro and in-vivo plant growth promoting (PGP) traits and for agroactive compounds. *Front Microbiol*. 2016;7:e1334. https://doi.org/10.3389/fmicb.2016.01334

33. Basavaraj KN, Chandrashekhara S, Shamarez AM, Goudanavar PS, Manvi FV. Isolation and morphological characterization of antibiotic producing actinomycetes. *Trop J Pharma Res.* 2010;9(3):231–236. https://doi.org/10.4314/tjpr.v9i3.56282

34. Seipke RF, Kaltenpoth M, Hutchings MI. Streptomyces as symbionts: an emerging and widespread theme? *FEMS Microbiol Rev*. 2012;36(4):862–876. https://doi.org/10.1111/j.1574-6976.2011.00313.x

35. Remya M, Vijayakumar R. Isolation and characterization of marine antagonistic actinomycetes from west coast of India. *Med Biol*. 2008;15(1):13–19.

36. Sharma D, Kaur T, Chadha BS, Manhas RK. Antimicrobial activity of actinomycetes against multidrug resistant Staphylococcus aureus, E. coli and various other pathogens. *Trop J Pharma Res*. 2011;10(6):801–808. https://doi.org/10.4314/tjpr.v10i6.14

37. Pandey B, Ghimire P, Agrawal VP. Studies on the antibacterial activity of the Actinomycetes isolated from the Khumbu region of Nepal. *J Biol Sci*. 2004;23:44–53.

38. Rana S, Salam MD. Antimicrobial potential of actinomycetes isolated from soil samples of Punjab. India. *J Microbiol Exp*. 2014;1(2): 63–68. https://doi.org/10.15406/jmen.2014.01.00010

39. Belyagoubi L, Belyagoubi-Benhammou N, Jurado V, et al. Antimicrobial activities of culturable microorganisms (actinomycetes and fungi) isolated from Chaabe Cave, Algeria. *Int J Speleol*. 2018;47(2):189–199. https://doi.org/10.5038/1827-806X.47.2.2148

40. Aedms H, Sheir DH, Eldewany AI. Production of antimicrobial agent from marine bacteria Isolated from Mediterranean. *Aust J Basic Appl Sci*. 2011;5(5):121–128.

Article QR

Title:	**Synthesis, Properties, and Applications of Carbon Nanotubes: An Overview**
Author (s):	Shabbir Hussain[1], Uzma Akbar[2], Muhammad Ahmad[3], Muhammad Ibrar[4], Zulfiqar Ali[5], Muhammad Waqas[4], Sheikh Asrar Ahmad[6], Syed Mustansar Abbas[7], Habib Ullah[4], Sehrish Anwar[4]
Affiliation (s):	[1]Khwaja Fareed University of Engineering and Information Technology Rahim Yar Khan, Pakistan [2]Minhaj University Lahore, Pakistan [3]University of Education, Lahore, Pakistan [4]Lahore Garrison University, Lahore, Pakistan [5]University of Engineering & technology Lahore, KSK Campus, Pakistan [6]University of Education, Lahore, Vehari Campus, Pakistan [7]National Centre for Physics, Islamabad, Pakistan

UMT

A publication of
The School of Science
University of Management and Technology, Lahore, Pakistan

Synthesis, Properties, and Applications of Carbon Nanotubes: An Overview

Shabbir Hussain[1*], Uzma Akbar[2], Muhammad Ahmad[3], Muhammad Ibrar[4], Zulfiqar Ali[5], Muhammad Waqas[4], Sheikh Asrar Ahmad[6], Syed Mustansar Abbas[7], Habib Ullah[4], and Sehrish Anwar[4]

[1]Institute of Chemistry, Khwaja Fareed University of Engineering and Information Technology, Rahim Yar Khan, Pakistan

[2]Department of Chemistry, Minhaj University, Lahore, Pakistan

[3]Department of Chemistry, Division of Science and Technology, University of Education, Lahore, Pakistan

[4]Department of Chemistry, Lahore Garrison University, Pakistan

[5]Department of Basic Sciences & Humanities, University of Engineering & Technology, Lahore, Pakistan

[6]Department of Chemistry, University of Education, Lahore, Vehari Campus, Pakistan

[7]Nanoscience and Technology Department, National Centre for Physics, Islamabad, Pakistan

ABSTRACT

The current study attempts to review the literature concerning the synthesis, properties, and application of carbon nanotubes (CNTs). The methods used to produce carbon nanotubes include laser ablation, electric arc discharge, chemical vapor deposition, plasma-enhanced chemical vapor deposition, pulsed laser deposition, use of low-frequency ultrasound waves, heating a bulk polymer, and bulk sputtering. CNTs have excellent mechanical and thermal properties that strongly depend upon their structure. Functionalized magnetic CNTs are involved in magnetic force microscopy used in biomedicine. The liquid and plastic limit of kaolinite can be increased by adding CNTs to it. In the medical field, CNTs have numerous applications including gene delivery to cells, cancer therapy, drug delivery, and tissue regeneration. Their antioxidant nature also enables them to be used in cosmetic products and in the field of dermatology. They are also used to purify the environment, water, and in modern food-packaging technology. The sensors containing CNTs composite pellets are sensitive to gases, such as NH_3, CO_2, and CO H_2O. CNTs are used to construct gas containers for hydrogen storage. They are also considered ideal for structural applications and their properties can be

* Corresponding Author: shabchem786@gmail.com

improved by making their composites with metals. Such metals may be introduced into the core of CNTs by different methods including solid-state reaction, arc-discharge method, and electrochemical techniques. The value of absorbed hydrogen gas in CNTs varies between 0.4 and 67 mass %. Recent advances encourage more research on CNTs to increase their clinical applications in the future.

Keywords: carbon nanotubes (CNTs), metals, properties, synthesis

1. INTRODUCTION

Carbon plays an important role in almost all fields of science and technology, especially as a source of energy [1]. Carbon nanotubes (CNTs) possess outstanding electrical and mechanical properties, which are used as an important component of flexible batteries [2]. They are hollow cylindrical structures rolled into a cylinder akin to a honeycomb lattice. The internal diameter of CNTs lies in the range of nanoscale or is 1µm in length. The history of carbon nanotubes (CNTs) started in 19th century, certainly from World War 2 when carbon fiber was first synthesized by Thomas A. Edison for electric light bulbs as a filament [3]. CNTs fall into two categories, namely single-walled carbon nanotubes (SWCNTs) and multi walled carbon nanotubes (MWCNTs). The toughness and higher thermal conductance are owed to the presence of sp^2 hybridization in CNTs. SWCNTs are insoluble in both organic and inorganic solvents, although they may be soluble after complexation and polymerization. When SWCNTs are added to aniline (organic solvent) then SWCNT-aniline charge transfer complex is formed that makes SWCNTs soluble in organic solvents and preserves their pristine nature, as proved by various analysis tools [4].

CNTs comprise graphite sheets rolled into a cylindrical pattern and have various applications in the fields of medicine and material sciences [5]. They have widespread applications in every aspect of life, such as film and coatings and also in the fields of biotechnology, electronics, environment, energy storage, and many others due to their unique higher thermal conductivities, toughness, and electrical conductivity [6].

Keeping in view the great importance of nanotechnology in various fields [7–10], the current study reviews the literature concerning the synthesis, properties, and uses of carbon nanotubes (CNTs).

2. SYNTHESIS OF CARBON NANOTUBES (CNTS)

The methods used to produce CNTs include laser vaporization, electric arc discharge, chemical vapor deposition [11], decomposition of SiC, dipping graphite in cold water, torsion of graphene layers, as well as, mechano-thermal, pyrolysis, solar energy, liquid phase, electrolysis, and heat treatment of polymers [12].

Historically, electric arc discharge was the first method used for the formation of CNTs. Arc discharge method technically resembled the laser evaporation process. Comparison between these two methods (laser evaporation process and electric arc discharge) that shows that there is a difference in the purity and quality of the obtained products. However, the most favorable and developed techniques used for the synthesis of CNTs and related to materials on a large scale, which include different types of chemical vapor deposition (CVD) and arc discharge [13]. Consequentially, CNTs were synthesized using various techniques, such as laser ablation or arc discharge. However, in present days, CVD ($<80^0$C) has replaced these techniques (laser ablation and arc discharge) because this method accurately controls the nanotube diameter, length, density, purity, orientation, and alignment [14].

2.1. Electrical Arc Discharge Method

The arc discharge method involves the vaporization of carbon by applying electric field at a high-temperature gradient. This process may be improved in the presence of numerous metal catalysts (for instance, iron, cobalt, nickel, yttrium, boron, and gadolinium) under the reduced pressure of the inert gas [15] It also creates plasma in a glass chamber due to the transfer of energy from the arc to the graphite anode doped with a catalyst. The arc discharge setup involves two graphite rods, which act as anode and cathode and have a diameter of 20 mm and 7 mm, respectively. An arc is produced when 100–200 ampere current is provided between the electrodes [16]. Generally, multi-walled carbon nanotubes (MWCNTs) are produced when no catalysts are applied. However, single walled carbon nanotubes (SWCNTs) are synthesized in the presence of a transitional metal catalyst. The high-temperature arc discharge method (above 1700°C) results in the formation of a mixture product and requires the separation of CNTs from both coal and the remaining metals (catalytic) [17]. The catalyst composed of nano-sized metal particles (such as Ni, Co, or Fe), which cause the disintegration of the precursor molecules of

gaseous hydrocarbon into carbon [18]. Needle-like CNTs with approximately 1 mm of length and 4-30 nm diameter can be produced on carbon cathode by using the direct arc discharge evaporation of carbon. Lijima et al. used the pressurized chamber filled with a gaseous mixture of 40 torr argon and 10 torr methane [19]. The high yield production of CNTs depends on the concentration and nature of catalysts, gases that are composed of plasma, the pressure of inert gas, the arc current intensity, and the distance between the electrodes [17]. Figure 1 displays a 15 kW xenon short-arc lamp used in the IMAX projection system.

Figure 1. A 15 kW xenon Short-Arc Lamp

Source. https://en.wikipedia.org/wiki/Arc_lamp

2.2. Laser Ablation Technique

CNTs can be produced using the laser ablation method (Figure 2). Normally, a laser is directed on the targeted carbon, which vaporizes a small quantity of material inside an oven warmed up to 1200°C. The smooth beam of laser on the target is ensured by a computer control system [20]. The plasma produced by this method is usually swept by nitrogen or argon from a high-temperature gradient and deposited onto the surface of the substrate, which is cooled by the external cooling system. Pulsed or continuous laser vaporizes 1.2% of Co/Ni with 98% composite of graphite target under 500 torr of the inert atmosphere of helium at 1200°C in quartz furnace. A plume forms vapors at this high temperature which rapidly expands and cools. A large cluster is formed by the quick

compression of small carbon molecules or atoms to cool down the vapors [21]. The growth of nanotubes is stopped when the carbon layer cannot absorb particles anymore because the surface is already occupied and has no space for the coming particles. MWCNTs are formed by using a pure graphite target. The SWCNTs yield depends strongly on the metal catalyst type and it can be increased by increasing the temperature of the furnace, among other factors [12]. Laser ablation is the best method to grow SWCNTs with a high purity and a high quality [17].
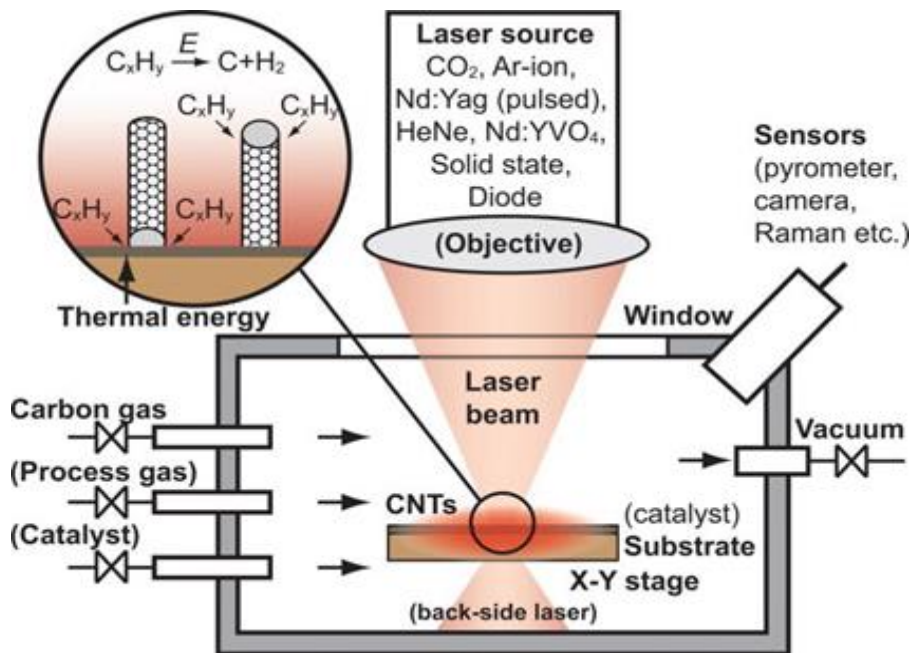
Figure 2. Laser Ablation Setup for CNT Synthesis [22]

2.3. Chemical Vapor Deposition (CVD) Method

In electronics and CMOS industry, chemical vapors deposition (CVD) is the most suitable technique for the synthesis of CNTs as compared to laser ablation and arc discharge methods. This technique can synthesize CNTs at a lower temperature [23]. CVD yields very pure and high-performance solid materials. This technique can be used to synthesize the materials in which vapor phase chemical components react at specific surfaces to form solid films [24].

CVD was first reported in 1996 for the production of nanotubes. In CVD, vacuum deposition occurs for the production of CNTs. In this process, the substrates are exposed to a volatile precursor which reacts or decompose on the surface of the substrates. This method is useful for the production of nanotubes in a high quantity and also to control the growth direction onto the substrate [25]. The synthesis of CNTs through CVD involves the sputtering of a transition metal catalyst onto the substrate. It also uses thermal annealing or chemical etching to induce nucleation in the catalyst particle. Clusters are formed on the substrate as a result of thermal annealing and nanotubes are grown [26].

In the reaction chamber, there is a gas phase in which the carbon source is placed. Then, by using an energy source such as plasma, carbon molecule or heating coil is converted to an atomic level. Carbon monoxide, methane, or acetylene can be used as a carbon source [27]. Generally, CVD utilizes a temperature range of 650–900ºC for the synthesis of nanotubes, with the consequent yield of about 30% [26]. MWCNTs are produced by thermal CVD methods, using acetylene or ethylene gas as the feedstock of carbon in the presence of Ni, Co, or Fe nanoparticles as a catalyst. At these temperatures, carbon atoms are dissolved into metal nanoparticles which finally become saturated and the precipitation of carbon forms CNTs. The size of the metal particles (catalysts) can help to determine the diameter of CNTs. When other elements such as Mn, Cr, and Cu are used, CNTs are formed only in minute amounts [28].

The percentage yield of CNTs varies depending upon their synthetic methodology. Table 1 gives a brief comparison between CVD, laser ablation, and arc discharge methods.

Table 1. Comparison between Different Synthesis Methods

Arc discharge method	Laser ablation method	Chemical vapor deposition
➤ With the help of the arc discharge tube method, we can synthesize up to 30% by weight of both MWCNTs and SWCNTs [29].	➤ The yield of the laser ablation method is about 70% of SWNTs with a measurable diameter, which is controlled by the	➤ For the synthesis of carbon nanotubes, CVD is known as the most widely used method [30]. ➤ The removal of catalyst by acid treatment may

Arc discharge method	Laser ablation method	Chemical vapor deposition
➤ The synthesis of carbon nanotubes requires a temperature above 1700 ºC. ➤ The synthesis is performed in an arc discharge tube. This method causes less structural distortions [14].	temperature of reaction. ➤ In comparison with chemical vapor deposition, arc discharge method is much expensive [29].	cause destruction of the original structure of carbon nanotubes. ➤ The yield may be increased by the use of catalysts like MgO or Al_2O_3 [31].

2.4. Plasma-enhanced Chemical Vapor Deposition (PECVD)

PECVD is a versatile technique that is used to obtain vertically dense aligned CNTs at lower temperature, as compared to the one's used in CVD. It is a latest procedure for the selective positioning and vertical alignment of CNTs. In PECVD, the activation energy for the CVD reaction is provided not only by elevating temperature gradient but also by the energetic plasma formation in an electric field [32].

2.5. Pulsed Laser Deposition Method

The CNTs can be synthesized by the pulsed laser deposition method. This is a thin film deposition method in which the targeted material is evaporated by a pulse of laser beam and a film is deposited on the substrate surface. The furnace contains the targeted substance placed at the bottom in which the substrate is placed at the top side of the furnace. The laser beam normally used is Nd: YAG. The laser beam strikes the targeted atom and vaporize them. The vaporized atoms are called a plume. The plume is moved towards the substrate, deposited and grows as carbon nanotubes upon the substrate surface [33]. The rate of deposition and the laser beam can be collaborated to control certain parameters of the CNTs. These CNTs are deposited in the substrate surface that can be separated from the carbon nanoparticles, amorphous carbon, and other unwanted impurities. These prepared CNTs can be purified by several methods that includes gas-phase purification and liquid phase purification, which are used most commonly for the purification procedure [34].

2.5.1. Gas-phase Purification. In the gas-phase purification method, CNTs are purified by applying high-temperature oxidation, which is continued by the repeated extractions with nitric acid and HCl. In this process, the synthesized CNTs have a high purity and stability, including little impurities or residual catalyst [34].

2.5.2. Liquid phase Purification. In liquid phase purification, the CNTs are purified in several steps, which mainly include:

i.   The preliminary filtration, which is done to remove the bulk residual graphite particles.

ii. Then the CNTs are dissolved in both conc., acid, and organic solvents to remove the unreacted catalyst and fullerenes.

iii. Next is the centrifugal separation of CNTs from the solution.

iv. Then microfiltration is done.

v.   The final step of purification is chromatography, which is used to separate the MWCNTs and SWCNTs [34].

2.6. Modification of CNTs by Low-Frequency Ultrasound Waves

Multi-walled carbon nanotubes (CNTs) can be modified by treating with 20 kHz ultrasound in combination with dilute HNO_3 and dilute H_2SO_4 for 30 min at 12 W cm^{-2} sonication. These specified conditions prevent the aggregation of the nanotubes and allow an efficient dispersion in ethanol or in chitosan [35].

2.7. Synthesis of CNTs through Bulk Polymer

The CNTs can be synthesized by heating a bulk polymer at about 400 $^{\circ}$C in the air. This can be obtained by polyesterfication reaction of ethylene glycol and citric acid. The formation of CNTs is confirmed by the number of spectroscopic analyses. The lengths of CNTs is generally less than 1 μm, whereas their diameter ranges from 5-20 nm [36].

2.8. Synthesis of CNTs through Bulk Sputtering

One of the most promising methods among all is bulk sputtering method, which may be employed for the mass production of CNTs, however, this process is overpriced[37]. During the process of sputtering, the targeted graphene is usually placed as the targeted material in the chamber. The reaction chamber is filled with an inert argon gas, which is

commonly used when an inert atmosphere is required or for the production of titanium and other reactive material. The electric field is applied between the two electrodes, which accelerate the ionization process of argon gas to produce the charged particles that strike the surface of the targeted graphene material and eject the carbon atoms from the surface of graphene [38]. The CNTs are grown on the surface of the substrate. Thus, the CNTs prepared by this method are impure and can be purified by several other methods [37].

3. PROPERTIES

Carbon nanotubes (CNTs) have unique properties due to which they are found in numerous applications, which have a great impact on human health. However, some chemicals have also evolved during CNTs production and handling, which are usually inhaled during the inhalation process [39]. The tensile strength of CNTs is hundred times greater than their steel and thermal/electrical conductivities, which are comparable to copper [25]. CNTs show significant properties including physicochemical properties, metallic or semi-metallic characteristics, great mechanical and electrical characteristics, good thermal conductivity, high electrical conductivity, and a large surface area [40]. They are considered ideal for the production of next-generation composite materials due to their specific properties [41]. The properties of CNTs can be modified by doping with heteroatoms such as nitrogen and boron to tune their physicochemical characteristics for specific applications [42].

3.1. Electronic Properties

CNTs possess hollow cylinders with approximately 20 carbon atoms around the circumference of the cylinders and microns in length. They can act as semiconductors or conductors depending on their structure and possess characteristic electronic properties. CNTs have unusual electronic properties due to their high electrical conductivities as compared to copper. The symmetry of the planner system can be broken down by rolling action, which causes a specific direction with respect to the hexagonal lattice and axial directions [43]. Different theoretical and experimental works suggest that single-walled CNTs are considered as quantum wires, which have one dimension [44]. The graphene sheet is the main site for single-walled CNTs having a main electronic structure and is considered to possess metal properties with bands of conduction [45].

Moreover, carbon nanotubes are also considered as an example of ideal quantized one-dimensional conductors [46].

3.2. Mechanical Properties of CNTs

CNTs are one-dimensional materials that display the mechanical properties, such as the tensile strength and young's modulus. However, it is difficult to produce the pure form of CNTs and to control and manage their properties. Due to these properties, CNTs are considered good for polymer enforcement. The extensive mechanical characteristics of CNTs are due to the sp^2 hybridization of carbon-carbon double bond. The densities of carbon nanoparticles are very low (1.3 gcm^{-3}) as compared to stainless steel. Young's modulus of CNTs is higher than carbon fibers with larger values than that of 1TPa, which is about five times larger than steel [43]. CNTs have excellent mechanical properties that strongly depend upon their structure. There are three kinds of nanotubes (SWNTs, MWNTs, and catalytic MWNTs) studied under laboratory actions that always consist of structural defects [47]. The calculation for the stiffness constant of SWNTs can be done by adopting the elastic modulus of graphite to understand the important properties like mechanical properties of graphite of a single crystal [48].

3.3. Thermal Properties of CNTs

One of the most important properties of CNTs is thermal property, which is directly related to their small sizes and unique structures. Thermal and specific heat conductivity of bulk MWNTs can help to measure the thermal properties of carbon nanoparticles [49]. The thermal characteristics of CNTs are directly related to each other's as the size of devices (electronic or mechanical) are reduced to the micro and nanometer level. With the help of molecular modeling predictions, the studies of nano-electronic devices became very easy, however, it is quite difficult to measure the accurate thermal properties [50]. The excellent thermal conductivity of 3000 W/m K at room temperature of SWNTs makes them important for thermal applications [51]. The high thermal conductivity of nanotubes has a number of applications in thermal management such as heat sinking of silicon processors, or increasing the thermal conductivity of plastics in areas of housing for electric appliances [52]. Carbon nanotubes show greater variations in thermal conductivities and the

conductivity of nanotubes is greater along the axis due to greater anisotropic property [53].

3.4. Magnetic Characteristics and Heat Generation

CNTs are widely accepted due to their fundamental properties. The basic field interest of CNTs is the magnetic functionalization, which has a wide applications as nano-scaled magnetic objects [54]. The semiconducting and metallic properties of CNTs can be predicted by both first principal calculation and tight binding that depends upon their size and helicity. Few unusual characteristics were demonstrated by many recent experiments [55]. For a magnetic field, high diamagnetic sensitivity is found in both perpendicular and parallel axis of the tube [56]. Specifically, the magnetic functionalization gives tremendous potential to CNTs that can provide a practical approach to give a stable coating for protection from degradation and oxidation. The functionalized magnetic CNTs are involved in magnetic force microscopy, which is used in biomedicine in the form of magnetic nano-vectors or spintronics [57].

3.5. Carbon Nanotubes (CNTs) Composites

Due to the magnificent physical properties of CNTs, they form a metal matrix with the metals to take the advantage of their high tensile strength and electric conductivity. They are also considered ideal for structural applications and their properties can be improved by making their composites with metals. The following techniques are used for the fabrication of CNTs polymer nanocomposite material.

3.5.1. Solvent Casting. It is an important procedure for the preparation of CNTs concentrated polymer nanocomposite materials. These solvents have a significant influence on the properties of nanocomposites. The in solvent casting of the nanotubes is facilitated by dispersion and it involves the preparation of a suspension of CNTs in the solution of a desirable polymer by energetic agitation. The process involves the dissolution of a polymer in an organic solvent and then the addition of particles (generally salts) with specific dimensions to the solution. It is followed by the shaping of consequent mixture, its final geometry a membrane that can be produced by casting it onto a glass plate or a scaffold is formed by using a three-dimensional mold. After evaporation of solvent evaporates, a composite material is produced, which contains the particles together with the polymer [58].

3.5.2. Melt Mixing Method. CNTs can also be synthesized by the melt mixing method, which is used for the thermoplastic polymers that gets soften on heating. This process involves an elevated temperature gradient to decrease the viscosity of the substrate and high shear forces to the nanotubes bundle. Templates of numerous shapes can then be obtained by various fabrication techniques, including injection molding, compression molding or extrusion formed composites of commercial polymers, such as acrylonitrile butadiene styrene (ABS) with MWCNT, polypropylene, and high impact polystyrene [59].

For the achievement of multifunction and high-performance stability, CNTs are considered to be an ideal filler for polymer type matrixes, due to their sizes in nanometers, high and well-known aspect ratio, and more specifically due to their amazing strength and high thermal and electrical conductivities [60]. Solution casting and melt blending are the most common methods that are used to produce polymer composites; inorganic fillers may also be used in making carbon nanotubes-polymer composites [61]. In recent times, fabrication of CNTs with the polymeric substances gives the characteristics synergistic effects to the host and boosts a vast interest in the development of multifunctional CNTs along with alternative materials [62].

4. APPLICATIONS OF CARBON NANOTUBES (CNTS)

Nanoparticles are found in a broad range of biological [63–66] and non-biological applications [67–70]. CNTs functional materials (CNTFMs) had shown a potential impact on the fields of science, engineering, and technology with the transformation of nanoscience towards a practical applications [71].

4.1. Carbon Nanotubes as Stabilizers

The liquid and plastic limit of kaolinite can be increased by the significant addition of CNTs to it. The resultant mixture would have lower soil strength, higher compressibility, and reduced hydraulic conductivity [72]. The presence of CNTs in construction materials increase the mechanical strength of a material. It has the capacity to increase the flexibility of a material [73]. It also decrease the breakability of a material. Soil cement itself is not a flexible material and it can be easily broken by applying stress. Consequently, materials which are made by only soil-

cement can be easily breakable by applying any kind of stress. CNTs have significantly solved such type of problems [74].

4.2. CNTs Applications in the Medical Field

In the medical field, CNTs have numerous applications including gene delivery to cells, cancer therapy, drug delivery, and tissue regeneration. MWNTs and SWNTs have a greater potential to improve the traditional drug delivery to the cells [75]. CNTs as compared to other nanocarriers that can be easily modified for conjugation of bioactive compounds and ligands for the targeting process. Additionally, they also found diagnostic applications to drug delivery [76]. The use of CNTs in the nerve tissue are explained in several reports [77].

CNTs applications are also found in drug delivery, genes, cells, and cytokines. Moreover, they can also develop tissue induction and cell activation properties along with futuristic biomaterials characteristics, which are beneficial for the human body. For the self-repaired potential of the human body, it is very important to use CNTs flexibly to adapt to their environment [78]. Their solubility is applicable in biocompatibility, secretion, blood transportation, and gastrointestinal absorption. The CNTs composites are also involved in therapeutic drug delivery systems [79]. Significantly, CNT dispersions should have a uniform and stable distribution to a sufficient degree for an accurate concentration. The solubility of pristine CNTs in the aqueous solution is an important factor for their use as a practical drug carrier, which can be owed to the hydrophobic property of the graphene sidewalls and also π-π strong interaction between CNTs. There had been a prime focus on nano-carbon biomaterial research and its development over the last 15 years. However, it is strongly believed that this focus would lead to paradigm shifts and lead to major advancements in global medicine by following the road towards clinical applications [80].

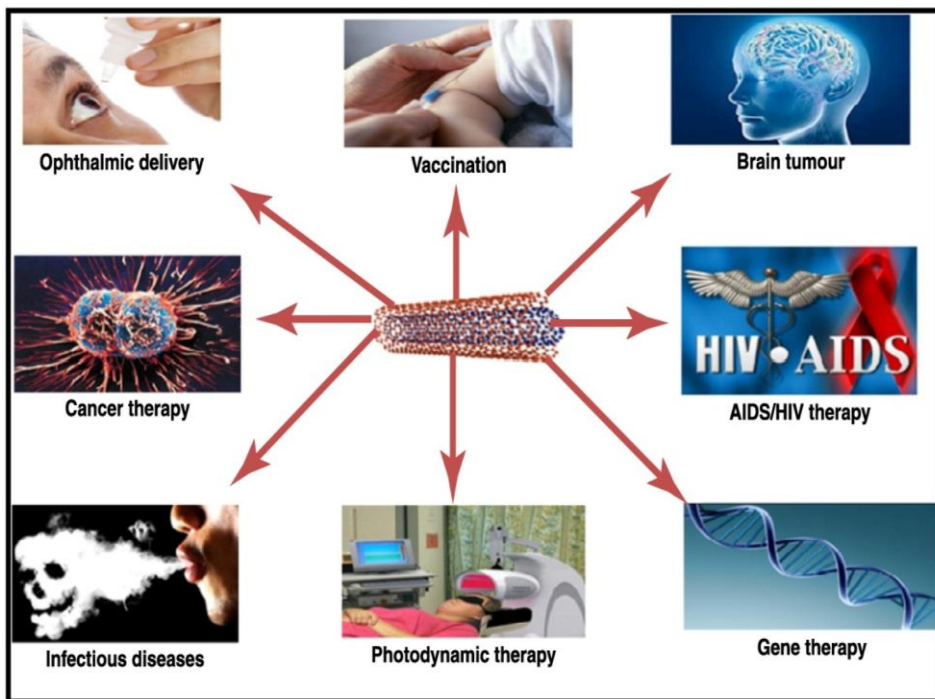Figures 3 and 4 display important applications of CNTs in the field of medical.

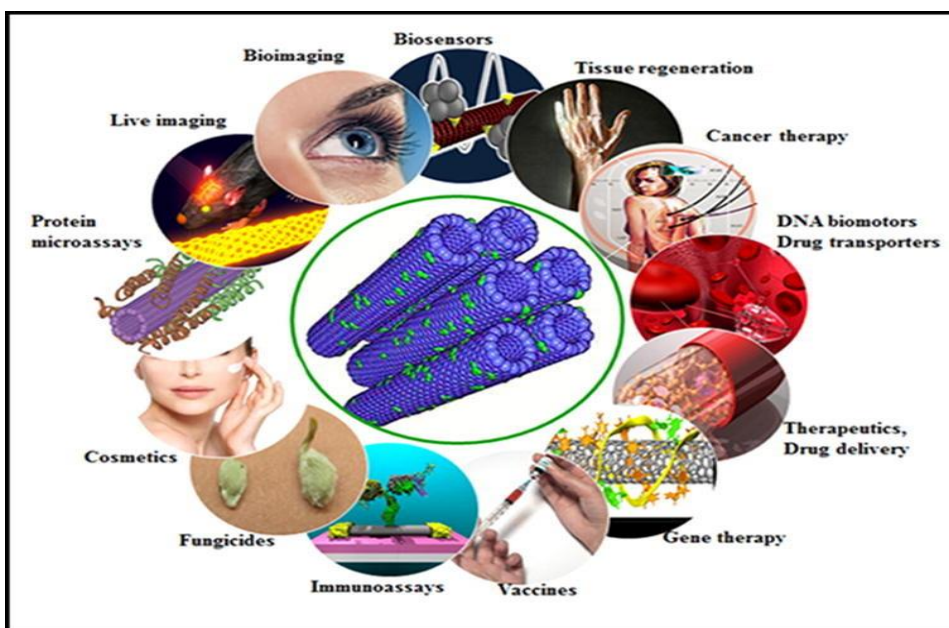**Figure 3.** Application of CNT in Biomedical Field [81]

Figure 4. Application of CNT in Biomedical Field [82]

4.3. Application of Carbon Nanotubes (CNTs) as a carrier of the Anticancer Drug

Chemotherapy is usually coupled with other treatment techniques to reduce the size of the tumor in traditional methods, however, this technique also causes toxicity to the other living cells, which has adverse side effects. To reduce the side effects, a new method has been developed in which anticancer drug is delivered to tumors by CNTs [83]. To deliver the drug to the target cell, CNTs are functionalized with the chemical receptor (protein or nucleic acid), and then the anticancer drug is fixed in functionalized CNTs with the open ends; this drug along with CNTs is introduced into the animal body either by oral or injection. Finally, drug carrier CNTs pass across the nuclear membrane and cytoplasmic membrane without generating toxic effects and reach the targeted cell. There are two targeted ways through which a drug is delivered to a cell; one is non-internalization, while the second one is the internalization method. Comparatively, the second method is considered better than the first method. In the internalization method, both drug and CNTs are entered inside the cell from the intracellular environment that assists to deteriorate the drug carrier conjugate for releasing drugs into the cell. While in the method of non-internalization, the extracellular status helps to deteriorate the drug carrier to conjugate, then the drug itself penetrates across the lipid membrane to enter into the cell; here the drug is degraded before reaching the targeted cell. There are two possible mechanisms of internalization of CNTs, which include insertion and diffusion and endocytosis. The whole procedure is used for cancer therapy [84].

4.4. Carbon Nanotubes as Preservatives

Many investigations have focused on the development of novel antioxidants due to their importance in food and pharmaceutical industry [85]. CNTs and nano-horns are antioxidants in nature. They can be used in drugs to reduce the process of oxidation in the human body. Their antioxidant nature also enables them to be utilized in cosmetic products and in the field of dermatology along with zinc oxide sunscreen, which is used to avoid oxidation of vital skin constituents [86]. For convenient and processed food, aromatic organic acids are used to inhibit a vast range of fungi, molds, bacteria, and yeasts [87]. Despite this, extensive consumption of these types of preservatives in food may be harmful for human health and can cause several allergic diseases like dermatitis, hives,

convulsion, and others in humans [88]. Currently, carbon nanomaterials have attracted significant attention worldwide in modern food-packaging technology due to their easy functionalization, high surface area-to-volume ratio, excellent antimicrobial activity, superb physico-mechanical and water resistance properties, strong adsorptive ability, high thermal, and electrical conductivity,. CNTs-based nano-sensors offer a better assessment of the freshness, security, safety, quality, and packaging of food products [89].

4.5. Application of Carbon Nanotubes (CNTs) as a Sensor

Sensors are mostly imported as detecting devices, which are used in different fields. There are different types of sensors such as biosensors and molecular sensors. The efficiency of sensors can be enhanced by attaching CNTs to them (Figure 5) [90]. CNTs have been employed in the sensing and detection of liver and pancreas cancer [91]. The usages of CNTs for the detection and sensing of NO_2 gas are well recognized [92]. CNTs incorporated sensors can be used to bring revolutionary changes in different sectors, especially in the biomedical industry [83]. The sensors containing CNTs composite pellets may be constructed by attaching different chemical groups onto the end; they are also sensitive to gases such as NH_3, CO_2, and CO H_2O [93]. Gas sensor are used in medical, industrial, and in commercial areas for the reduction of greenhouse gases and to monitor the environment of the combustion engine [94]. Ammonia, carbon dioxide, and oxygen gas can be detected using their conductivity and permittivity properties by multi-walled nanotubes [95].

The CNTs have unique physical, adsorption, and electrochemical properties. The strong adsorption capacity of the CNTs and their good sensitivity towards atoms and molecules adsorbed on their surface enable them to design sensors-based CNTs. Many gas sensors (detectors) based on the CNT have been reported in previous literature [96] that include:

 i. Shift gas sensors

 ii. Resonance frequency

iii. Capacitance gas sensors

iv. Ionization gas sensors

 v. Adsorption gas sensors

Their main operating principle involves adsorption during which an adsorbed gas molecule transfers an electron to or takes it from a nanotube. This changes the electrical properties of the CNTs, which can be detected and measured. There are numerous gas sensors based on pure SWCNTs and MWCNTs modified by metals, metal oxides, polymers or various functional groups [97].
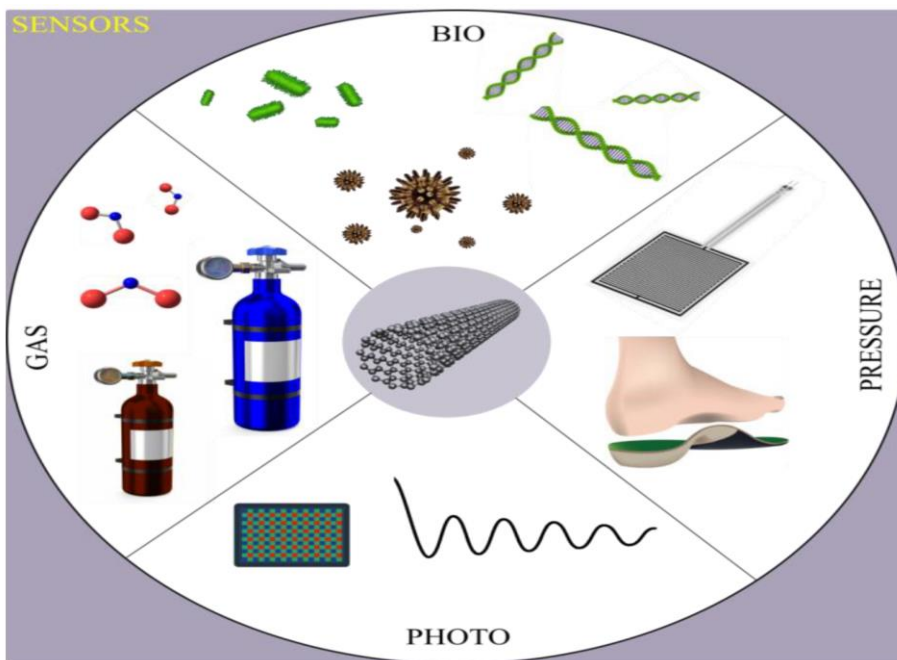

Figure 5. Application of CNT as a sensor [98]

4.6. Application of Carbon Nanotubes (CNTs) in Water Filtration and Environment

Carbon nanotubes (CNTs) find numerous applications in the purification of water [99] and the remediation of pollutants [100]. They can reduce the distillation cost by up to 75% and their membranes help in filtration. CNTs have a very small particle size, which enable smaller particles (like water molecules) to pass through them, while larger particles are blocked (they cannot pass through carbon nanotubes), such as chloride salts [101].

4.7. Carbon Nanotubes (CNTs) in Electronic Devices

In electronic devices, CNTs can be used as field emission sources, which is done by applying the potential between CNTs surface and anode.

Due to the curvature present in the form of pentagons in CNTs , electrons are discharged from their tips [102]. The use of CNTs as electron emitters is associated with several advantages, which include stable field emission, high current densities over prolonged periods, low emission threshold potential, and long lifetime of the components for the construction of field emission devices [103].

CNTs can be used in supercapacitors because they have a large surface area [104]. Therefore, by using carbon nanotubes (CNTs), the use of platinum can be reduced, which creates some problems specially in fuel cells [105].

4.8. Gas and Hydrogen Storage

Carbon nanotubes (CNTs) are used as a metal container because of their hollow cylindrical nature. Metals may be introduced into CNTs core by different methods, including solid-state reaction, arc-discharge method, and electrochemical techniques [106]. The environmental problems are rising day by day due to the overuse of fossil fuels. There are various primary energy sources, such as, wind, solar energy, thermonuclear energy, and geothermal. The best choice among all is hydrogen because of its adverse advantages. It can be easily produced, it has a high utilization efficiency and it transforms without any additional problems at the consumer end [107]. CNTs are used to construct gas containers, which are used to store hydrogen gas. Hydrogen gas is absorbed in single-walled nanotubes. The value of absorbed hydrogen gas in CNTs varies between 0.4 and 67 mass % [82].

5. CONCLUSION

Carbon nanotubes can be produced by laser ablation, electric arc discharge, chemical vapor deposition (CVD), plasma-enhanced chemical vapor deposition (PECVD), pulsed laser deposition, use of low-frequency ultrasound waves, by heating a bulk polymer and bulk sputtering etc. Chemical vapor deposition (CVD) and arc discharge are the most favorite methods for CNTs production on large scale; however, the latter is comparatively expensive. The CVD yields very pure and high-performance solid materials and has the ability to control accurately the nanotube diameter, length, density, purity, orientation, and alignment. Plasma-enhanced chemical vapor deposition (PECVD) is a latest technique for the selective positioning and vertical alignment of CNTs.

The laser ablation is the best suitable method to grow single-wall nanotubes with high purity and high quality. The CNTs prepared by pulsed laser deposition require either gas- or liquid-phase purification. CNTs show characteristic metallic/semi-metallic, mechanical, electrical, thermal and electrical properties which are improved by making their composites with metals. They can improve the mechanical strength and flexibility of a construction material. CNTs find applications in diagnosis, drug delivery, gene delivery to cells, cancer therapy, drug delivery, tissue regeneration, biomedicine, cosmetic products, dermatology, environmental science, water purification, modern food-packaging technology, electronic devices, gas sensors and in construction of gas containers for hydrogen storage.

REFERENCES

1. Karthik P, Himaja A, Singh SP. Carbon-allotropes: synthesis methods, applications and future perspectives. *Carbon Lett*. 2014;15(4):219–237. https://doi.org/10.5714/CL.2014.15.4.219

2. Zhu S, Sheng J, Chen Y, Ni J, Li Y. Carbon nanotubes for flexible batteries: recent progress and future perspective. *Nat Sci Rev*. 2021;8(5):nwaa261. https://doi.org/10.1093/nsr/nwaa261

3. Saito R, GD, Dresselhaus G, Dresselhaus MS. *Physical properties of carbon nanotubes*. London; Imperial College Press; 1998.

4. Chen J, Hamon MA, Hu H, et al. Solution properties of single-walled carbon nanotubes. *Science*. 1998;282(5386):95–98. https://doi.org/10.1126/science.282.5386.95

5. Tasis D, Tagmatarchis N, Bianco A, Prato M. Chemistry of carbon nanotubes. *Chem Rev*. 2006;106(3):1105–1136. https://doi.org/10.1021/cr050569o

6. De Volder MFL, Tawfick SH, Baughman RH, Hart AJ. Carbon nanotubes: present and future commercial applications. *Science*. 2013;339(6119):535–539. https://doi.org/10.1126/science.1222453

7. Javed M, Abbas SM, Hussain S, Siddiq M, Han D, Niu L. Amino-functionalized silica anchored to multiwall carbon nanotubes as hybrid electrode material for supercapacitors. *Mat Sci Energy Technol*. 2018;1(1):70–76. https://doi.org/10.1016/j.mset.2018.03.002

8. Munir M, Hussain S, Anwar R, Waqas M, Ali J. The role of nanoparticles in the diagnosis and treatment of diseases. *Scie Inq Rev*. 2020;4(3):14–26. https://doi.org/10.32350/sir.43.02

9. Shahzad K. synthesis, characterization, and photocatalytic degradation of nickel doped copper oxide nanoparticles. *Lahore Garrison Univ J Life Sci*. 2020;4(02):130–138. https://doi.org/10.54692/lgujls.2019.0402103

10. Iqbal MF, Yousef AK, Hassan A, et al. Significantly improved electrochemical characteristics of nickel sulfide nanoplates using graphene oxide thin film for supercapacitor applications. *J Energy Storage*. 2021;33:e102091. https://doi.org/10.1016/j.est.2020.102091

11. Singh E, Srivastava R, Kumar U, Katheria AD. Carbon nanotube: A review on introduction, fabrication techniques and optical applications. *Nanosci Nanotechnol Res*. 2017;4(4):120–126.

12. Akbari GH, Mirabootalebi SO. Methods for synthesis of carbon nanotubes. *Int J Bio-Inorg Hybr Nanomater*. 2017;6(2):1–10.

13. Szabó A, Perri C, Csató A, Giordano G, Vuono D, Nagy JB. Synthesis methods of carbon nanotubes and related materials. *Materials*. 2010;3(5):3092–140. https://doi.org/10.3390/ma3053092

14. Eatemadi A, Daraee H, Karimkhanloo H, et al. Carbon nanotubes: properties, synthesis, purification, and medical applications. *Nanoscale Res Lett.* 2014;9(1):eD393.

15. Ando Y, Zhao X. Synthesis of carbon nanotubes by arc-discharge method. *New Diamond Front Carbon Technol*. 2006;16(3):123–138.

16. Sharma R, Sharma AK, Sharma V. Synthesis of carbon nanotubes by arc-discharge and chemical vapor deposition method with analysis of its morphology, dispersion and functionalization characteristics. *Cogent Eng*. 2015;2(1):e1094017. https://doi.org/10.1080/23311916.2015.1094017

17. Rashad AA, Mohammed SA, Yousif E. Synthesis of carbon nanotube : A review. *J Nanosci Technol*. 2016;2(5):e7.

18. Awasthi K, Srivastava A, Srivastava ON. Synthesis of carbon nanotubes. *J Nanosci Nanotechnol*. 2005;5(10):1616–1636. https://doi.org/10.1166/jnn.2005.407

19. Rafique MMA, Iqbal J. Production of carbon nanotubes by different routes—a review. *J Encapsul Adsorp Sci*. 2011;1:29–34. https://doi.org/10.4236/jeas.2011.11004

20. Chrzanowska J, Hoffman J, Małolepszy A, et al. Synthesis of carbon nanotubes by the laser ablation method: effect of laser wavelength. *Physica Status Solidi (b)*. 2015;252(8):1860–1867. https://doi.org/10.1002/pssb.201451614

21. Mahajan D. Carbon nanotubes: a review on synthesis, electrical and mechanical properties and applications. *Asian J Appl Sci Technol*. 2017;1(7):15–20.

22. van de Burgt Y. Laser-assisted growth of carbon nanotubes—a review. *J Laser Appl*. 2014;26(3):e032001. https://doi.org/10.2351/1.4869257

23. Emmenegger C, Bonard JM, Mauron P, et al. Synthesis of carbon nanotubes over Fe catalyst on aluminium and suggested growth mechanism. *Carbon*. 2003;41(3):539–547. https://doi.org/10.1016/S0008-6223(02)00362-7

24. Yadav BC, Kumar R, Srivastava R, Shukla T. Flame Synthesis of Carbon Nanotubes using Camphor and its Characterization. *Intl J Green Nanotechnol*. 2011;3(3):170–179. https://doi.org/10.1080/19430892.2011.628579

25. Ibrahim KS. Carbon nanotubes-properties and applications: a review. *Korea Sci*. 2013;14(3):131–144.

26. Bode Y. *Vibration Analysis of Coupled Coaxial Carbon Nanotube With Damping In The Presence Of Graphene Sheet* (master's thesis) University of Akron; 2018.

27. Varshney K. Carbon nanotubes: A review on synthesis, properties and applications. *Int J Eng Res General Sci*. 2015;2(4):660–670.

28. Fonseca A, Hernadi K, Nagy JB, Bernaerts D, Lucas AA. Optimization of catalytic production and purification of buckytubes. *J Molecul Catal A: Chemical*. 1996;107(1):159–168. https://doi.org/10.1016/1381-1169(95)00211-1

29. Collins PG, Avouris P. Nanotubes for electronics. *Sci Am*. 2000;283(6):62–69.

30. Kumar M, Ando Y. Chemical vapor deposition of carbon nanotubes: a review on growth mechanism and mass production. *J Nanosci Nanotechnol*. 2010;10(6):3739–3758. https://doi.org/10.1166/jnn. 2010.2939

31. Eftekhari A, Jafarkhani P, Moztarzadeh F. High-yield synthesis of carbon nanotubes using a water-soluble catalyst support in catalytic chemical vapor deposition. *Carbon*. 2006;44(7):1343–1345. https://doi.org/10.1016/j.carbon.2005.12.006

32. Franz G. Plasma enhanced chemical vapor deposition of organic polymers. *Processes*. 2021;9(6):e980. https://doi.org/10.3390 /pr9060980

33. Mirakabad FST, Nejati-Koshki K, Akbarzadeh A, et al. PLGA-based nanoparticles as cancer drug delivery systems. *Asian Pacific J Can Preven*. 2014;15(2):517–535. http://dx.doi.org/10.7314/APJCP. 2014.15.2.517

34. Jagadeesan AK, Thangavelu K, Dhananjeyan V. C*arbon Nanotubes: Synthesis, Properties and Applications*. IntechOpen; 2020.

35. Price GJ, Nawaz M, Yasin T, Bibi S. Sonochemical modification of carbon nanotubes for enhanced nanocomposite performance. *Ultrason Sonochem*. 2018;40:123–130. https://doi.org/10.1016/j. ultsonch.2017.02.021

36. Cho WS, Hamada E, Kondo Y, Takayanagi K. Synthesis of carbon nanotubes from bulk polymer. *Appl Phy Lett*. 1996;69(2):278–279. https://doi.org/10.1063/1.117949

37. Tran TQ, Lee JKY, Chinnappan A, et al. Strong, lightweight, and highly conductive CNT/Au/Cu wires from sputtering and electroplating methods. *J Mater Sci Technol*. 2020;40:99–106. https://doi.org/10.1016/j.jmst.2019.08.033

38. Chapin JS. *Sputtering Process and Apparatus*. Google Patents; 1979.

39. Ogura I, Kotake M, Hashimoto N, Gotoh K, Kishimoto A. Release characteristics of single-wall carbon nanotubes during manufacturing and handling. *J Phy: Conf Ser*. 2013;429:e012057. https://doi.org/10. 1088/1742-6596/429/1/012057

40. Hirlekar R, Yamagar M, Garse H, Vij M, Kadam V. Carbon nanotubes and its applications: a review. *Asian J Pharmac Clinic Res*. 2009;2(4):17–27.

41. Dubey R, Dutta D, Sarkar A, Chattopadhyay P. Functionalized carbon nanotubes: synthesis, properties and applications in water purification, drug delivery, and material and biomedical sciences. *Nanoscale Adv*. 2021;3(20):5722–5744. https://doi.org/10.1039/D1NA00293G

42. Sawant SV, Patwardhan AW, Joshi JB, Dasgupta K. Boron doped carbon nanotubes: Synthesis, characterization and emerging applications–a review. *Chem Eng J*. 2022;427:e131616. https://doi.org/10.1016/j.cej.2021.131616

43. Saifuddin N, Raziah AZ, Junizah AR. Carbon nanotubes: a review on structure and their interaction with proteins. *J Chem*. 2012;2013:e676815. https://doi.org/10.1155/2013/676815

44. Odom TW, Huang J-L, Kim P, Lieber CM. Atomic structure and electronic properties of single-walled carbon nanotubes. *Nature*. 1998;391(6662):62–64. https://doi.org/10.1038/34145

45. Wallace P. The band structure of graphite. *Phys Rev*. 1947;71(9):622–634.

46. Dresselhaus MS, Dresselhaus G, Eklund PC. *Science of Fullerenes and Carbon Nanotubes: Their Properties and Applications*. Elsevier; 1996.

47. Salvetat J-P, Bonard J-M, Thomson N, et al. Mechanical properties of carbon nanotubes. *Appl Phy*. 1999;69(3):255–260. https://doi.org/10.1007/s003390050999

48. Ashby MF. Overview no. 80: on the engineering properties of materials. *Acta Metallur*. 1989;37(5):1273–1293. https://doi.org/10.1016/0001-6160(89)90158-2

49. Hone J, Llaguno, M., Biercuk, M. et al. Thermal properties of carbon nanotubes and nanotube-based materials. *Appl Phys A*, 2002;74: 339–343. https://doi.org/10.1007/s003390201277

50. Che J, Çagin T, Goddard WA. Thermal conductivity of carbon nanotubes. *Nanotechnology*. 2000;11(2):65–69. https://doi.org/10.1088/0957-4484/11/2/305

51. Llaguno MC, Hone J, Johnson AT, Fischer JE. Thermal conductivity of single wall carbon nanotubes: Diameter and annealing dependence. *AIP Conf Proc*. 2001;591(1):384–387. https://doi.org/10.1063/1.1426893

52. Choi S, Zhang Z, Yu W, Lockwood F, Grulke E. Anomalous thermal conductivity enhancement in nanotube suspensions. *Appl Phy lett*. 2001;79(14):2252–2254. https://doi.org/10.1063/1.1408272

53. Small JP, Shi L, Kim P. Mesoscopic thermal and thermoelectric measurements of individual carbon nanotubes. *Solid State Commun*. 2003;127(2):181–186. https://doi.org/10.1016/S0038-1098(03)00341-7

54. Mönch I, Leonhardt A, Meye A, et al. Synthesis and characteristics of Fe-filled multi-walled carbon nanotubes for biomedical application. *J Phy*. 2007;61:820–824. https://doi.org/10.1088/1742-6596/61/1/164

55. Lu JP. Novel magnetic properties of carbon nanotubes. *Phy Rev Lett*. 1995;74(7):e1123.

56. Ramirez A, Haddon R, Zhou O, et al. Magnetic susceptibility of molecular carbon: nanotubes and fullerite. *Science*. 1994;265(5168):84–86. https://doi.org/10.1126/science.265.5168.84

57. Klingeler R, Hampel S, Büchner B. Carbon nanotube based biomedical agents for heating, temperature sensing and drug delivery. *Int J Hyper*. 2008;24(6):496–505. https://doi.org/10.1080/02656730802154786

58. Ponnamma D, Ninan N, Thomas S. Carbon nanotube tube filled polymer nanocomposites and their applications in tissue engineering. In *Applications of Nanomaterials: Advances and Key Technologies*. Elsevier; 2018:391–414. https://doi.org/10.1016/B978-0-08-101971-9.00014-4

59. El Achaby M, Arrakhiz FE, Vaudreuil S, el Kacem Qaiss A, Bousmina M, Fassi-Fehri O. Mechanical, thermal, and rheological properties of graphene-based polypropylene nanocomposites prepared

by melt mixing. *Polym Comp*. 2012;33(5):733–744. https://doi.org/10.1002/pc.22198

60. Dalton AB, Collins S, Munoz E, et al. Super-tough carbon-nanotube fibres. *Nature*. 2003;423(6941):e703. https://doi.org/10.1038/423703a

61. Liu T, Phang IY, Shen L, Chow SY, Zhang W-D. Morphology and mechanical properties of multiwalled carbon nanotubes reinforced nylon-6 composites. *Macromolecules*. 2004;37(19):7214–7222. https://doi.org/10.1021/ma049132t

62. Karim MR, Lee CJ, Park Y-T, Lee MS. SWNTs coated by conducting polyaniline: synthesis and modified properties. *Synth Met*. 2005;151(2):131–135. https://doi.org/10.1016/j.synthmet.2005.03.012

63. Hussain S, Amjad M. A review on gold nanoparticles (GNPs) and their Advancement in cancer therapy. *Int J Nanom Nanotechnol Nanomed*. 2021;7(1):019–025. https://dx.doi.org/10.17352/2455-3492.000040

64. Hussain S, Amjad M, Khan A, et al. A Perspective Study on Copper Oxide Nanoparticles and Their Role in Different Fields of Biomedical Sciences. *Int J Sci Res Eng Develop*. 2020;3(6):1246–1256.

65. Zulfiqar H, Hussain S, Riaz M, et al. Nature of nanoparticles and their applications in targeted drug delivery. *Pak J Sci*. 2020;72(1):30–36.

66. Mueez A, Hussain S, Ahmad M, Raza A, Ahmed I, Amjad M. Green synthesis of nanosilver particles from plants extract. *Int J Agricul Environ Biores*. 2022;7(1):96–122.

67. Rehman H, Ali Z, Hussain M, et al. Synthesis and characterization of ZnO nanoparticles and their use as an adsorbent for the arsenic removal from drinking water. *Dig J Nanomat Biostruc*. 2019;14(4):1033–1040.

68. Abbas SM, Ahmad N, Rana UA, et al. High rate capability and long cycle stability of Cr2O3 anode with CNTs for lithium ion batteries. *Electroch Acta*. 2016;212:260–269. https://doi.org/10.1016/j.electacta.2016.06.156

69. Raza MW, Kiran S, Razaq A, et al. Strategy to enhance the electrochemical characteristics of lanthanum sulfide nanorods for

supercapacitor applications. *J Nanopart Res*. 2021;23(9):1–12. https://doi.org/10.1007/s11051-021-05307-0

70. Javed M, Hussain S. Synthesis, characterization and photocatalytic applications of p (aac) microgels and its composites of ni doped ZnO nanorods. *Dig J Nanomater Bios*. 2020;15(1):217–230.

71. Wu Y, Zhao X, Shang Y, Chang S, Dai L, Cao A. Application-driven carbon nanotube functional materials. *ACS nano*. 2021;15(5):7946–7974. https://doi.org/10.1021/acsnano.0c10662

72. Taha MR, Ying T. *Effects of Carbon Nanotube on Kaolinite: Basic Geotechnical Behavior*. Anchorage, Alaska, USA. 2010.

73. Chappell MA. Solid-Phase characteristics of engineered nanoparticles. In: Linkov I, Steevens J, eds., *Nanomaterials: Risks and Benefits*. NATO Science for Peace and Security Series C: Environmental Security. Springer; 2009. https://doi.org/10.1007/978-1-4020-9491-0_8

74. Garboczi EJ. Concrete nanoscience and nanotechnology: definitions and applications. In: Bittnar Z, Bartos PJM, Němeček J, Šmilauer V, Zeman J, eds., *Nanotechnology in Construction 3*. Springer, Berlin, Heidelberg; 2009. https://doi.org/10.1007/978-3-642-00980-8_9

75. Akiladevi D, Basak S. Carbon nanotubes (CNTs) production, characterization and its applications. *Int J Adv Pharm Sci*. 2010;1:187–195.

76. Prajapati SK, Malaiya A, Kesharwani P, Soni D, Jain A. Biomedical applications and toxicities of carbon nanotubes. *Drug Chemical Toxicol*. 2022;45(1):435–450. https://doi.org/10.1080/01480545.2019.1709492

77. Mattson MP, Haddon RC, Rao AM. Molecular functionalization of carbon nanotubes and use as substrates for neuronal growth. *J Molecul Neurosci*. 2000;14(3):175–182. https://doi.org/10.1385/JMN:14:3:175

78. Saito N, Usui Y, Aoki K, et al. Carbon nanotubes: biomaterial applications. *Chem Soc Rev*. 2009;38(7):1897–1903. https://doi.org/10.1039/B804822N

79. Bianco A, Prato M. Can carbon nanotubes be considered useful tools for biological applications? *Adv Mat*. 2003;15(20):1765–1768. https://doi.org/10.1002/adma.200301646

80. Saito N, Haniu H, Aoki K, Nishimura N, Uemura T. Future Prospects for clinical applications of nanocarbons focusing on carbon nanotubes. *Adv Sci*. 2022;9(24):e2201214. https://doi.org/10.1002/advs.202201214

81. Mehra NK, Jain K, Jain NK. Pharmaceutical and biomedical applications of surface engineered carbon nanotubes. *Drug Discov Today*. 2015;20(6):750–759. https://doi.org/10.1016/j.drudis.2015.01.006

82. Merum S, Veluru JB, Seeram R. Functionalized carbon nanotubes in bio-world: Applications, limitations and future directions. *Mater Sci Eng*. 2017;223:43–63. https://doi.org/10.1016/j.mseb.2017.06.002

83. Wong BS, Yoong SL, Jagusiak A, et al. Carbon nanotubes for delivery of small molecule drugs. *Adv Drug Deliv Rev*. 2013;65(15):1964–2015. https://doi.org/10.1016/j.addr.2013.08.005

84. Zhang Y, Bai Y, Yan B. Functionalized carbon nanotubes for potential medicinal applications. *Drug Discov Today*. 2010;15(11):428–435. https://doi.org/10.1016/j.drudis.2010.04.005

85. Mahmood A, Saqib M, Ali M, Abdullah MI, Khalid B. Theoretical investigation for the designing of novel antioxidants. *Canad J Chem*. 2013;91(2):126–130. https://doi.org/10.1139/cjc-2012-0356

86. Pai P NK, Jamade S, Shah R, Ekshinge V, Jadhav N. Pharmaceutical applications of carbon tubes and nanohorns. *Current Pharma Res. J.* 2006;1:11–15.

87. Sun Y, Wang X, Huang Y, Pan Z, Wang L. Derivatization following hollow-fiber microextraction with tetramethylammonium acetate as a dual-function reagent for the determination of benzoic acid and sorbic acid by GC. *J Separa Sci*. 2013;36(14):2268–2276. https://doi.org/10.1002/jssc.201300239

88. Han F, He Y-Z, Li L, Fu G-N, Xie H-Y, Gan W-E. Determination of benzoic acid and sorbic acid in food products using electrokinetic flow analysis–ion pair solid phase extraction–capillary zone

electrophoresis. *Analytica Chimica Acta*. 2008;618(1):79–85. https://doi.org/10.1016/j.aca.2008.04.041

89. Hui S, Das NC. Surface modified carbon nanotubes in food packaging. In: Aslam J, Hussain CM, Aslam R. *Surface Modified Carbon Nanotubes Volume 2: Industrial Applications*. ACS Publications; 2022:199–233. https://doi.org/10.1021/bk-2022-1425.ch009

90. Wong SS, Joselevich E, Woolley AT, Cheung CL, Lieber CM. Covalently functionalized nanotubes as nanometre-sized probes in chemistry and biology. *Nature*. 1998;394(6688):52–55. https://doi.org/10.1038/27873

91. Ahmadian E, Janas D, Eftekhari A, Zare N. Application of carbon nanotubes in sensing/monitoring of pancreas and liver cancer. *Chemosphere*. 2022;302:e134826. https://doi.org/10.1016/j.chemosphere.2022.134826

92. Hussain S, Nazir K, Ata-ur-Rehman, Abbas SM. Nitrogen dioxide sensing technologies. In: *Toxic Gas Sensors and Biosensors*. Materials Research Foundations;2021:1–38. https://doi.org/10.21741/9781644901175-1

93. Collins PG, Bradley K, Ishigami M, Zettl A. Extreme oxygen sensitivity of electronic properties of carbon nanotubes. *Science*. 2000;287(5459):e1801.https://doi.org/10.1126/science.287.5459.1801

94. Ivers-Tiffée E, Härdtl K, Menesklou W, Riegel J. Principles of solid state oxygen sensors for lean combustion gas control. *Electroch Acta*. 2001;47(5):807–814. https://doi.org/10.1016/S0013-4686(01)00761-7

95. Ong KG. *Design and application of planar inductor-capacitor resonant circuit remote query sensors* [doctoral thesis]. University of Kentucky; 2000.

96. Schroeder V, Savagatrup S, He M, Lin S, Swager TM. Carbon nanotube chemical sensors. *Chem Rev*. 2018;119(1):599–663. https://doi.org/10.1021/acs.chemrev.8b00340

97. Matos MA, Pinho ST, Tagarielli VL. Application of machine learning to predict the multiaxial strain-sensing response of CNT-polymer composites. *Carbon*. 2019;146:265–275. https://doi.org/10.1016/j.carbon.2019.02.001

98. Camilli L, Passacantando M. Advances on sensors based on carbon nanotubes. *Chemosensors*. 2018;6(4):e62. https://doi.org/10.3390/chemosensors6040062

99. Sajid M, Asif M, Baig N, Kabeer M, Ihsanullah I, Mohammad AW. Carbon nanotubes-based adsorbents: Properties, functionalization, interaction mechanisms, and applications in water purification. *J Water Process Eng*. 2022;47:e102815. https://doi.org/10.1016/j.jwpe.2022.102815

100. Chung JH, Hasyimah N, Hussein N. Application of carbon nanotubes (CNTs) for remediation of emerging pollutants-a review. *Trop Aqu Soil Pollut* 2022;2(1):13–26. https://doi.org/10.53623/tasp.v2i1.27

101. Kaushik1 BK, Majumder MK. *Carbon Nanotube Based VLSI Interconnects. Analysis and Design*. Springer; 2015.

102. Car ADV-CCB. Electronic structure at carbon nanotube tips. *Applied Physics A*. 1999;68(3):283–286. https://doi.org/10.1007/s003390050889

103. Sharma A, Kim HS, Kim D-W, Ahn S. A carbon nanotube field-emission X-ray tube with a stationary anode target. *Microelec Eng*. 2016;152:35–40. https://doi.org/10.1016/j.mee.2015.12.021

104. Wu Z-S, Zhou G, Yin L-C, Ren W, Li F, Cheng H-M. Graphene/metal oxide composite electrode materials for energy storage. *Nano Energy*. 2012;1(1):107–131. https://doi.org/10.1016/j.nanoen.2011.11.001

105. Matsumoto T, Komatsu T, Arai K, et al. Reduction of Pt usage in fuel cell electrocatalysts with carbon nanotube electrodes. *Chemical Commun*. 2004(7):840–841. https://doi.org/10.1039/B400607K

106. Banhart F, Grobert N, Terrones M, Charlier JC, Ajayan PM. Metal atoms in carbon nanotubes and related nanoparticles. *Int J Modern Phy B*. 2001;15(31):4037–4069. https://doi.org/10.1142/S0217979201007944

107. Veziro TN, Barbir F. Hydrogen: the wonder fuel. *Int J Hydrogen Energy*. 1992;17(6):391–404. https://doi.org/10.1016/0360-3199(92)90183-W